1997

An Integrated GPS-GIS Methodology for Performing Travel Time Studies.

Cesar A. Quiroga
Louisiana State University and Agricultural & Mechanical College

INFORMATION TO USERS

This manuscript has been reproduced from the microfilm master. UMI films the text directly from the original or copy submitted. Thus, some thesis and dissertation copies are in typewriter face, while others may be from any type of computer printer.

The quality of this reproduction is dependent upon the quality of the copy submitted. Broken or indistinct print, colored or poor quality illustrations and photographs, print bleedthrough, substandard margins, and improper alignment can adversely affect reproduction.

In the unlikely event that the author did not send UMI a complete manuscript and there are missing pages, these will be noted. Also, if unauthorized copyright material had to be removed, a note will indicate the deletion.

Oversize materials (e.g., maps, drawings, charts) are reproduced by sectioning the original, beginning at the upper left-hand corner and continuing from left to right in equal sections with small overlaps. Each original is also photographed in one exposure and is included in reduced form at the back of the book.

Photographs included in the original manuscript have been reproduced xerographically in this copy. Higher quality 6" x 9" black and white photographic prints are available for any photographs or illustrations appearing in this copy for an additional charge. Contact UMI directly to order.

UMI

A Bell & Howell Information Company
300 North Zeeb Road, Ann Arbor MI 48106-1346 USA
313/761-4700 800/521-0600

AN INTEGRATED GPS-GIS METHODOLOGY FOR PERFORMING TRAVEL TIME STUDIES

A Dissertation

Submitted to the Graduate Faculty of the
Louisiana State University and
Agricultural and Mechanical College
in partial fulfillment of the
requirements for the degree of
Doctor of Philosophy

in

The Department of Civil and Environmental Engineering

by
Cesar A. Quiroga
Ingeniero Civil, Escuela Colombiana de Ingenieria, 1982
M.S. in Civil Engineering, Louisiana State University, 1986
August, 1997

ACKNOWLEDGMENTS

This dissertation originated in the Congestion Management System (CMS) research project conducted by the Remote Sensing and Image Processing Laboratory (RSIP) at Louisiana State University. Funding for this project was provided by the Louisiana Department of Transportation and Development, through the Louisiana Transportation Research Center (Awards No. 95-755 and 97-755).

Many people and institutions provided invaluable help to make my research contribution to the CMS project possible. Giving credit to all of them is practically impossible. However, some key names must be mentioned: At DOTD, Jim Joffrion, Art Rogers, and Masood Rasoulian; at CRPC, Huey Dugas and Jay Naidu; at RPC, Walter Brooks and Nitin Kamath; at NLCOG, Chris Petro; at RSIP, Chris Schwehm, Hong-Lie Qiu, Tom Smailus, Margaret Brewer, and all the undergraduate students who collected travel time data and helped with data processing. A very special expression of gratitude, of course, goes to Darcy Bullock who, as my major professor and principal investigator in the CMS project, always provided me with sound advice, a sense of direction, and focus. I also have to mention the extremely useful assistance provided by the members of my committee. I gratefully acknowledge their invaluable criticism and suggestions as well as their thorough revision of this document.

Finally, I thank my wife Tosca and our daughters Pamela and Sophia for their love, patience, and understanding while I was completing this work.

TABLE OF CONTENTS

LIST OF TABLES

LIST OF FIGURES

ABSTRACT

This dissertation describes a methodology for conducting travel time studies based on global positioning system (GPS) receivers and geographic information system (GIS) technology. Compared to traditional approaches, the new methodology provides consistency, automation, finer levels of resolution, and better accuracy in measuring travel time and speed. These characteristics enable the detection of localized traffic effects much more efficiently than with traditional techniques. The new methodology automates the data collection and data reduction procedures, and provides improved procedures for documenting and analyzing travel time and speed data. As a result, large amounts of reliable travel time and speed data can be collected and processed.

The new methodology was used to process 28,000 miles of travel time runs on 4,000 highway segments (nominally 0.2-mi long) along 660 miles of highways in three metropolitan areas in Louisiana (Baton Rouge, Shreveport, and New Orleans). Nearly 183,000 segment travel time and speed records based on GPS data collected every 1 second were obtained.

Using 0.2-mi segments was justified by an analysis which showed that segment lengths shorter than 0.5 mi were needed to detect localized traffic effects. These traffic disturbances became visible only when segment lengths were at most half the length of the associated disturbance. The analysis also showed that traditional link-based segments, which are typically longer than 0.5 mi, were not sufficient to characterize localized effects properly.

GPS time intervals larger than one second were simulated. The analysis showed that all segments had GPS data only when the GPS time interval was at most half the shortest segment travel time observed for the run. The analysis also showed a direct relationship between segment speed uncertainties and GPS time intervals.

Median speeds were shown to be more robust estimators of central tendency than harmonic mean speeds. Segment speed coefficient of variation maps were shown to be powerful indicators of traffic flow variability along highways.

The ITE Manual of Transportation Engineering Studies was shown to seriously underestimate required sample sizes for travel time studies (or alternatively, to overestimate confidence levels associated with specified sample sizes). A new formulation was then developed to correct the shortcomings.

Chapter 1
INTRODUCTION

Two mandates of the Intermodal Surface Transportation Efficiency Act [ISTEA, 1991] were the development of congestion management systems (CMSs) and statewide highway traffic monitoring systems. An important component in the development of these systems is the capability to document congestion accurately and reliably. Although analytical procedures using estimated volumes and Highway Capacity Manual (HCM) [TRB, 1994] techniques can be used, direct travel time measurements are much more accurate.

Many congestion management measures, particularly those dealing with improved traffic control, are essentially local in nature (0.1-0.2 mi around the location of the traffic control). However, most existing techniques to quantify the performance of congestion management measures are targeted at relatively long segments and corridors (2-5 mi) and, consequently, do not properly measure localized traffic problems. In addition to this, current techniques are labor intensive; tend to be expensive, and are prone to frequent errors both in the field and in the office. As a result, only a few runs, which tend to be affected by significant accuracy problems, are usually made. To address these problems, updated procedures need to be implemented for documenting localized problems accurately along relatively short highway segments (say 0.1-0.2 mi long). Such procedures must be quick and easy to implement.

The goal of this dissertation is to document a set of GPS-GIS procedures developed to conduct travel time studies. The primary contribution is the development of

a cost-effective methodology that automates data collection. This simplified methodology allows operators to analyze a statistically significant amount of data with little effort. Specific contributions addressed in subsequent chapters include:

- An appropriate spatial model necessary for handling vast amounts of GPS point data.
- Data reduction procedures to compute travel time, speed, and delay along highway segments directly from the GPS data.
- Documentation of data collection, data reduction, and data reporting procedures.
- Updated formulation for estimating minimum sample sizes. This formulation replaces an erroneous formulation that has been widely used for the past 20 years.
- Procedures to analyze aggregation levels, central tendency estimators, and dispersion estimators.

This material is covered in the next seven chapters. Chapter 2 provides background information on urban congestion; travel time as a performance measure; and travel time data collection techniques including GPS. Chapter 3 discusses the spatial model used to map GPS point data to highway segments and the mathematical model developed to aggregate GPS travel time data into highway segment travel time data. Chapter 4 discusses limitations of existing formulations for estimating minimum sample sizes and proposes a new, updated methodology. Chapter 5 describes the geographic database and queries used to obtain specific travel time and speed information. Chapter 6 summarizes the procedures followed to collect GPS travel time data; methods to reduce raw GPS data to meaningful summary data; and procedures to generate both graphic and tabular reports. It also summarizes the application of the GPS-GIS methodology to three metropolitan areas in Louisiana: Baton Rouge, Shreveport, and New Orleans. Chapter 7

analyzes the GPS-GIS methodology from the following points of view: aggregation levels, sampling rates, central tendency, and dispersion. Finally, Chapter 8 presents a summary and a set of conclusions and recommendations.

This dissertation originated in the Congestion Management System (CMS) research project [Bullock and Quiroga, 1996]. Like other large research projects, the CMS project involved the work of many individuals, including that of this author. For clarity, Table 1-1 summarizes the level of involvement and responsibility of this author in each phase of the research.

Table 1-1: Level of involvement and responsibility of this author in the CMS research project

Item	Dissertation Chapter	Involvement Level (%)	Responsibility and Contributions
Literature review	2	100	Gathered and compiled all pertinent previous work
Spatial model	3	100	Developed spatial model and constructed GIS vector maps
Aggregation model	3	100	Developed mathematical model for aggregating GPS travel time data into segment travel time data
Sample size requirements	4	100	Found errors in ITE methodology and developed updated formulation
Database schema	5	100	Developed geographic database schema and coordinated the population of all database tables
Database queries	5	100	Constructed all spatial and non-spatial queries
Purchase and installation of GPS equipment	6	0	
Data collection in Baton Rouge	6	100	Coordinated all travel time data collection
Data collection in Shreveport	6	0	
Data collection in New Orleans	6	0	
Data reduction GIS utility	6	10	Designed graphical interface specifications, tested application, and provided feedback for application improvement
Data reduction in Baton Rouge, Shreveport, and New Orleans	6	100	Coordinated all data reduction, including data management and quality control
Color coded maps	6	100	Designed map layout and developed procedure for production of color coded maps
Archival tabular reports	6	30	Helped in the design of the tabular report layout, and coordinated the production of all tabular reports
WWW reports	6	20	Designed project home page
Analysis	7	100	Designed and conducted analyses on the following topics: aggregation levels, GPS sampling rate, central tendency estimators, and dispersion estimators

Chapter 2
BACKGROUND

Congestion in Urban Areas

Traffic congestion has become a critical problem nationwide. Several indicators confirm this trend. For example, between 1973 and 1993 (Figure 2-1), the number of vehicle-miles traveled (VMT) increased 75% [FHWA, 1995]. This increase was due in part to increases in the number of vehicles registered (54%) and the number of licensed drivers (43%). These two increases were higher than the increase in population (22%), and much higher than the increase in mileage of roads and streets (3%). As a result of these trends, traffic flow became much more demanding on the transportation system, particularly in urban areas. This resulted in more congested highways and in longer congestion periods, as evidenced in the 32% increase in percentage (from approximately 37% in 1973 to 69% in 1993) of the peak-hour VMT that occurred under congested conditions on the urban Interstate system. Here, congestion is assumed to occur for volume/service flow ratios ≥ 0.8. It is also interesting to note that total highway fuel use also increased (23%), despite improvements in fuel consumption (39%).

Congestion usually results in time delays for passengers, goods and services. It also results in increased fuel consumption, pollution, stress, health hazards, and added vehicle wear. The net result is a social cost that is paid directly and indirectly by users and nonusers. This cost is huge. For example, in a recent study that included 50 major urban areas around the country, Schrank, Turner, and Lomax [1993] concluded that the

total annual cost of congestion in those urban areas was more than $40 billion. This amount included time and fuel consumption, and it is not hard to imagine that it would be even higher if environmental costs had been included. While assigning a dollar amount to these environmental costs is highly speculative and many times impractical, it may be interesting to observe that whenever they have been included, the resulting amount is usually astronomical. For example, the Organization for Economic Cooperation and Development (OECD) has recently estimated the average annual cost of congestion in time, energy, and pollution for its member countries to be around 5% of the gross domestic product (GDP) [Konvitz, 1995]. By comparison, the estimated economic contribution of transportation (including transport, storage, and communications) to the US GDP in 1994 was 6% [FHWA, 1996].

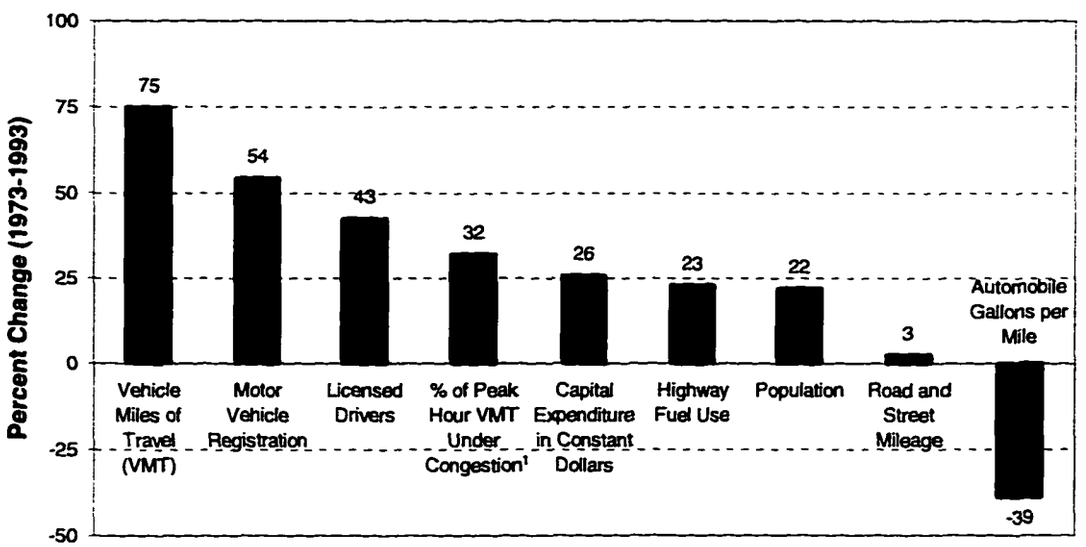

[1] On the urban Interstate System. Congestion is assumed to occur for Volume/Service Flow ratios ≥ 0.8

Figure 2-1: Highway and congestion indicators in the United States (adapted from FHWA [1995])

Travel delay is perceived by many as the most noticeable impact of congestion. Not surprisingly, numerous efforts have been made to eliminate it or, at least, to alleviate its effects. In the past, adding capacity was considered as the main solution to eliminate or reduce travel delays. However, this approach has frequently proved to be insufficient. Faced with this reality, many urban areas have opted for implementing alternative management measures such as improved traffic controls (in the form of intelligent transportation systems (ITS)); dedicated high-occupancy vehicle (HOV) lanes; improved transit service; and congestion and parking pricing [OECD, 1994]. The objective of these measures is to manage and reduce congestion by improving traffic flow, enhancing mobility and safety, and reducing demand for car use. Many of these management measures are the result of federal, state or local legislation. Such is the case, for example, of the measures that need to be implemented in urban areas designated as non-attainment for ozone or carbon monoxide [CAAA, 1990] [ISTEA, 1991].

The effect of many congestion management measures, particularly those dealing with improved traffic control, is essentially local. For example, signalized intersections typically affect traffic flow within a 0.1-0.2 mi radius [Reilly, Gardner, and Kell, 1976]. However, most existing techniques to quantify the performance of congestion management measures are targeted at relatively long segments and corridors. For example, the Highway Capacity Manual (HCM) [TRB, 1994] recommends using long segments (at least 1 mi long in downtown areas and at least 2 mi long in other areas) for computing average speeds on arterial streets. This level of resolution makes it very difficult to evaluate local effects accurately. It also indicates a need for the development of improved procedures to document localized conditions effectively.

Travel Time as a Performance Measure

Over the years, departments of transportation nationwide, city traffic engineering offices, and other agencies have developed various performance measures to quantify congestion. Commonly used performance measures are level of service (LOS), v/c ratio, delay, and travel time/speed. However, other performance measures are also used, including vehicle occupancy, lane occupancy, queue duration, and duration of peak period. In a survey conducted by Lomax et al. [1995] on more than 450 government agencies nationwide, approximately 90% of respondents acknowledged using LOS to quantify congestion. By comparison, only 19% of respondents acknowledged using delay, and only 13% of respondents acknowledged using travel time/speed. The degree of satisfaction with these performance measures was completely different, though. Only 9% of respondents considered LOS to be an appropriate performance measure. In contrast, 31% of respondents considered delay to be appropriate, and 24% of respondents considered travel time/speed to be appropriate. Interestingly, only 18% of respondents acknowledged having travel time data collection programs. Inadequate staffing and budget constraints were two of the main reasons cited for travel time data collection not to be used more frequently .

According to Lomax et al. [1995], an appropriate performance measure should be easy to understand; unambiguous, accurate, and consistent; applicable across modes of transportation; flexible to describe different geographic and time settings; able to assess existing and future conditions; and relatively inexpensive and easy to collect. HCM performance measures such as LOS are easy to understand by the professional transportation community, but not so much by the traveling public. HCM measures are

not well suited for multimodal comparisons. They require detailed, site-specific input data which can be difficult and expensive to obtain. In some cases, they use complex models which, unfortunately, tend to be rather limited in their functionality. Finally, HCM measures are difficult to use for long-range comparisons because concepts such as capacity and speed-flow rate relationships tend to change over time [HRB, 1950] [HRB, 1965] [TRB, 1985] [TRB, 1994].

In contrast, travel time-based measures are easy to understand by both the professional transportation community and the traveling public. They are flexible enough to describe traffic conditions at various levels of resolution both in space and time. This makes travel time-based measures appropriate for handling specific locations as well as entire corridors. It also allows analysts to perform comparisons over long periods of time, say years or decades. Travel time-based measures translate easily into other measures like user costs, and can be used directly to validate planning models such as travel demand forecasting models [Laird, 1996]. Travel time-based measures are applicable across modes. So important is travel time in this regard that the year 2000 edition of the HCM is being structured around travel time as a common measure of effectiveness for all modes [JHK, 1996]. All these reasons make travel time-based measures extremely powerful, versatile, and desirable.

Travel Time Data Collection Techniques

Two techniques have traditionally been used to measure travel time: the license plate technique, and the floating car technique [May, 1990] [Robertson, 1994]. With the automation provided by computers and other electronic devices, additional techniques have emerged over the years, including automatic vehicle identification (AVI), automatic

vehicle location (AVL), cellular phone tracking, and video imaging [Liu and Haines, 1996] [Turner, 1996]. For convenience, these techniques can be grouped into two categories: roadside techniques and vehicle techniques.

Roadside Techniques

These techniques are based on the use of detecting devices physically located along the study routes at pre-specified intervals. They obtain travel time information from vehicles traversing the route by recording passing times at predefined checkpoints. Examples of these techniques include license plate matching and AVI. License plate matching is based on recording of the license plate number of individual vehicles and the corresponding time stamps as they pass checkpoints (Figure 2-2). Travel times are determined as differences in time stamps between checkpoints. An assumption of this technique is that each individual vehicle does not make intermediate stops. This may be limiting, particularly if there are intersections, on-ramps, off-ramps, or interchanges between checkpoints.

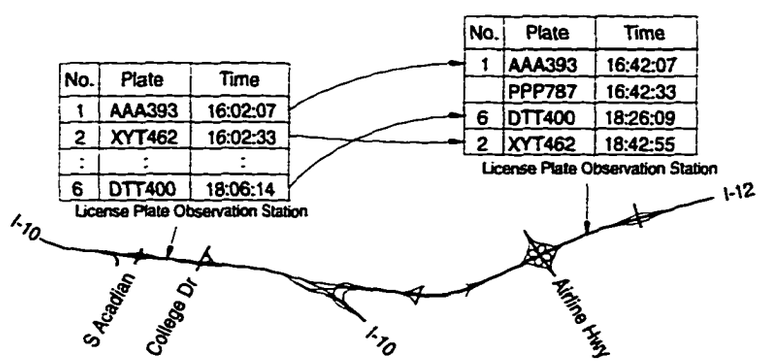

Figure 2-2: License plate travel time example

Computer vision video-based systems are now being developed to automate this technique. They reduce the amount of field manual work, but still do not provide an

accurate measurement of behavior between checkpoints. In addition, these automated systems tend to be quite expensive. For example, the video recording equipment for a single observation station could cost nearly $3,000 [Liu and Haines, 1996] [Turner, 1996]. The corresponding data processing is estimated to cost around $50 per hour of video [Turner, 1996].

AVI is a technology that is now being used in several metropolitan areas both in the United States and abroad. AVI systems consist of in-vehicle transponders (or tags), roadside reading units, a communication network, and a central computer system. The roadside reading units detect individual vehicles equipped with transponders as they pass nearby and transmit the corresponding transponder data to the central computer system. Travel times between consecutive checkpoints are computed in a similar manner as with the license plate technique, except that transponder identification numbers are used to compare time stamps instead of vehicle license plate numbers. AVI systems are typically very expensive. For example, each roadside reader unit costs about $30,000 [Turner, 1996]. Because of this, distances between consecutive checkpoints tend to be large (1-5 mi) and, consequently, detecting localized problems becomes much more difficult. One advantage of AVI technology is that area-wide real-time travel time data collection and dissemination are possible. With Internet tools, for example, cities like Houston, Chicago, and Seattle are using AVI technology to disseminate up-to-date geo-referenced travel time and speed data to the traveling public.

Vehicle Techniques

These techniques are based on the use of detection devices carried inside the vehicle. Examples of these techniques include the traditional floating car technique,

AVL, and cellular phone tracking. In the floating car technique, a single probe vehicle is driven with the traffic flow, i.e., passing as many cars as cars pass the probe vehicle. Travel time and passage of specific landmarks are recorded along the route. In the traditional approach, two people, usually technicians, are required in the car: one of them to drive the vehicle, and the other one to manually record the location and time of individual checkpoints, and the length and time spent in queues. Figure 2-3a shows a typical form used to record these data. The level of accuracy obtained with this technique varies from technician to technician. Realistically, technicians can log checkpoint data if the distance between contiguous checkpoints is at least 0.25 mi [Benz and Ogden, 1996]. With this level of resolution only average speeds can be calculated. At any level of resolution, queue information is highly subjective because it depends on the technician's estimation of queue lengths. In addition to this, problems such as missing checkpoints or inaccurately marked checkpoints are common.

The floating car technique is one of several techniques grouped under the general names of test vehicle techniques [May, 1990], moving vehicle [Robertson, 1994], or moving observer techniques [Taylor, Young, and Bonsall, 1996]. In the general case, a probe vehicle is used to measure both travel time and other data such as flow rates, vehicle-miles, and time spent in queues. Flow rates are used, among other things, to refine observed travel time values when the number of vehicles passed by the probe vehicle is not the same as the number of vehicles that pass the probe vehicle. Figure 2-3b shows a form typically used to collect travel time data using the moving vehicle technique.

(a) Average vehicle technique[1]

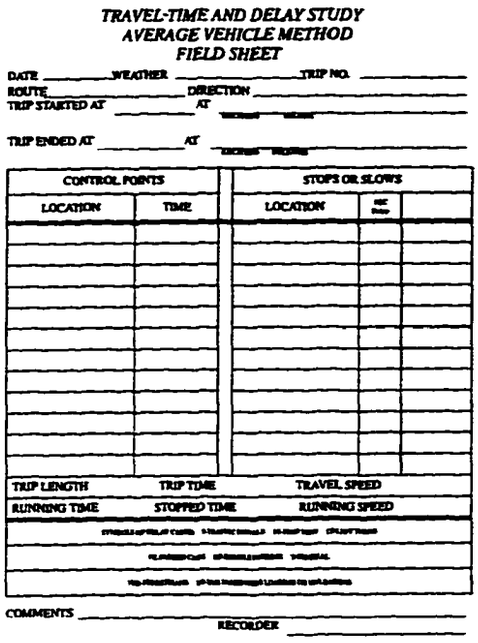

TRAVEL-TIME AND DELAY STUDY
AVERAGE VEHICLE METHOD
FIELD SHEET

DATE _____ WEATHER _____ TRIP NO. _____
ROUTE _____ DIRECTION _____
TRIP STARTED AT _____ AT _____
TRIP ENDED AT _____ AT _____

CONTROL POINTS		STOPS OR SLOWS		
LOCATION	TIME	LOCATION		

TRIP LENGTH	TRIP TIME	TRAVEL SPEED
RUNNING TIME	STOPPED TIME	RUNNING SPEED

COMMENTS _____
RECORDER _____

(b) Moving vehicle technique

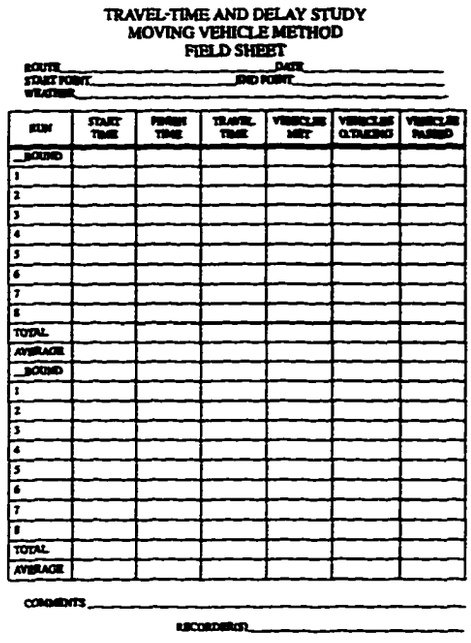

TRAVEL-TIME AND DELAY STUDY
MOVING VEHICLE METHOD
FIELD SHEET

ROUTE _____ DATE _____
START POINT _____ END POINT _____
WEATHER _____

RUN	START TIME	FINISH TIME	TRAVEL TIME	VEHICLES MET	VEHICLES OVERTAKING	VEHICLES PASSED
_____BOUND						
1						
2						
3						
4						
5						
6						
7						
8						
TOTAL						
AVERAGE						
_____BOUND						
1						
2						
3						
4						
5						
6						
7						
8						
TOTAL						
AVERAGE						

COMMENTS _____
RECORDER(S) _____

[1] The average vehicle technique is similar to the floating car technique. In the average car technique, the car travels according to the driver's perception of the average speed of the traffic stream [Robertson, 1994]

Figure 2-3: Forms used by technicians to manually log travel time data (Source: Robertson [1994])

To improve accuracy in estimating flow rates, a second vehicle driving in the opposite direction can be used to count the number of vehicles traveling in the same direction as the first probe vehicle. Notice, however, that using a second vehicle adds to the total cost of the travel time study. Having only one vehicle drive both directions of travel could result in some savings but, unfortunately, the trade off is a decrease in accuracy because counts in both directions of travel are not made simultaneously [Taylor, Young, and Bonsall, 1996]. Also, counting vehicles traveling in the opposite direction while driving is feasible only for low to moderate volumes. This is clearly not the case of most urban congested areas. Furthermore, all portions of the opposing segment must be visible. For this reason, probe vehicles are generally used to measure travel time only. In

general, an effort is made to pass as many cars as cars pass the probe vehicle. Under congested conditions, this is relatively easy to accomplish as speed variation by lane is usually very low. During non-congested conditions, speed variation by lane may be quite significant. In this case, approximately average speeds can be obtained by driving in the middle lane [May, 1990].

With a manual travel time data collection technique like the floating car technique it is possible to obtain link-based speed-distance profiles and cumulative travel time-distance profiles (Figure 2-4a). Nowadays, distance measuring instruments (DMIs) can be attached to the vehicle's transmission to automatically record distance, time and speed. These devices enable the production of more detailed distance-time profiles (Figure 2-4b). When using DMIs, only one technician is needed in the probe vehicle. In some models, it is even possible to store route and checkpoint location in memory to avoid some of the problems associated with missing or inaccurately marked checkpoints. However, DMIs are not free of difficulties. For example, Benz and Ogden [1996] reported a need for weekly calibrations of the probe vehicles and constant verification of the vehicles' tire pressure (an incorrect tire pressure provides inaccurate speed and distance readings). This indicates the vehicle dependence of the DMI approach. In addition to this, DMIs tend to be relatively expensive. Including a notebook computer for data storage, each unit costs about $2,000.

AVL is a generic term that groups several techniques that use receivers or transmitters on-board to determine vehicle location (in latitude and longitude) and speed. Examples of these techniques are ground-based radio navigational systems and GPS. GPS is particularly advantageous because it does not need receiving towers on the ground

as traditional radio navigational systems do. One of the significant advantages of AVL compared to other techniques is that traffic monitoring is network and driver independent. This makes AVL suitable for many applications, including tracking the motion of special-purpose probe vehicles and entire fleets. When used with single probe vehicles, AVL systems are usually configured so that data are collected and stored on board, and then post-processed in the office. When used with entire fleets, AVL systems are usually configured so that data are collected and transmitted via radio or cellular phone to a central location where they are immediately processed. AVL costs vary widely depending on the particular application, but in general, they range from $1,000 to $4,500 per vehicle [Turner, 1996].

(a) Speed-distance and time-distance profiles using a manual data collection technique

(b) Distance-time profile using a DMI

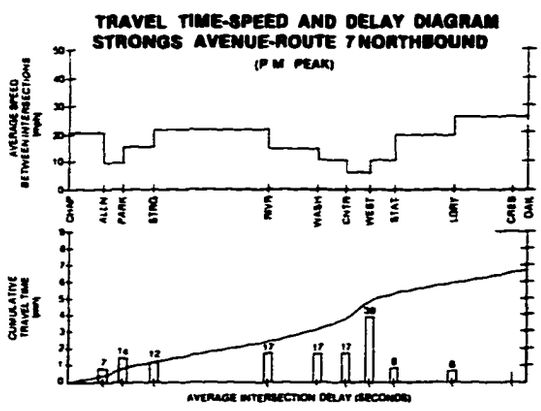

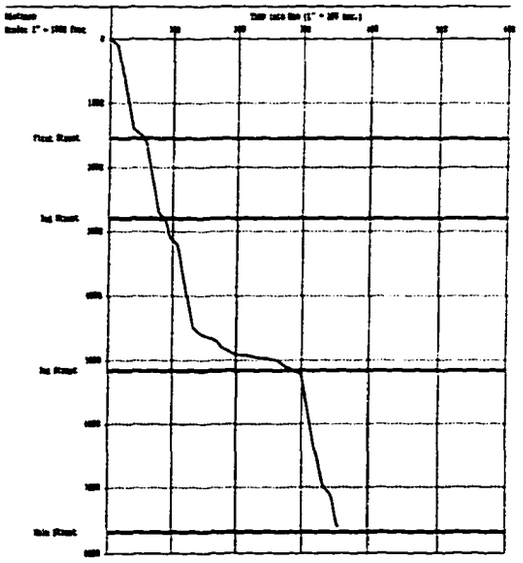

Figure 2-4: Traditional reporting of travel time data (Source: Robertson [1994])

Cellular phone tracking is an experimental technique that involves locating cellular phones that are being used by motorists on the road. Geolocation is done using

cellular phone tower triangulation methods and techniques involving differences in signal time of arrival to those phone towers. Cellular phone tracking systems are increasingly being used because the use of cellular phones among motorists is also increasing [Turner, 1996]. Total costs are expected to be relatively low because private motorists can more easily absorb the cost of using their cellular phones. However, system operation is highly dependent on the motorists' willingness to use their cellular phones when they cross pre-specified checkpoints. Overall, cellular phone systems appear to be more feasible for reporting traffic incidents.

Comparison of Techniques

Table 2-1 is a summary of characteristics and applicability of the travel time data collection techniques described previously. Roadside techniques are obviously infrastructure dependent, as opposed to vehicle techniques. Roadside techniques have lower levels of resolution and accuracy than vehicle techniques. However, vehicle techniques, specifically those based on DMIs and AVL, are generally based on a limited number of probe vehicles, which means that area wide coverage is limited. This makes roadside techniques (specifically AVI) better suited for daily or real-time monitoring. In contrast, vehicle techniques are best for determining initial conditions and for annual monitoring.

In practice, most travel time studies are made using vehicle techniques. Many government agencies use DMIs. However, as mentioned before, DMIs are not exactly error free. For this reason and because of budgetary constraints, many other agencies still conduct their travel time studies with the traditional two-people clipboard and stopwatch approach. Not surprisingly, runs made during most travel time studies tend to be

extremely low in number and subject to significant accuracy problems [Laird, 1996] [CUTR, 1996]. Consequently, there is a need to develop automated procedures that reduce data collection and data reduction errors, and that increase productivity. Such procedures would result in an increased number of runs in travel time studies so that a statistically significant amount of data could be obtained with little effort [Laird, 1996].

Table 2-1: Comparison of travel time data collection techniques (adapted from Liu and Haines [1996] and Turner [1996])

Criteria	Travel Time Collection Technique					
	Roadside techniques			Vehicle techniques		
	License plate matching		AVI	DMI	AVL	Cellular phone
	Traditional	Video				
Characteristics:						
Infrastructure dependent	yes	yes	yes	no	no	no
Travel time/speed resolution	low	low	low	high	high	unknown
Travel time/speed accuracy	good	good	good	good	very good	unknown
Area wide coverage	low	low	very good	low	low	unknown
Technology status	proven	being tested	proven	proven	proven[1]	being tested
Capital costs	low	high	high	low	low to mod.	mod. to high
Operating costs per unit	moderate	moderate	low	high	low to mod.	low to mod.
Applicability:						
Annual monitoring	yes	yes	yes	yes	yes	yes
Daily monitoring	limited	limited	yes	limited	limited	limited
Real-time travel information	limited	limited	yes	no	yes	limited
Incident detection	limited	limited	yes	limited	limited	yes

[1] GPS is a proven technology. However, its applicability to travel time studies has been limited until recently.

Travel Time Studies with GPS

GPS is a positional and navigational system developed and operated by the US Department of Defense. Its main component is a constellation of 24 satellites that broadcast signals that provide data on their position and trajectory. For strategic military reasons, those signals may be subject to a random intentional degradation process known as selective availability (SA) [Leick, 1995]. When SA is disabled, horizontal positional accuracy on the ground may vary from a few millimeters to tens of meters, depending on the GPS receiver used. When SA is enabled, an additional random error is added to the

satellite signal which results in the horizontal positional accuracy on the ground to degrade to about 100 m (two sigmas) [Leick, 1995]. In practice, this limitation can be bypassed by operating two GPS receivers simultaneously (one mobile and the other one stationary) and by using the data collected with the stationary unit to differentially correct the data collected with the mobile unit. This correction process is termed differential because differences between the true coordinates of the stationary unit location (determined previously following established surveying and/or geodetic standards) and the coordinates read with the stationary unit are used to correct the coordinates read with the mobile unit. The differentially corrected GPS points are then called DGPS points.

It may be worth noting that the US Government intends to discontinue the use of SA over the next 10 years [OSTP, 1996]. If SA is phased out, the intentional degradation of the GPS signal will disappear. However, this does not necessarily mean that differential correction will become superfluous. With current technology, GPS positional accuracy is usually higher with differential correction than without differential correction, even when SA is disabled. For example, the positional accuracy of a GPS receiver such as the Trimble GPS Placer 400 is 2-5 m spherical error probability (SEP) when using differential correction, even if SA is enabled. By comparison, the positional accuracy of the same receiver without differential correction is around 25 m SEP when SA is disabled [Trimble, 1993]. The reason for this is that differential correction techniques can also substantially reduce the effect of a number of non-SA-related errors including satellite errors (atomic clock errors, frequency offsets, and hardware delay) and atmospheric errors (mainly ionospheric errors) [Leick, 1995] [Sandlin, McDonald, and Donahue, 1995].

Obviously, as accuracy increases so does cost, as shown in Figure 2-5. With the floating car technique, only one probe vehicle is needed to characterize traffic flow along a specific direction of travel. As a result, it is sufficient to use GPS receivers having a positional accuracy of around 2-3 m. Including differential correction and a laptop computer for data storage, such receivers now cost less than $2,000. This makes GPS data collection price competitive with other techniques such as those based on the use of DMIs. Actually, GPS receivers are much more versatile than DMIs because they can also be used for other purposes such as sign inventories, fleet tracking, and origin-destination (O-D) studies. In contrast, DMIs are good for just one thing: measuring distances along pre-specified routes.

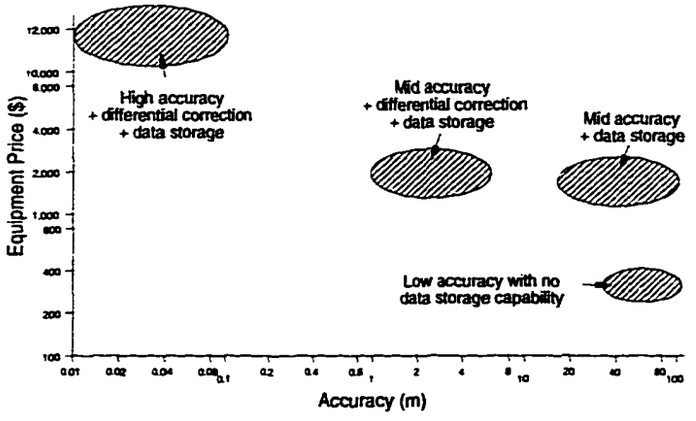

Figure 2-5: Relationship between GPS equipment cost and positional accuracy (adapted from Advanstar [1996])

However, GPS receivers only produce a tabular log of time and speed values at various latitude and longitude locations (Table 2-2). In practice, GPS data files (and DMI files, for that matter) tend to have huge numbers of records. This poses a serious data management problem. For example, collecting GPS data every one second translates to

3,600 position and speed records per hour. This number is then multiplied by the number of hours a particular run takes to complete and by the number of runs on all routes considered. A possible solution is to keep only travel time information between specific checkpoints along the corridor. However, this approach is valid only when total travel time data are of interest and when local variations in traffic behavior are not of concern. Moreover, because only a handful of travel time data points are actually used, it is reasonable to expect the accuracy of the results to closely resemble those of the traditional, manual floating car technique.

Table 2-2: Example GPS data

Time (s)	Latitude (°)	Longitude (°)	Speed (mph)
7:02:19	30.4079608	-91.1860431	33.4
7:02:20	30.4080936	-91.1860955	34.4
7:02:21	30.4081597	-91.1861196	33.2
7:02:22	30.4083609	-91.1861840	32.8
7:02:23	30.4084293	-91.1862008	32.7

Another solution is to keep all the GPS points and build detailed speed-time or speed-distance profiles along corridors (Figure 2-6) [Harding et al., 1996] [Guo and Poling, 1995] [Zito, D'Este, and Taylor, 1995]. For visualization purposes, the procedure is usually augmented with the display of GPS points on maps containing corridors and other geographic features. Because one gets a very detailed and rich picture of the traffic situation [Harding et al., 1996], the solution is suitable for detecting local variations in traffic behavior. However, it overlooks the inevitability that traffic may vary greatly from one day to the next both in space and time. For example, at specific locations in the I-10&I-12 corridor in Baton Rouge it is not unusual to observe speed differences of 30 mph or more from one day to another during the same time period (Figure 2-6). This means

that keeping all GPS data for analysis may actually become counterproductive and some kind of aggregation may be both desirable and necessary. The next chapter describes the spatial model developed to allow this aggregation.

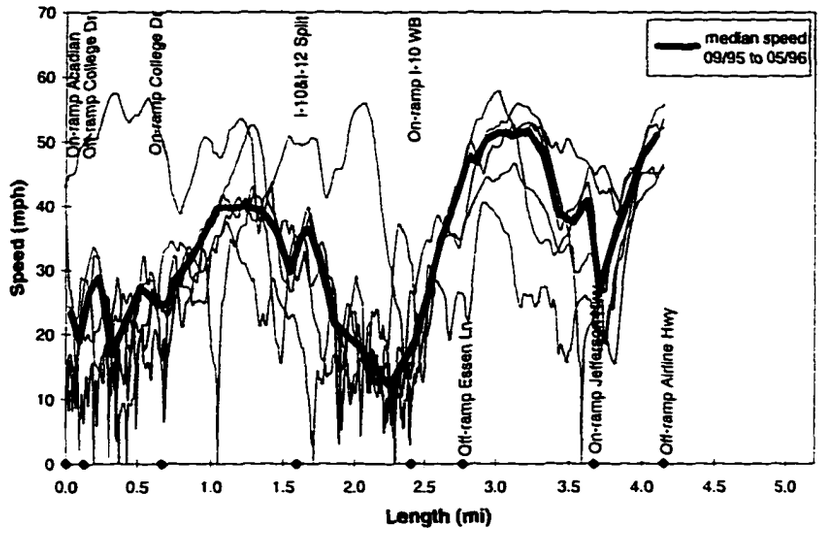

Figure 2-6: Speed-distance profiles using GPS data on the I-10 & I-12 corridor east bound (EB) in Baton Rouge (September 1995 - May 1996, 4:30 - 5:30 pm)

Chapter 3
SPATIAL MODEL

This chapter discusses a spatial model used to map GPS point data to highway segments and the mathematical model developed to aggregate GPS travel time and speed data into highway segment travel time and speed data. As shown in Table 2-2, GPS receivers record time, location (latitude, longitude), and speed. GPS receivers do not record location as cumulative distances along paths. Rather, they record location as longitude, latitude pairs. As a result, additional tools are required to provide a linear reference to these point locations. Fortunately, this linear referencing can be created quite easily with the help of GIS tools. During the linear referencing process, travel time data can be extracted and entered into existing geographic databases. This is a significant benefit of the GPS approach, more so if one considers that most municipalities already have or are in the process of implementing geographic databases to manage everything from land use to highway networks to traffic signals.

Base Map Preparation Procedure

In conducting travel time studies with GPS and GIS, the first step is to obtain a good base vector map with links to a database. One approach is to use digitized quad maps or TIGER files, but such maps provide only a crude representation of the corridors and their surroundings. Most existing digital maps were developed for area-wide planning purposes at a time when the need to provide an accurate representation of geographic features was not evident. In many cases, for example, highway interchanges

were represented by single straight lines or by lines connecting bi-directional vector elements. As a result, when GPS points are displayed on GIS maps containing this kind of features, the offset between GPS points and the physical discontinuity features is usually quite significant. For example, Figure 3-1a and Figure 3-1b show two samples of maps normally used in Baton Rouge to represent the I-10 corridor between Acadian and College Drive. For comparison purposes, Figure 3-1c shows a digital representation of the same area based on GPS data. Notice that the offset of some of the physical discontinuities indicated in the first two maps (Figure 3-1a and Figure 3-1b) with respect to the actual location of these physical discontinuities (Figure 3-1c) is quite large: between 0.1 and 0.2 miles. This would also be the offset associated with GPS travel time data when trying to map these data to physical discontinuities such as those shown in Figure 3-1a or Figure 3-1b.

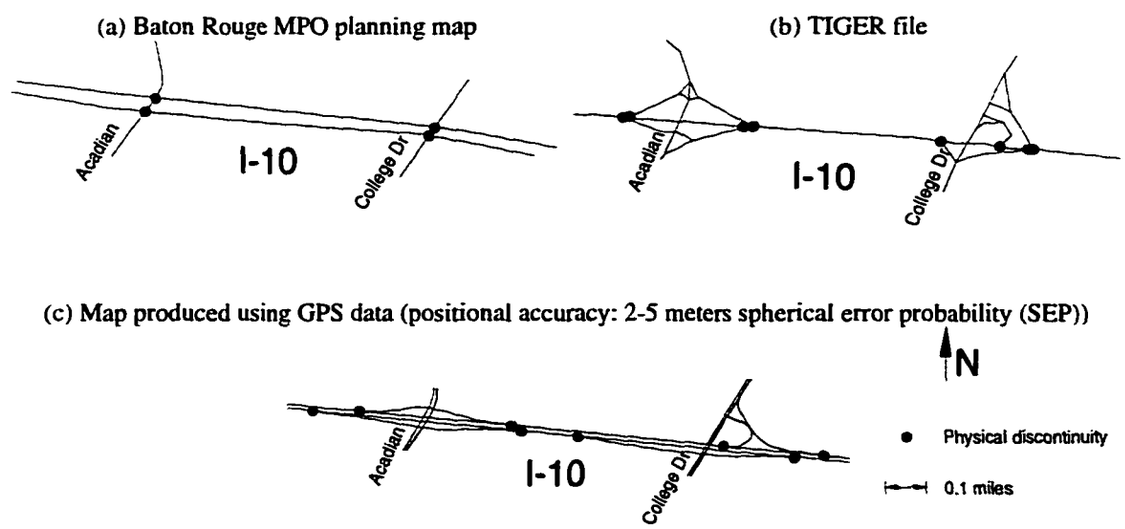

Figure 3-1: Digital representation of I-10 between Acadian and College Drive in Baton Rouge, Louisiana

For comparison purposes, Figure 3-2 illustrates some of the differences among GIS maps in the case of arterial streets. The dots represent major physical discontinuities (signalized intersections, on-ramps, and off-ramps) along the Florida Boulevard corridor. In the case of arterial streets, the problem of misplacement of physical discontinuity points still remains, although it tends to be smaller for signalized intersections than for interchanges. However, even if a signalized intersection is misplaced by only 0.03 mi (50 m) (compare the relative position of the Bon Marche Mall intersection with respect to the Lobdell intersection in Figure 3-2b and Figure 3-2c), this would be enough to map GPS points on the wrong side of the intersection. Another common problem is the absence or incorrect modeling of signalized intersections. For example, notice the absence of a high number of signalized intersections in Figure 3-2a. Notice also the incorrect modeling of the Bon Marche Mall and Wooddale Boulevard intersections in Figure 3-2b. As Figure 3-2c shows, the entrance to Bon Marche Mall is actually located on the north side of Florida Boulevard. Also, Wooddale Boulevard actually crosses Florida Boulevard.

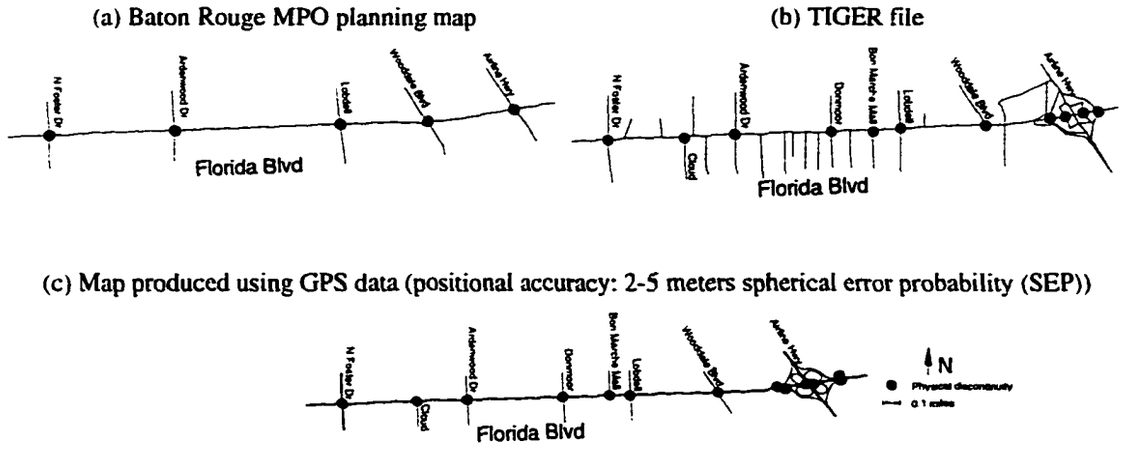

Figure 3-2: Digital representation of Florida Boulevard between North Foster Drive and Airline Highway in Baton Rouge, Louisiana

The offset between the GPS points and the linear graphical features can make the mapping process extremely difficult, particularly if the representation of physical discontinuities is as crude as that shown in Figure 3-1a and Figure 3-1b. To address this problem, some applications allow users to manually select individual GPS points to estimate travel time between checkpoints [Zito, D'Este, and Taylor, 1995] [Gallagher, 1996]. Other applications include the use of shape matching algorithms [Roden, 1996] which are used to "distort" or fit GPS points to network features based on the identification of corners and curves in the GPS data. Included in these algorithms are maximum allowed displacements so that users have some control regarding which GPS points can be linked to the linear graphical features. The percentage of GPS points rejected depends primarily on whether differential correction is used and how inaccurate the underlying GIS map is. This percentage can be quite significant, possibly as high as 20-30% [DeVivo, 1997]. Obviously, using DGPS data instead of uncorrected GPS data can help to reduce this percentage. But the question of whether using highly inaccurate GIS maps is really practical or convenient still remains.

It is possible to reduce the level of sophistication and demand for shape matching algorithms by developing alternative, GPS-derived network maps for processing GPS travel time data. Because most GIS packages are based on relational database models, attribute tables can be easily constructed to relate the new GPS-derived links to the original, inaccurate links. This is a one-time operation that actually makes the best use of two different scenarios. First, accurate GPS-derived maps can be used right now, despite the fact that most planning organizations may still be using their "inaccurate" maps for quite some time, say 5 to 10 years. And second, with the advent of GIS, GPS-derived

maps may very well provide the foundation for the next generation of planning models. If so, travel time data collected and processed today with the GPS-derived maps will still be available for use in the future without major changes.

Building a GPS-derived map requires surveying both directions of travel, as well as on-ramps, off-ramps, interchanges, and signalized intersecting streets (Figure 3-3a). The resulting GPS data are then imported into a GIS map to create a directional centerline network map (Figure 3-3b). Because this base map is constructed directly from GPS data, GPS data collected during future travel time studies are guaranteed to match the vector base map.

Traditional travel time studies record travel time and average speed between checkpoints along study routes. Checkpoints in the GIS map can be formalized using the following rules [Quiroga and Bullock, 1996]:

1. Establish checkpoints at all physical discontinuities such as signalized intersections, significant unsignalized intersections, lane drops, on-ramps, and off-ramps (Figure 3-3c).
2. Segment sections of road between physical discontinuity checkpoints so that there are nominally n checkpoints every mile. Figure 3-3d illustrates how the relatively large distances between exit and entrance ramps are segmented to create intermediate checkpoints.
3. Link each of the discrete segments to a relational database by assigning unique identification numbers to each segment. For example, segment 12444 in Figure 3-3e always represents the section of I-10 east bound (EB) immediately before the I-10 & I-12 split. Similarly, segment 12478 in Figure 3-3e always represents the segment of

I-12 EB immediately after the interchange from I-10 west bound (WB). By creating these unique identifiers, each segment can have fixed data associated with it, including number of lanes and posted speed limit. These identifiers can also be used to index travel time data from travel time studies performed on different dates and times. Details of the relational database schema used in this dissertation are discussed in Chapter 5.

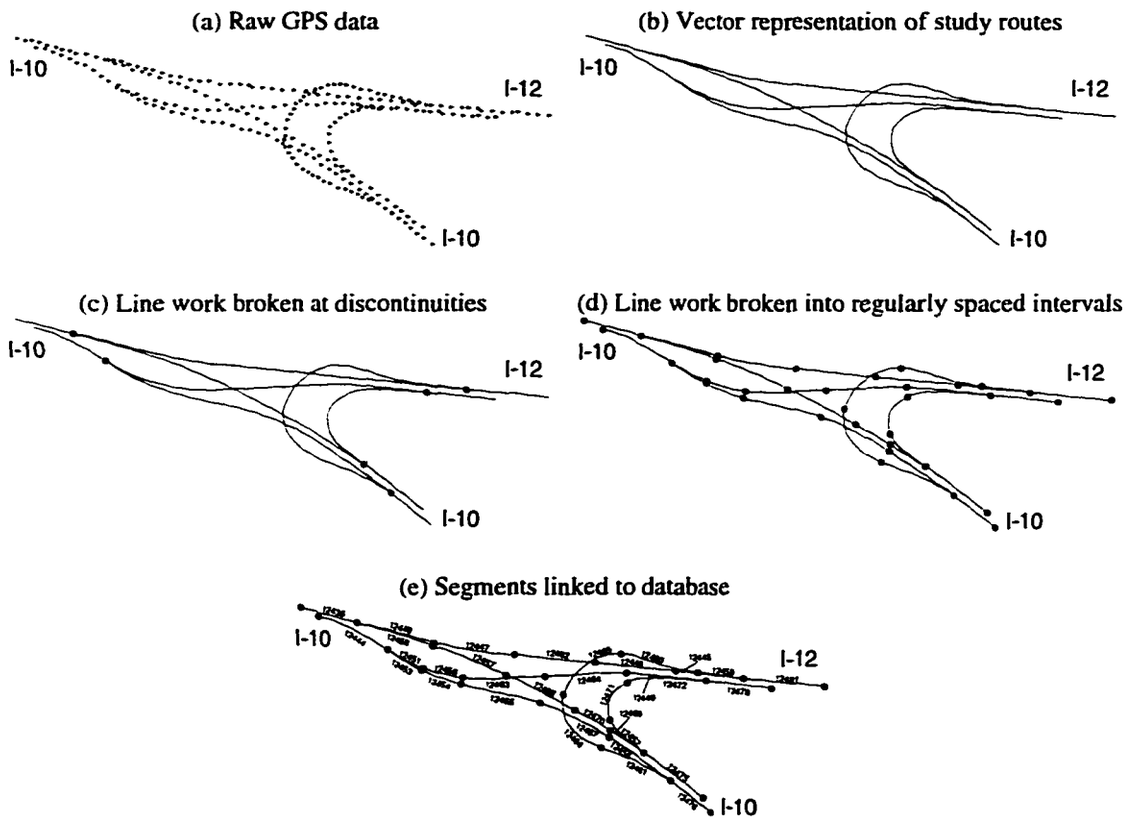

Figure 3-3: Sample network map geocoding and segmentation of the I-10 & I-12 split in Baton Rouge, Louisiana

Theoretically, the number of checkpoints per mile, n, can be set at any value. In practice, it is necessary to balance the need for accuracy, the need to derive meaningful

information from GPS-derived travel time data, and the need to develop a consistent procedure. During the data reduction process, GPS travel time and speed data are converted into segment-wise travel time and speed information. To minimize the error associated with the new aggregated values, the original GPS travel times and speeds should be as uniform as possible. This can be accomplished by limiting the number of GPS points that can be linked to any particular segment. At the same time, however, the number of GPS samples per segment should be large enough to ensure statistical significance. In practice, this means defining a balance between sampling rate, segment length, and vehicle speed.

Table 3-1 shows the maximum number of GPS points that could be associated with a segment for various combinations of segment length and speed. Assuming GPS data every 1 second (most low and moderately priced GPS receivers have a maximum sampling rate of 1 Hz), the values shown also indicate the travel time associated with a segment for each segment length-vehicle speed pair. For example, the maximum number of GPS points that could be associated with a 0.20-mile segment while traveling at 45 mph would be 16. This would also be the corresponding segment travel time in seconds.

Table 3-1: Maximum number of GPS points per segment, assuming GPS data every one second (values also represent segment travel time in seconds)

Segment length (mi)	Probe vehicle speed (mph)				
	25	35	45	55	65
5.0	720	514	400	327	276
2.0	288	205	160	130	110
1.0	144	102	80	65	55
0.5	72	51	40	32	27
0.2	28	20	16	13	11
0.1	14	10	8	6	5
0.05	7	5	4	3	2
0.02	2	2	1	1	1
0.01	1	1	-	-	-

Lower sampling rates, which involve using time intervals larger than 1 second, would result in a lower number of GPS points per segment. The minimum sampling rate is that which allows at least one GPS point to be associated with a segment. Following well established spatial sampling theory principles [Tobler, 1987], this is possible only if the time interval between consecutive GPS points is at most half the segment travel time (Table 3-2a). For example, if the travel time resulting from traveling at 45 mph on a 0.20-mile segment is 16 seconds (Table 3-1), the largest time interval between consecutive GPS points would have to be 8 seconds (Table 3-2a). In practice, it is recommended to set the time interval at about one fifth the segment travel time to allow for imperfections in the data collection process [Tobler, 1987]. This means, in the case of the example discussed above, that the largest time interval between consecutive GPS points would have to be around 3 seconds (Table 3-2b) instead of 8 seconds. Notice in Table 3-2b that, as long as GPS data are collected every one second, the shortest segment length which would be able to handle speeds ranging from 25 to 65 mph is 0.1 miles. Shorter segment lengths would increase the risk of leaving segments without any GPS data.

Table 3-2: Largest time interval between consecutive GPS points

(a) Time interval = 1/2 segment travel time

Segment length (mi)	Probe vehicle speed (mph)				
	25	35	45	55	65
5.0	360	257	200	164	138
2.0	144	102	80	65	55
1.0	72	51	40	32	28
0.5	36	26	20	16	14
0.2	14	10	8	6	5
0.1	7	5	4	3	2
0.05	4	2	2	1	1
0.02	1	1	-	-	-
0.01	-	-	-	-	-

(b) Time interval = 1/5 segment travel time

Segment length (mi)	Probe vehicle speed (mph)				
	25	35	45	55	65
5.0	144	103	80	65	55
2.0	58	41	32	26	22
1.0	29	20	16	13	11
0.5	14	10	8	6	5
0.2	6	4	3	3	2
0.1	3	2	2	1	1
0.05	1	1	1	-	-
0.02	-	-	-	-	-
0.01	-	-	-	-	-

Computation of Segment Travel Time and Speed

To illustrate how GPS data are used to compute segment travel time and speed data, Figure 3-4 shows an enlarged diagram of Figure 3-3e. Example GPS point data are overlaid along a section of I-12 WB that merges with I-10 WB. The GPS Point Data table shows that the vehicle entered segment 12447 at 8:30:01 am, then segment 12448 at 8:30:11 am, and finally segment 12436 at 8:30:21 am. The Segment Aggregated Data table shows net travel times through segments 12447, 12448, and 12436. That table also tabulates the corresponding average vehicle speed values. It is these two values: travel time and average speed that are the important summary statistics.

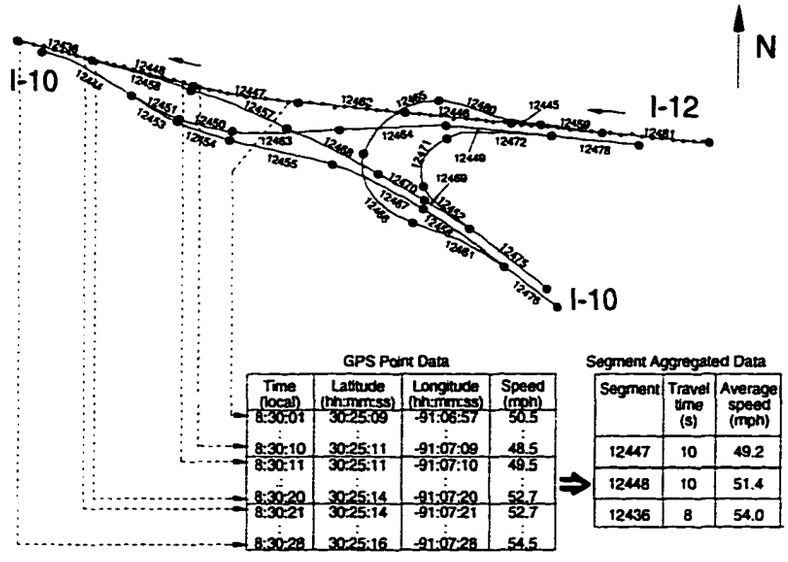

Figure 3-4: GPS data mapping onto highway segments

To efficiently transform the GPS point data into segment travel times and average speeds, it is necessary to develop a systematic procedure. Figure 3-5 shows the time-distance diagram of the probe vehicle as it traverses a segment of length L. The dots represent GPS data points. The GPS equipment in the probe vehicle receives information

from the constellation of satellites on a continuous basis and computes coordinates and speed values.

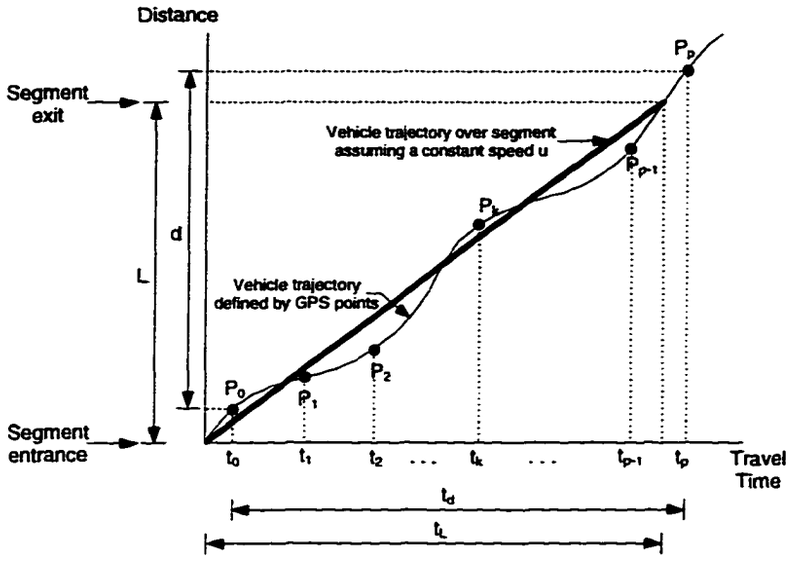

Figure 3-5: Time-Distance diagram for GPS points on a segment

Consider a procedure that defines the points that can be associated with the segment by searching the closest points to the segment entrance and exit. Since GPS points can occur anywhere along the segment, it is very unlikely that the cutoff points will coincide with the segment entrance and exit points. This is illustrated in Figure 3-5 with GPS points P_0 and P_p. P_0 is closest to the segment entrance (detected when selected the previous segment), and P_p is closest to the segment exit. Segment travel time and average speed could be obtained by interpolating the time stamps of the two GPS points located immediately before and after the segment entrance, and the time stamps of the two GPS points located immediately before and after the segment exit. However, in order to perform a time interpolation, the location of the GPS points involved is also needed. Because of uncertainties regarding the effect of GPS point positional errors on the

computation of segment travel time and speed (see Appendix A), an alternative procedure, based on GPS speeds, was developed. This procedure bypasses the need for interpolation.

The alternative GPS speed procedure is based on the assumption that the GPS receiver used for the travel time study has the capability to record speeds in addition to coordinates and time. For the procedure to work properly, it is necessary that the GPS receiver compute speeds independently of position fix calculations by using fairly standard formulations based on pseudorange data (distance from satellite to receiver) and pseudorange rate data. A receiver such as the Trimble GPS Placer 400 complies with this requirement (according to information provided by telephone by Trimble officials). For speed computations, the receiver polls satellite data for a fraction of a second and, as a result, the computed speeds are almost instantaneous. In the case of the Trimble GPS Placer 400, which was the receiver used for this research, the specified accuracy of speed measurements was 0.1 mph (1 sigma) [Trimble, 1993].

In Figure 3-5, let the instantaneous speeds associated with points P_0 to P_p be v_0 to v_p, respectively. The total distance covered by the probe vehicle between t_0 and t_p is

$$d = \int_{t_0}^{t_p} v\,dt \approx v_0\left(\frac{t_1 - t_0}{2}\right) + \left[\sum_{k=1}^{p-1} v_k\left(\frac{t_{k+1} - t_{k-1}}{2}\right)\right] + v_p\left(\frac{t_p - t_{p-1}}{2}\right) \qquad (3\text{-}1)$$

The corresponding average speed u is

$$u = \frac{d}{t_d} = \frac{1}{t_d}\left\{v_0\left(\frac{t_1 - t_0}{2}\right) + \left[\sum_{k=1}^{p-1} v_k\left(\frac{t_{k+1} - t_{k-1}}{2}\right)\right] + v_p\left(\frac{t_p - t_{p-1}}{2}\right)\right\} \qquad (3\text{-}2)$$

where t_d is the travel time over the distance d. If GPS data are collected at regular time intervals Δt, equation (3-2) can be reduced to

$$u = \frac{\Delta t}{t_d}\left[\frac{v_0}{2} + \left(\sum_{k=1}^{p-1} v_k\right) + \frac{v_p}{2}\right] = \frac{1}{p}\left[\frac{v_0}{2} + \left(\sum_{k=1}^{p-1} v_k\right) + \frac{v_p}{2}\right] \tag{3-3}$$

If the variation of GPS speeds within the segment is small, v_0 should be very similar to v_p. In this case, equation (3-3) could be approximated to

$$u = \frac{1}{p}\sum_{k=1}^{p} v_k \tag{3-4}$$

Normally, the segment length L is known. If the initial and final GPS points associated with the segment are close to the entrance and exit points, respectively, d and L should be very similar. In this case, the mean speed u can be assumed to apply over the entire segment length and, as a result, the travel time t_L along the segment can be estimated as

$$t_L = \frac{L}{u} \tag{3-5}$$

If d and L are similar, t_d and t_L should also be similar.

Equations (3-2) and (3-5) are valid for a single run on a single segment and provide the necessary tools to transform a set of GPS point time stamp and speed values into a single pair of segment travel time and average speed values for the segment. In general, however, several runs involving several contiguous segments may be made [Robertson, 1994]. In this case, it may be of interest to compute not only speed values for individual segments due to individual runs, but also representative speed values for each segment and for all segments combined. To keep the discussion general, the number of runs per segment is assumed to be different. This is particularly important if there are interchanges or intersections along the route and some segments have more records than

other segments. Because of this, the procedure to compute representative speed values involves aggregating the data at the segment level first.

Let the number of runs (or sample size) per segment be m_i. The average travel time per segment is

$$\bar{t}_i = \frac{1}{m_i}\sum_{j=1}^{m_i} t_{L_j} = \frac{1}{m_i}\sum_{j=1}^{m_i}\frac{L_i}{u_{ij}} = L_i\frac{1}{m_i}\sum_{j=1}^{m_i}\frac{1}{u_{ij}} \tag{3-6}$$

where L_i is the length of each segment, and u_{ij} is the j^{th} speed record associated with segment i. Let the number of segments be n. The total distance L_T is

$$L_T = \sum_{i=1}^{n} L_i \tag{3-7}$$

The total travel time t_{T_L} over L_T is

$$t_{T_L} = \sum_{i=1}^{n}\left[L_i\frac{1}{m_i}\sum_{j=1}^{m_i}\frac{1}{u_{ij}}\right] \tag{3-8}$$

The average speed for all runs over L_T is

$$\bar{u}_L = \frac{L_T}{t_{T_L}} \tag{3-9}$$

Equation (3-9) can be rewritten as

$$\bar{u}_L = \frac{1}{\sum_{i=1}^{n}\left[\frac{L_i}{L_T}\frac{1}{m_i}\sum_{j=1}^{m_i}\frac{1}{u_{ij}}\right]} \tag{3-10}$$

This equation represents a weighted harmonic mean, where the weight is the ratio of the length of each segment to the total length considered. If all segments have the same length, the weight associated with each segment will be the same.

Notice that equations (3-8) and (3-10) are general in the sense that they can be used either for one or several runs, and either for one or several contiguous segments. To check their accuracy, an alternative formulation based on t_d values (Figure 3-5) is also provided. For m_i samples per segment and n segments, it can be shown that the total travel time t_{T_d} is

$$t_{T_d} = \sum_{i=1}^{n} \left[\frac{1}{m_i} \sum_{j=1}^{m_i} t_{d_j} \right] \tag{3-11}$$

An approximate value of the average speed for all runs is

$$\overline{u}_d = \frac{L_T}{t_{T_d}} \tag{3-12}$$

The methodology described above can be used to obtain travel time and speed for a variety of scenarios ranging from a single segment to an entire corridor, and from a single run to a complete set of runs. From a practical perspective, it is of interest to obtain and compare travel time data for various traffic conditions, including AM peak, off peak, and PM peak. Off peak travel time data can be used to define minimum travel time conditions. Travel time data from any other period can be compared with the off peak travel time data to compute travel delay. In this case, delay can be written as

$$d_t = t - t_m \tag{3-13}$$

where t_m is the minimum travel time, and t is travel time under any other traffic condition.

Strictly speaking, it is possible to define two types of minimum travel time conditions: (1) based on posted speed limits; and (2) based on "free-flow" driving patterns. Posted speed limits provide a fixed reference to define minimum travel times. Unfortunately, as often happens on freeways, drivers tend to exceed speed limits. This

would result in some delay values being negative. "Free-flow" driving patterns provide a better representation of the actual behavior of drivers both on freeways and on signalized streets. In the case of freeways, it represents what the drivers, on average, perceive as a comfortable speed to drive. In the case of signalized streets, it includes the combined effect of signal spacing and timing and other discontinuities on the road. In general, it is desirable to use both the speed limit and the "free-flow" approaches and compare the results. Depending on the circumstances, one might be considered better than the other one.

The expressions for travel time and delay described above depict the situation for a typical vehicle. Using count data, the total delay in vehicle-hours could be obtained as

$$d_T = n_c d_t \tag{3-14}$$

where n_c is the number of vehicles using the facility during a period of time T, which is related to the flow rate q by the expression

$$q = \frac{n_c}{T} \tag{3-15}$$

Combining equations (3-14) and (3-15),

$$d_T = qTd_t \tag{3-16}$$

For example, if T is the peak hour and q is the peak-hour flow rate, equation (3-16) gives the total delay in vehicle-hours for the peak hour.

Examples

To illustrate the use of this methodology, three examples with AM data collected in Baton Rouge during the Summer of 1995 are used. Table 3-3 shows a sample of travel time records (t_d and u) for selected segments. Figure 3-4 shows the location of the

segments considered. For completeness, two values of u are included: one obtained with equation (3-2), and the other one obtained with equation (3-4). The first example involves the computation of total travel time and average speed for a single run. The second example involves several runs. The third example involves entire corridors.

Example 1

Find individual travel time, total travel time, and average speeds for segments 12444, 12453, and 12454 on I-10 EB (Figure 3-4) using data from the August 13, 1995 run shown in Table 3-3.

Table 3-3: Sample of AM travel time and data associated with selected segments in Figure 3-4

Date	Segment Code	L (mi)	t_d (seconds)	u Eqn. (3-2) (mph)	u Eqn. (3-4) (mph)
06/25/95	12444	0.200	12.5	53.19	52.92
	12453	0.106	8.0	51.31	51.25
	12454	0.106	10.0	51.51	51.53
07/23/95	12444	0.200	11.0	60.90	60.86
	12451	0.104	7.0	58.58	58.52
	12450	0.104	5.5	58.89	59.08
	12463	0.200	12.5	60.48	60.64
	12464	0.200	11.5	62.18	62.21
07/25/95	12444	0.200	11.5	56.46	56.50
	12451	0.104	6.5	56.82	56.85
	12450	0.104	7.0	57.11	57.30
	12463	0.200	12.5	58.72	58.78
	12464	0.200	12.5	59.13	59.17
08/13/95	12444	0.200	11.5	61.20	61.27
	12453	0.106	6.0	60.03	59.94
	12454	0.106	7.0	58.60	58.38

Table 3-4 summarizes the computational procedure. For example, for segment 12444, using equation (3-1),

$$d = \frac{1}{3600}\left[\frac{61.1*2.0}{2} + \frac{61.3*4.0}{2} + \ldots + \frac{61.2*2.5}{2} + \frac{60.9*1.0}{2}\right] = 0.196 \text{ mi}$$

Using equation (3-2),

$$u = \frac{1}{11.5}\left[\frac{61.1*2.0}{2} + \frac{61.3*4.0}{2} + ... + \frac{61.2*2.5}{2} + \frac{60.9*1.0}{2}\right] = 61.20 \text{ mph}$$

Using equation (3-5),

$$t_L = 3600\left[\frac{0.200}{61.20}\right] = 11.76 \text{ s}$$

For segments 12453 and 12454, the corresponding u values are 60.03 mph and 58.60 mph (Table 3-3, Table 3-4). The corresponding t_L values are 6.36 and 6.51 seconds.

Table 3-4: Computation of travel time and speed for run of August 13, 1995

GPS travel time data			Segment		Equation (3-2) Procedure			Equation (3-4) Proc.		Equation (3-12) Proc.	
Time (AM)	Δt (sec)	Speed (mph)	Code	L (mi)	d Eqn (3-1) (mi)	u Eqn. (3-2) (mph)	t_L Ean. (3-5) (sec)	u Eqn. (3-4) (mph)	t_L Ean. (3-5) (sec)	u Eqn. (3-12) (mph)	t_d (sec)
6:26:51.3		60.5									
6:26:53.3	2.0	61.1									
6:26:55.3	2.0	61.3									
6:26:56.8	1.5	61.4									
6:26:57.8	1.0	61.4									
6:26:58.8	1.0	61.4									
6:27:59.8	1.0	61.3									
6:27:00.3	0.5	61.4									
6:27:01.8	1.5	61.2									
6:27:02.8	1.0	60.9	12444	0.200	0.196	61.20	11.76	61.27	11.75	62.61	11.50
6:27:03.8	1.0	60.5									
6:27:04.8	1.0	60.2									
6:27:06.3	1.5	59.8									
6:27:06.8	0.5	59.8									
6:27:08.8	2.0	59.4	12453	0.106	0.100	60.03	6.36	59.94	6.37	63.60	6.00
6:27:10.3	1.5	59.3									
6:27:11.3	1.0	59.5									
6:27:12.3	1.0	59.2									
6:27:14.8	2.5	57.2									
6:27:15.8	1.0	56.7	12454	0.106	0.114	58.60	6.51	58.38	6.54	54.51	7.00

Now, for segment 12444, using equation (3-4),

$$u = \frac{1}{9}[61.1 + 61.3 + ... + 61.2 + 60.9] = 61.27 \text{ mph}$$

For segments 12453 and 12454, the corresponding u values are 59.94 and 58.38 mph (Table 3-3, Table 3-4). The resulting t_L values are 11.75, 6.37 and 6.54 seconds. These values are practically identical to those obtained previously (11.76, 6.36, and 6.51

seconds). They also compare well with the measured values of t_d (11.5, 6.0, and 7.0 seconds, respectively), as shown in Table 3-3 and Table 3-4. Notice that the differences between t_L and t_d are less than one second, even though in relative terms they range from 2 to 6%. This is obviously due to the order of magnitude of the travel times considered.

Using now equation (3-12), the value of u_d for segment 12444 is

$$u_d = \frac{0.200 * 3600}{11.5} = 62.61 \text{ mph}$$

For segments 12453 and 12454, the corresponding values of u_d are 63.69 and 54.57 mph. In relative terms, the difference between these speeds and those based on equations (3-2) or (3-4) is still between 2 and 6%. However, in absolute terms, the three values of u_d do not compare well with those based on equations (3-2) or (3-4) . The first two values are higher while the third value is smaller. Inspection of the original GPS speeds (Table 3-4) reveals that the probe vehicle was gradually reducing speed as it traversed segments 12444, 12453, and 12454. The u values (61.20, 60.03, and 58.60 mph; or 61.27, 59.94, and 58.38 mph) confirms this trend.

If longer segments are used, or as more contiguous segments are considered, the difference between u_d and u_L and that between t_d and t_L should decrease. For example, for segments 12444, 12453, and 12454, the total length L is

$$L = 0.200 + 0.106 + 0.106 = 0.412 \text{ mi}$$

Using equation (3-8) results in

$$t_{T_L} = 3600\left[\frac{0.200}{61.20} + \frac{0.106}{60.03} + \frac{0.106}{58.60}\right] = 11.76 + 6.36 + 6.51 = 24.63 \text{ s}$$

for speeds computed with equation (3-2), or in 24.65 s for speeds computed with equation (3-4). By comparison, the total travel time using t_d values is

$$t_{T_d} = 11.5 + 6.0 + 7.0 = 24.5 \text{ s}$$

which is less than 1% different with respect to t_{T_L}. Now, using equation (3-9),

$$\bar{u}_L = \frac{0.412 * 3600}{24.63} = 60.22 \text{ mph}$$

or 60.17 mph when using 24.65 seconds instead of 24.63 seconds. By comparison,

$$\bar{u}_d = \frac{0.412 * 3600}{24.5} = 60.5 \text{ mph}$$

which is less than 1% different with respect to $\bar{u}_L$.

Example 2

Find the average travel time and speed for the freeway section defined by the following segments: 12444, 12451, 12450, 12463, and 12464. The number of segments n is 5. Using equation (3-7), the total length L is

$$L = 0.200 + 0.104 + 0.104 + 0.200 + 0.200 = 0.808 \text{ mi}$$

Using equation (3-8),

$$\begin{aligned} t_{T_L} = 3600 * \Bigg[& \frac{0.200}{4}\left(\frac{1}{53.19} + \frac{1}{60.90} + \frac{1}{56.46} + \frac{1}{61.20}\right) + \frac{0.104}{2}\left(\frac{1}{58.58} + \frac{1}{56.82}\right) \\ & + \frac{0.104}{2}\left(\frac{1}{58.89} + \frac{1}{57.11}\right) + \frac{0.200}{2}\left(\frac{1}{60.48} + \frac{1}{58.72}\right) + \frac{0.200}{2}\left(\frac{1}{62.18} + \frac{1}{59.13}\right)\Bigg] \\ = & 12.47 + 6.49 + 6.46 + 12.08 + 11.88 = 49.38 \text{ s} \end{aligned}$$

for speeds computed with equation (3-2), or 49.34 s for speeds computed with equation (3-4). Using equation (3-9),

$$\bar{u}_L = \frac{0.808 * 3600}{49.38} = 58.91 \text{ mph}$$

for speeds computed with equation (3-2), or 58.95 mph for speeds computed with equation (3-4). By comparison, when using equations (3-11) and (3-12),

$$t_{T_d} = \frac{12.5+10.97+11.5+11.5}{4} + \frac{7.0+6.5}{2} + \frac{5.5+7.0}{2} + \frac{12.5+12.5}{2} + \frac{11.5+12.5}{2}$$
$$= 11.62 + 6.75 + 6.25 + 12.5 + 12.0 = 49.12 \text{ s}$$

$$\bar{u}_d = \frac{0.808 * 3600}{49.12} = 59.21 \text{ mph}$$

Notice that differences in travel time and speed are around 0.5%.

Example 3

An extension of Example 2 is the computation of total travel time and average speed for entire corridors. These results are useful when measuring global corridor characteristics. As an example, consider all existing records for Baton Rouge between May and August, 1995 (7:00-8:00 am). Table 3-5 shows a summary of travel time and average speed values for each direction of travel on 21 corridors in Baton Rouge. Notice that the differences between t_{T_L} and t_{T_d}, and those between $\bar{u}_L$ and $\bar{u}_d$, are very small.

In the case of the Baton Rouge network (and the Shreveport and New Orleans networks), all segment speeds based on GPS speeds were computed using equation (3-4). As shown in Examples 1 and 2, this formulation produces good results most of the time because, in most cases, the variation of GPS speeds within a segment tends to be relatively small. Most results shown in Table 3-5 confirm this trend. However, in some cases, for instance when the probe vehicle approaches a signalized intersection, GPS speeds do vary greatly. For cases such as these, it may be advisable to use equation (3-2) instead of equation (3-4) to compute segment speeds. Current work involving extensions to the methodology described here will use equation (3-2) directly. Details of this additional work are discussed in Chapter 8.

Table 3-5: Total travel time and average speed for selected corridors in Baton Rouge (Summer 1995, 7:00-8:00 am data)

Corridor				Equation (3-4) Procedure		Equation (3-12) Procedure		$t_{T_L} - t_{T_d}$
Name	Dir.	# Segments w/ Records	Length (mi)	t_{T_L} (mm:ss)	$\bar{u}_L$ (mph)	t_{T_d} (mm:ss)	$\bar{u}_d$ (mph)	(mm:ss)
I-10	EB	93	16.18	17:16	56.23	17:21	55.96	00:05
	WB	78	13.51	15:22	52.77	15:23	52.71	00:01
I-110	NB	58	8.84	09:46	54.25	09:47	54.21	00:00
	SB	57	8.58	09:46	52.70	09:43	53.02	00:03
I-12	EB	97	17.56	18:05	58.23	18:03	58.34	00:02
	WB	96	17.62	23:13	45.53	23:07	45.72	00:06
LA 19	NB	27	4.68	07:50	35.87	07:44	36.35	00:06
	SB	34	5.61	09:27	35.63	09:26	35.67	00:01
Plank Rd	NB	83	13.87	29:03	28.64	28:26	29.25	00:36
	SB	89	14.63	26:08	33.59	26:54	32.64	00:46
Airline Hwy	SB	126	20.72	35:57	34.58	35:48	34.71	00:08
	NB	125	20.57	37:33	32.86	37:12	33.18	00:21
Florida Blvd	EB	92	14.62	32:31	26.97	32:29	27.00	00:02
	WB	86	14.12	29:12	29.01	28:52	29.35	00:20
Mickens Rd	EB	17	3.01	04:41	38.64	04:35	39.47	00:06
	WB	17	3.01	04:45	38.05	04:39	38.76	00:05
Sherwood For.	NB	43	6.76	17:29	23.20	16:58	23.90	00:31
	SB	42	6.73	17:14	23.43	17:21	23.28	00:07
Siegen Lane	NB	16	2.47	06:52	21.56	06:25	23.04	00:26
	SB	16	2.47	05:42	25.99	05:48	25.52	00:06
N Foster Dr	NB	6	0.77	01:24	33.13	01:26	32.38	00:02
	SB	5	0.78	04:14	11.03	03:25	13.67	00:49
Government	EB	20	2.88	07:50	22.02	07:57	21.71	00:07
	WB	26	3.45	08:48	23.50	08:36	24.05	00:12
Jefferson Hwy	EB	32	5.01	10:21	29.01	10:15	29.28	00:06
	WB	32	4.91	10:42	27.51	10:33	27.90	00:09
Staring Lane	NB	10	1.99	03:17	36.34	03:17	36.30	00:00
	SB	10	1.99	04:25	26.95	04:15	28.04	00:10
Essen Lane	NB	14	1.86	05:14	21.30	05:13	21.36	00:01
	SB	11	1.56	04:12	22.31	04:16	22.03	00:03
Bluebonnet Rd	NB	7	1.21	04:21	16.70	04:13	17.21	00:08
	SB	8	1.29	04:19	17.86	04:05	18.92	00:14
Burbank Dr	EB	5	0.92	01:26	38.57	01:29	37.17	00:03
	WB	5	0.92	02:17	24.18	02:19	23.76	00:02
LA 1	NB	2	0.27	00:20	49.77	00:20	50.16	00:00
	SB	3	0.45	00:30	53.28	00:31	52.11	00:01
Greenwell Sp.	EB	35	5.23	11:21	27.66	11:19	27.77	00:03
	WB	35	5.24	17:48	17.67	17:36	17.87	00:12
Scenic Hwy	NB	43	8.27	09:03	54.89	08:59	55.23	00:03
	SB	49	9.21	12:10	45.42	12:16	45.03	00:06
Range Ave	NB	12	1.87	04:01	27.97	03:54	28.83	00:07
	SB	11	1.77	06:13	17.07	05:53	18.04	00:20

To illustrate the convenience of using equation (3-2) instead of equation (3-4), consider a hypothetical segment 0.025 mi long. A probe vehicle collecting GPS data every 1 second enters the segment at 30 mph and decelerates at a uniform rate of 5 mph/second during 6 seconds until it stops at the end of the segment. The vehicle

remains stopped for 4 seconds after which it resumes its journey. Figure 3-6 shows the corresponding time-distance diagram. The total travel time is 10 seconds. As a result, the average speed along the segment is calculated to be 0.025*3600/10 = 9 mph. Equation (3-2) produces this same result. In contrast, equation (3-4) produces 7.5 mph.

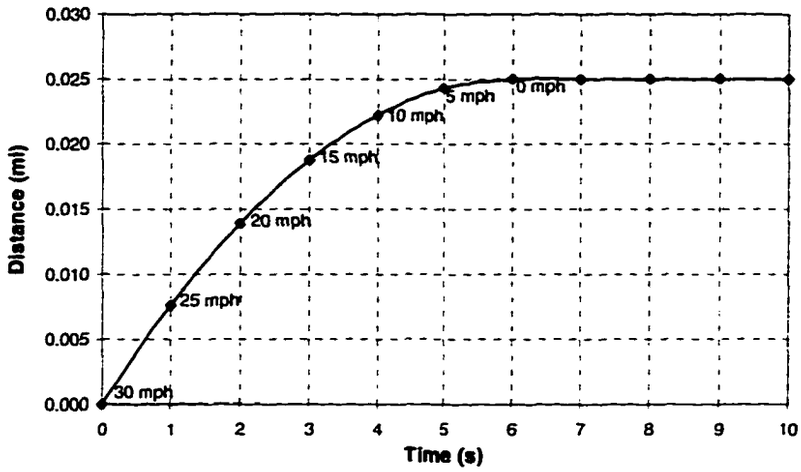

Figure 3-6: Time-Distance diagram for a hypothetical 0.025-mi segment

Chapter 4
SAMPLE SIZE REQUIREMENTS

Chapter 3 describes a spatial model that provides the capability to aggregate data from one or several travel time runs. In practice, the number of runs made should comply with acceptable error tolerance specifications. For the past 20 years, many travel time studies have been executed following guidelines included in the Institute of Transportation Engineers (ITE) manuals of traffic and transportation engineering studies [Box and Oppenlander, 1976] [Robertson, 1994]. Unfortunately, the ITE methodology seriously underestimates required sample sizes (or alternatively, it overestimates confidence levels associated with specified sample sizes). This chapter discusses this issue, compares existing approaches for estimating sample size requirements, and proposes a new formulation that solves the shortcomings of existing methodologies.

Sample Size Formulations

There are basically two types of formulations which are commonly used for estimating minimum sample sizes: (1) based on sample ranges, and (2) based on sample standard deviations. This section describes and compares these formulations.

Sample Range Formulation

The best known example of a sample range formulation is the one included in the ITE methodology. This formulation defines minimum sample sizes as a function of permitted errors in the estimate of the mean speed, average ranges in speed, and specified levels of confidence. It was originally developed using concepts adapted from quality

control theory [Oppenlander, 1976] where the lower and upper control limits for the mean are used to determine the need for additional sampling. Such concepts are widely used in industrial processes where the requirement to detect "out of control" situations early is critical so that corrective actions can be taken. Two basic assumptions used in quality control theory are that estimates of the population's mean μ and standard deviation σ are reliable and that a simple direct relationship between σ and the average sample range $\overline{R}$ can be established. For travel time studies, these assumptions imply that all travel time runs are made under the same traffic and environmental conditions and that a comprehensive set of initial runs is made to obtain reliable estimates for μ and σ. Traditional practice in industrial quality control suggests around 20 samples of size 4 to 5 each for this purpose [Milton and Arnold, 1990]. However, for most travel time studies, obtaining such a high number of initial samples is not practical. For this reason, it is usually accepted that one initial sample composed of four to five runs [Oppenlander, 1976], or even as low as two runs [Robertson, 1994], is sufficient to characterize the route under consideration. Based upon the observed range, a decision can be made whether there is a need for additional sampling.

Following Oppenlander [1976], the required sample size n is given by

$$n = \left[\frac{Z_\alpha \overline{R}}{d\varepsilon} \right]^2 \tag{4-1}$$

where Z_α is the normal, two-tailed statistic for a confidence level of $1-\alpha$, d is the ratio of $\overline{R}$ to σ; and ε is a user-selected allowable error or interval half-length. The ratio d is a function of n and is usually presented in a tabular form, as shown in Table 4-1. Typical

confidence levels are 95 and 99.73% [Robertson, 1994] [Oppenlander, 1976] which result in $Z_{0.05} = 1.96$ and $Z_{0.0027} = 3.00$, respectively. Since d is a function of n, an iterative procedure must be followed to solve for n. For illustration purposes, Table 4-2 shows values of n for various combinations of $\overline{R}$ and ε.

Table 4-1: Factor d as a function of sample size (adapted from Duncan [1986] and Oppenlander [1976])

Sample size n	d	Sample size n	d	Sample size n	d	Sample size n	d
2	1.128	12	3.258	22	3.819	60	4.639
3	1.693	13	3.336	23	3.858	65	4.699
4	2.059	14	3.407	24	3.895	70	4.755
5	2.326	15	3.472	25	3.931	75	4.806
6	2.534	16	3.532	30	4.086	80	4.854
7	2.704	17	3.588	35	4.213	85	4.898
8	2.847	18	3.640	40	4.322	90	4.939
9	2.970	19	3.689	45	4.415	95	4.978
10	3.078	20	3.735	50	4.498	100	5.015
11	3.173	21	3.778	55	4.572		

Table 4-2: Minimum sample size using the sample range formulation of equation (4-1)

a) Confidence level: 99.73%

Average Range (mph)	Specified Permitted Error				
	±1 mph	±2 mph	±3 mph	±4 mph	±5 mph
1	4	2	2	2	2
2	6	4	3	2	2
3	10	5	4	3	3
4	13	6	4	4	3
5	18	8	5	4	4
6	23	10	6	5	4
7	28	11	7	6	5
8	34	13	8	6	5
9	40	16	10	7	6
10	46	18	11	8	6
11	53	20	12	9	7
12	61	23	13	10	8
13	68	25	15	11	8
14	77	28	16	11	9
15	85	31	18	12	10
16	94	34	19	13	10
17	>100	37	21	15	11
18	>100	40	23	16	12
19	>100	43	24	17	13
20	>100	46	26	18	13
25	>100	65	36	24	18
30	>100	85	46	31	23

b) Confidence level: 95%

Average Range (mph)	Specified Permitted Error				
	±1 mph	±2 mph	±3 mph	±4 mph	±5 mph
1	3	2	2	2	2
2	4	3	2	2	2
3	6	4	3	2	2
4	8	4	3	3	2
5	11	5	4	3	3
6	13	6	4	4	3
7	16	7	5	4	3
8	19	8	6	4	4
9	22	9	6	5	4
10	25	11	7	5	4
11	29	12	8	6	5
12	33	13	8	6	5
13	37	14	9	7	5
14	41	16	10	7	6
15	45	17	11	8	6
16	49	19	11	8	7
17	54	20	12	9	7
18	59	22	13	9	7
19	64	24	14	10	8
20	69	25	15	11	8
25	97	35	20	14	11
30	-	45	25	17	13

Table 4-3 shows the original sample size values presented by Oppenlander [1976]. These values gave origin to those included in Box and Oppenlander [1976] and Robertson [1994]. Notice that for a 99.73% confidence level, most sample sizes shown in Table 4-2 match those shown in Table 4-3. In contrast, for a 95% confidence level, the sample sizes shown in Table 4-2 are around 20% higher than those shown in Table 4-3.

Table 4-3: Minimum sample size (using original values included in Tables 2 and 3 of Oppenlander [1976])

a) Confidence level: 99.73%

Average Range (mph)	Specified Permitted Error				
	±1 mph	±2 mph	±3 mph	±4 mph	±5 mph
1	4	2	2	2	2
2	6	4	3	2	2
3	10	5	4	3	3
4	13	6	4	4	3
5	18	8	5	4	4
6	23	10	6	5	4
7	28	12	7	6	5
8	34	13	8	6	5
9	40	15	10	7	6
10	47	18	11	8	6
11	52	20	12	9	7
12	61	23	13	10	8
13	74	25	15	11	8
14	79	28	17	12	9
15	85	31	18	12	10

b) Confidence level: 95%

Average Range (mph)	Specified Permitted Error				
	±1 mph	±2 mph	±3 mph	±4 mph	±5 mph
1	2	2	2	2	2
2	3	2	2	2	2
3	5	3	2	2	2
4	6	3	2	2	2
5	8	4	3	2	2
6	10	5	3	3	2
7	12	6	3	3	3
8	15	6	4	3	3
9	18	7	5	3	3
10	21	8	5	4	3
11	23	9	6	4	3
12	27	10	6	5	4
13	32	11	7	5	4
14	34	12	8	6	4
15	37	14	8	6	5

The values shown in Table 4-3 for a 95% confidence level (Table 3 of Oppenlander [1976]) are wrong, as shown in the following examples:

Example 1

Suppose an average range $\overline{R}$ of 15 mph and a permitted error ε of ± 1 mph. Since the confidence level is 95%, $Z_{0.05} = 1.96$. Assume n = 40. From Table 4-1, d = 4.322. Solving for ε in equation (4-1) yields $\varepsilon = 1.08$ mph. Clearly n must be larger. Assume now n = 45. From Table 4-1, d = 4.415. Solving for ε in equation (4-1) yields $\varepsilon = 0.993$ mph. which is practically the same as 1 mph. As a result, the required sample size is 45.

This value is the same as that shown in Table 4-2, but around 20% higher than that shown in Table 4-3.

Example 2

Suppose an average range $\overline{R}$ of 13 mph and a permitted error ε of ±3 mph. Since the confidence level is 95%, $Z_{0.05}$ = 1.96. Assume n = 8. From Table 4-1, d = 2.847. Solving for ε in equation (4-1) yields ε = 3.16 mph. Clearly n must be larger. Assume now n = 9. From Table 4-1, d = 2.970. Solving for ε in equation (4-1) yields ε = 2.86 mph. As a result, the required sample size is 9. This value is the same as that shown in Table 4-2, but almost 30% higher than that shown in Table 4-3.

In addition to the numerical error in the table, there is a problem with the methodology. The ITE manual [Robertson, 1994] recommends a procedure to estimate $\overline{R}$ where the absolute differences in running speed v between each pair of sequential runs in the initial study (or moving ranges) are computed and then averaged. $\overline{R}$ would then be computed as

$$\overline{R} = \frac{1}{m-1}\sum_{i=2}^{m}\left|v_i - v_{i-1}\right| \qquad (4\text{-}2)$$

where m is the sample size of the initial study. However, this procedure tends to be biased because the moving ranges are correlated through their common speed value [Messina, 1987]. For example, $v_2 - v_1$ and $v_3 - v_2$ have v_2 in common. This correlation can induce patterns which make the value of $\overline{R}$ lower than the true average range. Alternatively, Oppenlander [1976] suggests to estimate the average range simply by subtracting the minimum speed from the maximum speed measured in the initial study. In this case, $\overline{R}$ would be computed as

$$\overline{R} = \max_{i=1}^{m} v_i - \min_{i=1}^{m} v_i \qquad (4\text{-}3)$$

This approach is statistically more acceptable than that of equation (4-2) and, consequently, is adopted here.

Standard Deviation Formulation

Other approaches available in the literature use the sample standard deviation s instead of $\overline{R}$ to determine minimum sample sizes [May, 1990] [Srinivasan and Jovanis, 1996]. By using s instead of $\overline{R}$, these approaches bypass the assumption that a direct relationship between $\overline{R}$ and σ exists. Unfortunately, the result is that a simple-to-use, intuitive statistic such as $\overline{R}$ is replaced by a somewhat abstract statistic such as s that is frequently more difficult to conceptualize and calculate by field personnel.

In the sample standard deviation approach [May, 1990], n is given by

$$n = \left[\frac{t_\alpha s}{\varepsilon}\right]^2 \qquad (4\text{-}4)$$

where t_α is the t distribution statistic (used instead of the normal distribution Z_α statistic when dealing with small sample sizes). The statistic t_α is a function of n and, as a result, an iterative procedure must be followed to solve for n. For illustration purposes, Table 4-4 shows values of n for various combinations of s and ε, assuming confidence levels of 99.73% and 95%. The standard deviation approach approach is widely used and is generally considered to be sound and robust. Consequently, in this dissertation, n values using equation (4-4) are expected to be the most reliable sample size estimates. The other formulations were measured against the standard deviation formulation to evaluate their feasibility.

Table 4-4: Minimum sample size using the sample standard deviation formulation of equation (4-4)

a) Confidence level: 99.73%

Sample Standard Deviation (mph)	Specified Permitted Error				
	±1 mph	±2 mph	±3 mph	±4 mph	±5 mph
1	15	8	6	5	5
2	42	15	10	8	6
3	87	26	15	11	9
4	>100	42	22	15	12
5	>100	63	31	20	15
6	>100	87	42	26	19
7	>100	>100	55	34	24
8	>100	>100	70	42	29
9	>100	>100	87	52	35
10	>100	>100	-	63	42

b) Confidence level: 95%

Sample Standard Deviation (mph)	Specified Permitted Error				
	±1 mph	±2 mph	±3 mph	±4 mph	±5 mph
1	7	4	4	3	3
2	19	7	5	4	4
3	38	12	7	6	5
4	65	19	11	7	6
5	>100	28	14	10	7
6	>100	38	19	12	9
7	>100	51	25	16	11
8	>100	65	31	19	14
9	>100	82	38	23	16
10	>100	>100	47	28	19

It should be noted that equation (4-4) (and equation (4-1) for that matter) is valid under the assumption that ε is a deterministic variable. Strictly speaking, however, ε itself is a random variable that cannot be determined exactly ahead of time because σ is unknown [Hahn and Meeker, 1991]. If ε is assumed to be a random variable, it can be shown that the end result will be an even larger value of n than that computed with equation (4-4) [Hahn and Meeker, 1991].

Hybrid Formulation

As mentioned before, the range is a simple-to-use, intuitive statistic. Therefore, it is desirable to keep $\overline{R}$ in the formulation to compute n. Notice that $\overline{R}/d$, as used in equation (4-1), can provide a reasonable estimate for s in equation (4-4). At the same time, it is desirable to use t_α instead of Z_α because n is almost always less than 30. As a result, a hybrid formulation is proposed here in which n is computed as

$$n = \left[\frac{t_\alpha \overline{R}}{d\varepsilon}\right]^2 \qquad (4\text{-}5)$$

with $\overline{R}$ computed using equation (4-3). Since both d and t_α are functions of n, an iterative procedure must be followed to solve for n. Table 4-5 shows values of n for various combinations of $\overline{R}$ and ε, assuming confidence levels of 99.73% and 95%. For completeness, values of n for 85% and 75% confidence levels are also included.

Equation (4-5) produces larger values of n than equation (4-1) does. Dividing equation (4-5) by equation (4-1) yields

$$\frac{n_5}{n_1} = \left[\frac{t_{\alpha_5}}{Z_{\alpha_1}}\right]^2 \Big/ \left[\frac{d_5}{d_1}\right]^2 \tag{4-6}$$

where the subscripts 1 and 5 indicate the variables associated with equations (4-1) and (4-5), respectively. Both $t_{\alpha_5}/Z_{\alpha_1}$ and d_5/d_1 are larger than one. However, $t_{\alpha_5}/Z_{\alpha_1}$ dominates, particularly at high confidence levels, say 95% and above. For example, assume $\overline{R}$ = 9 mph, ε = 5 mph, and α = 0.0027 (99.73% confidence level). This means $Z_{\alpha_1} = 3.00$. Using equation (4-1), $n_1 = 6$ and $d_1 = 2.53$. Now, using equation (4-5), n_5 = 9, $t_{\alpha_5} = 4.28$, and $d_5 = 2.97$. As a result, $t_{\alpha_5}/Z_{\alpha_1} = 4.28/3.00 = 1.43$, $d_5/d_1 = 2.97/2.53$ = 1.17, and $n_5/n_1 = \left[1.43/1.17\right]^2 = 1.49$. This is the approximate ratio of the correct value in Table 4-5 (n = 9) to the incorrect value in Table 4-2 (n = 6).

Application

Two applications are included here to demonstrate the applicability of the hybrid formulation. First, a section of the eastbound (outbound) I-10 & I-12 corridor between the eastbound on-ramp at College Drive and the southbound off-ramp at Airline Highway is used to compare the formulations described previously. Second, significance levels for all segments in the Baton Rouge network using the hybrid formulation are determined.

Table 4-5: Minimum sample size using the proposed formulation of equation (4-5)

a) Confidence level: 99.73%

Average Range (mph)	Specified Permitted Error				
	±1 mph	±2 mph	±3 mph	±4 mph	±5 mph
1	6	5	4	4	4
2	9	6	5	5	4
3	13	8	6	5	5
4	17	9	7	6	6
5	21	11	8	7	6
6	26	13	9	8	7
7	32	15	10	8	7
8	37	17	12	9	8
9	44	19	13	10	9
10	50	21	14	11	9
11	57	24	15	12	10
12	65	26	17	13	11
13	73	29	18	14	11
14	81	32	20	15	12
15	89	35	21	16	13
16	98	37	23	17	14
17	>100	41	25	18	14
18	>100	44	26	19	15
19	>100	47	28	20	16
20	>100	50	30	21	17
25	>100	69	40	28	21
30	>100	89	50	35	26

b) Confidence level: 95%

Average Range (mph)	Specified Permitted Error				
	±1 mph	±2 mph	±3 mph	±4 mph	±5 mph
1	4	3	3	3	3
2	6	4	3	3	3
3	8	5	4	4	3
4	10	6	5	4	4
5	12	7	5	4	4
6	15	8	6	5	4
7	18	9	6	5	5
8	21	10	7	6	5
9	24	11	8	6	5
10	27	12	8	7	6
11	31	13	9	7	6
12	34	15	10	8	6
13	38	16	11	8	7
14	43	18	11	9	7
15	47	19	12	9	8
16	51	21	13	10	8
17	56	22	14	10	8
18	61	24	15	11	9
19	66	25	16	12	9
20	71	27	17	12	10
25	99	36	22	15	12
30	>100	47	27	19	15

a) Confidence level: 85%

Average Range (mph)	Specified Permitted Error				
	±1 mph	±2 mph	±3 mph	±4 mph	±5 mph
1	3	3	2	2	2
2	4	3	3	3	3
3	6	4	3	3	3
4	7	4	4	3	3
5	9	5	4	3	3
6	10	6	4	4	3
7	12	6	5	4	4
8	14	7	5	4	4
9	16	8	6	5	4
10	18	9	6	5	4
11	20	9	7	5	5
12	23	10	7	6	5
13	25	11	7	6	5
14	28	12	8	6	5
15	30	13	9	7	6
16	33	14	9	7	6
17	36	15	10	7	6
18	39	16	10	8	6
19	42	17	11	8	7
20	45	18	11	9	7
25	62	24	15	11	9
30	81	30	18	13	10

d) Confidence level: 75%

Average Range (mph)	Specified Permitted Error				
	±1 mph	±2 mph	±3 mph	±4 mph	±5 mph
1	3	2	2	2	2
2	4	3	3	2	2
3	5	3	3	3	2
4	6	4	3	3	3
5	7	4	3	3	3
6	8	5	4	3	3
7	9	5	4	3	3
8	11	6	4	4	3
9	12	6	5	4	3
10	14	7	5	4	4
11	15	7	5	4	4
12	17	8	6	5	4
13	19	9	6	5	4
14	20	9	6	5	4
15	22	10	7	5	5
16	24	11	7	6	5
17	26	11	8	6	5
18	28	12	8	6	5
19	30	13	8	6	5
20	33	14	9	7	6
25	44	18	11	8	7
30	58	22	14	10	8

I-10 & I-12 Corridor Application

The total length of the I-10 & I-12 corridor between College Drive and Airline Highway is 3.48 miles (Figure 4-1). For comparison purposes, data from three short 0.2-mile segments (12444, 12478, and 12530) as well as aggregated data from the entire 3.48-mile section of highway were used. Only data collected between September 1995 and May 1996 on Tuesdays, Wednesdays, and Thursdays from 7:00 to 8:00 am (uncongested traffic conditions) and from 4:30 to 5:30 pm (congested traffic conditions) were used in the analysis.

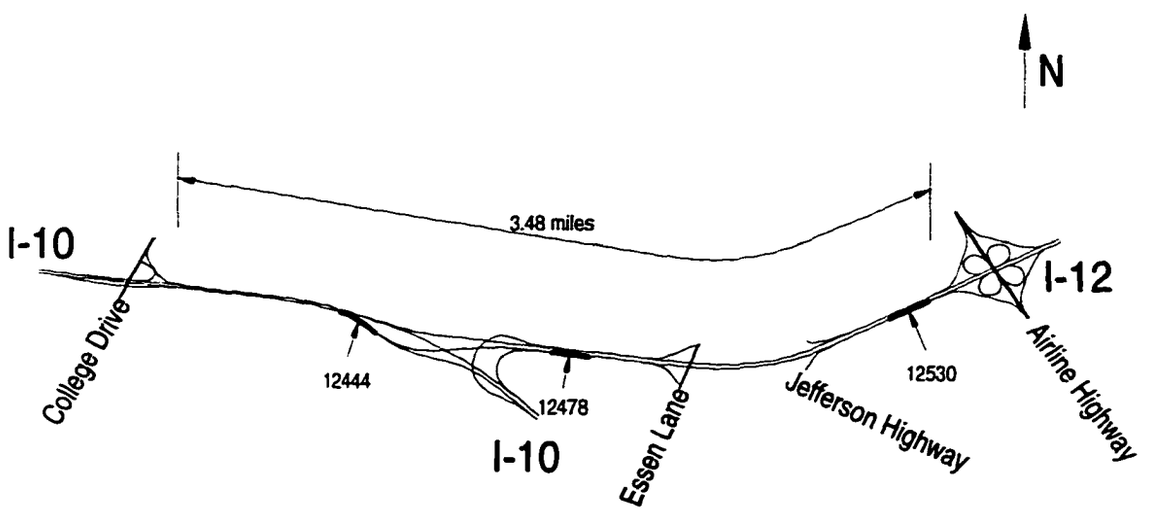

Figure 4-1: I-10 & I-12 corridor in Baton Rouge, Louisiana (5-digit numbers indicate location of selected 0.2-mile segments)

As an illustration, Table 4-6 shows speed data collected on segment 12444 from 7:00 to 8:00 am (column 2). Table 4-6 also shows the computational procedure to estimate $\bar{R}$ and s following the approaches described before. Column 3 represents cumulative sample size m and increases in value as each successive sample is collected

for segment 12444. Two columns show values for $\overline{R}$. Column 5 uses equation (4-2) to compute $\overline{R}$ based on absolute differences in speed between sequential runs (column 4). Column 6 uses equation (4-3) to compute $\overline{R}$ based on differences between maximum and minimum speeds (column 2). Finally, column 7 shows standard deviations based on speed data (column 2). For example, for m = 5, i.e. for i = 1 to 5, Table 4-6 shows that $\overline{R}$ is 2.69 mph when using equation (4-2) and 5.65 mph when using equation (4-3). It also shows that s = 2.27 mph. For m = 10, i.e. for i = 1 to 10, it shows that $\overline{R}$ is 1.41 mph when using equation (4-2) and 6.61 mph when using equation (4-3). It also shows that s = 1.90 mph. For the sake of brevity, speed data for other segments and time periods are not included in this document. However, the procedure to compute $\overline{R}$ and s is the same for all of them.

Table 4-6: AM peak speed data for segment 12444 (I-10 EB, before I-10 & I-12 split)

i (1)	Speed v (mph) (2)	m (3)	Speed dif. v_i-v_{i-1} (mph) (4)	Range Eqn. (4-2) (mph) (5)	Range Eqn. (4-3) (mph) (6)	Standard deviation (mph) (7)
1	52.59					
2	52.03	2	0.56	0.56	0.56	0.40
3	47.93	3	4.11	2.33	4.67	2.55
4	53.58	4	5.65	3.44	5.65	2.49
5	53.15	5	0.43	2.69	5.65	2.27
6	53.31	6	0.16	2.18	5.65	2.12
7	53.96	7	0.65	1.93	6.04	2.06
8	54.53	8	0.57	1.73	6.61	2.05
9	54.00	9	0.53	1.58	6.61	1.97
10	54.07	10	0.07	1.41	6.61	1.90
11	51.09	11	2.97	1.57	6.61	1.89
12	59.36	12	8.27	2.18	11.43	2.62
13	55.75	13	3.61	2.30	11.43	2.60
14	48.95	14	6.80	2.64	11.43	2.78
15	53.56	15	4.61	2.78	11.43	2.68
16	51.68	16	1.88	2.72	11.43	2.62
17	54.93	17	3.25	2.76	11.43	2.57
18	59.11	18	4.18	2.84	11.43	2.86
19	59.50	19	0.39	2.70	11.58	3.10
20	62.43	20	2.93	2.72	14.50	3.57
21	48.17	21	14.26	3.29	14.50	3.73
22	57.28	22	9.11	3.57	14.50	3.71

Table 4-7 shows the results of applying Table 4-2, Table 4-4, and Table 4-5 to the $\overline{R}$ and s data of Table 4-6 to compute n, assuming a permitted error ε of ±5 mph at the 95% confidence level. For the sake of brevity, Table 4-7 only shows the results for m = 5, 10, 15, 20, and 22. Table 4-7 also shows the results for other segments and time periods. For illustration purposes, consider the 7:00-8:00 am data on segment 12444. Assume m = 5. When using the ITE formulation, which involves using $\overline{R}$ = 2.69 mph as computed with equation (4-2), Table 4-7 shows that the required sample size n would be 2. In other words, no additional sampling would be required. When using Oppenlander's formulation, which involves using $\overline{R}$ = 5.65 mph as computed with equation (4-3), n would be 3. When using the standard deviation formulation, which involves using s = 2.27 mph, n would be 5. Finally, when using the hybrid formulation, which involves using $\overline{R}$ = 5.65 mph as computed with equation (4-3) (and Table 4-5 instead of Table 4-2), n would be 4.

In general, the ITE formulation produced the lowest values of n, between 50% and 80% lower than those obtained with the standard deviation formulation, clearly indicating that the ITE formulation seriously underestimates minimum sample sizes. Oppenlander's formulation produced n values that were much closer to, although consistently smaller than, those produced with the standard deviation formulation. Finally, the hybrid formulation produced values of n that were the closest to those produced with the standard deviation formulation. This trend is clearly shown in the case of the 4:30-5:30 pm data on segment 12444. The ITE formulation estimated a need for only 6 runs (both m = 5 and m = 10 produced n = 6). In contrast, the standard deviation formulation estimated a need for 15 to 18 runs (m = 15 produced n = 18; m = 20 produced n = 15).

Oppenlander's formulation estimated a need for 13 runs, which is slightly smaller than 15 runs. The hybrid formulation estimated a need for 15 runs, i.e. essentially the same number of runs as with the standard deviation formulation.

Table 4-7: Sample size requirements (for a permitted error of 5 mph at the 95% confidence level)

Segment	Time period	m	Formulation							
			ITE		Oppenlander's		Standard deviation		Hybrid	
			Range Eqn. (4-2) (mph)	n	Range Eqn. (4-3) (mph)	n	Standard deviation (mph)	n	Range Eqn. (4-3) (mph)	n
12444	7:00-8:00 am	5	2.69	2	5.65	3	2.27	5	5.65	4
		10	1.41	2	6.61	3	1.90	4	6.61	5
		15	2.78	2	11.43	5	2.68	5	11.43	6
		20	2.72	2	14.50	6	3.57	6	14.50	8
		22	3.57	2	14.50	6	3.71	6	14.50	8
12444	4:30-5:30 pm	5	15.47	6	29.67	13	11.01	22	29.67	15
		10	13.28	6	29.67	13	10.64	21	29.67	15
		15	9.76	4	29.67	13	9.53	18	29.67	15
		20	8.95	4	29.77	13	8.56	15	29.77	15
		23	8.26	4	29.77	13	8.41	15	29.77	15
12478	7:00-8:00 am	5	5.59	3	14.34	6	5.81	9	14.34	8
		7	5.42	3	14.34	6	4.85	7	14.34	8
12478	4:30-5:30 pm	5	4.59	3	10.22	5	3.83	6	10.22	6
		7	6.99	3	15.54	7	5.48	8	15.54	8
12530	7:00-8:00 am	5	2.36	2	4.61	3	2.13	5	4.61	4
		7	2.27	2	8.14	4	3.05	5	8.14	5
12530	4:30-5:30 pm	5	3.74	2	8.99	4	3.65	6	8.99	5
		8	4.79	3	11.76	5	3.89	6	11.76	6
3.48-mi	7:00-8:00 am	5	5.79	3	11.69	5	5.18	8	11.69	6
		7	4.82	3	11.69	5	4.08	6	11.69	6
3.48-mi	4:30-5:30 pm	5	10.85	5	18.96	8	8.66	16	18.96	9
		7	9.76	4	18.96	8	7.27	12	18.96	9

In most cases, using Table 4-4 and Table 4-5 to look up values of n for any given combination of $\overline{R}$ (or s) and ε provides accurate results. In some cases, however, using Table 4-4 and Table 4-5 may result in a slight overestimation of n because these tables contain n values which are rounded to the next higher integer. For example, when using the standard deviation formulation for the 7:00-8:00 am data on segment 12444 (assuming m = 5), use of Table 4-4 results in n = 5. In contrast, when applying equation (4-4) directly, n would be 4. Similarly, when using the hybrid formulation for the 7:00-

8:00 am data on segment 12478 (assuming m = 5), use of Table 4-5 results in n = 8. In contrast, when applying equation (4-5) directly, n would be 7. This is an indication that Table 4-4 and Table 4-5, while very useful for obtaining a quick estimation of required sample sizes, do not completely replace the use of the underlying formulations of equations (4-4) and (4-5).

Significance Levels for All Segments in Baton Rouge

Equation (4-5) (and equation (4-4) for that matter) can also be used to determine significance levels (or type I errors) associated with existing segment speed records. For example, for the 22 records associated with segment 12444 in Table 4-6, $\overline{R}$ = 14.50 mph and s = 3.71 mph. From Table 4-1, d = 3.819. Assume a permitted error ε of ±4 mph. Using equation (4-5), the resulting value of t_α would be

$$t_\alpha = \frac{\sqrt{n}d\varepsilon}{\overline{R}} = \frac{\sqrt{22}*3.819*4}{14.50} = 4.941$$

The corresponding value of α would be 0.01%. Similarly, when using equation (4-4), the resulting value of t_α would be

$$t_\alpha = \frac{\sqrt{n}\varepsilon}{s} = \frac{\sqrt{22}*4}{3.71} = 5.057$$

The corresponding value of α would be 0.01%.

Significance levels for other segments/conditions can be obtained in a similar way. As an illustration, Figure 4-2 and Figure 4-3 show the distribution of significance levels for nearly 1,900 segments in Baton Rouge, using data collected from September 1995 to May 1996. Figure 4-2 and Figure 4-3 are based on the use of equation (4-5) and a permitted error ε of ±4 mph. For completeness, Figure 4-2 and Figure 4-3 also show

the corresponding distribution of number of records per segment (Figure 4-2b and Figure 4-3b) and segment speed ranges (Figure 4-2c and Figure 4-3c).

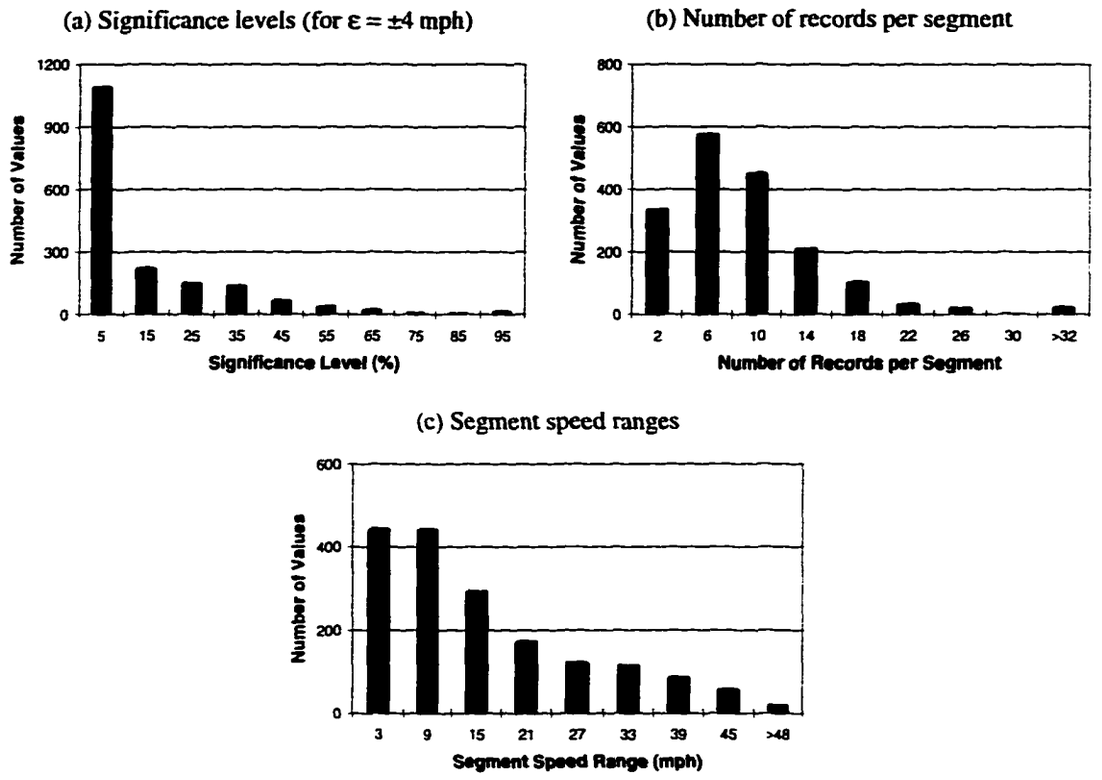

Figure 4-2: Distribution of significance levels, number of records per segment, and segment speed ranges in Baton Rouge (September 1995 - May 1996 7:00 - 8:00 am data)

The shapes of the AM peak and PM peak distributions are similar. The significance level for most segments is low as indicated in the number of segments with significance levels lower than 10% (more than 1,000 for the AM peak runs, and more than 700 for the PM peak runs). The number of records for most segments is less than 12. However, this is balanced by the fact that most sample speed ranges are less than 20 mph. These results also indicate that only a few extra runs on selected corridors would be needed to bring all significance levels below a certain threshold, say 25%.

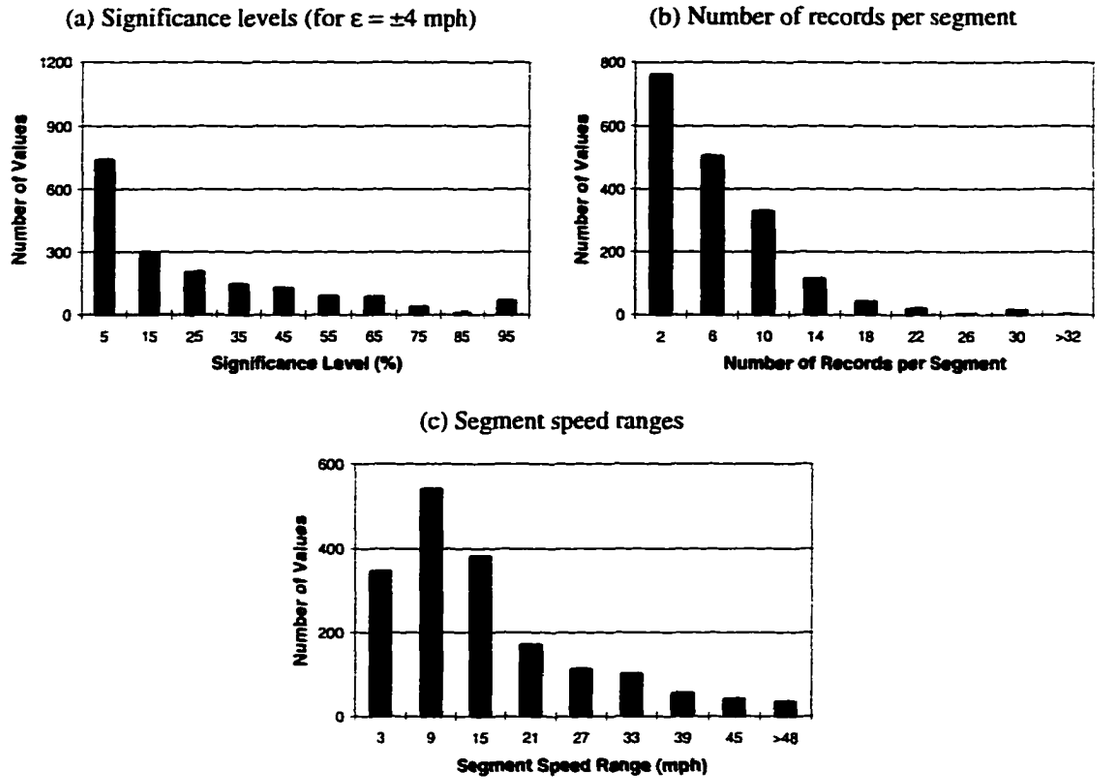

Figure 4-3: Distribution of significance levels, number of records per segment, and segment speed ranges in Baton Rouge (September 1995 - May 1996 4:30 - 5:30 pm data)

Charts such as those shown in Figure 4-2 and Figure 4-3, but based on equation (4-4) to estimate significance levels, can also be obtained. The resulting charts are very similar and, for this reason, they are not included here. It may be of interest, however, to analyze the differences in significance levels between the two approaches. Figure 4-4 shows the distribution of differences in significance levels, where the difference for each segment is computed as the significance level based on equation (4-4) minus the significance level based on equation (4-5). Notice that the differences for most segments are less than ±5 percentage points (87% of the segments for the AM peak and 84% of the segments for the PM peak). This is an indication that equation (4-5) yields almost identical results to equation (4-4).

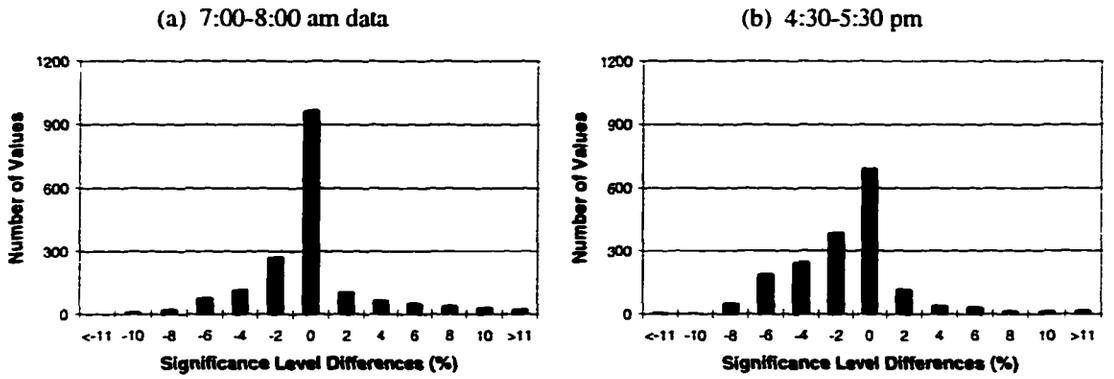

Figure 4-4: Distribution of significance level differences in Baton Rouge (September 1995 - May 1996 data)

The fact that equation (4-4) and equation (4-5) yield similar results is an indication that the ratio of $\overline{R}$ to s (or observed d values) for individual segments is similar to the theoretical d values shown in Table 4-1. Figure 4-5 shows both theoretical (Table 4-1) and observed d values for nearly 1,900 segments in Baton Rouge. The observed d values were calculated using more than 3,400 $\overline{R}$ and s values based on 26,000 segment records collected from September 1995 to May 1996 during the AM and PM peak periods. The overall trend of the observed d values follows that of the theoretical curve. Some scatter becomes evident, particularly for sample sizes larger than 10. The increased scatter for sample sizes larger than 10 indicates that, for large sample sizes, using equation (4-5) may be less reliable than equation (4-4). This observation is consistent with the literature [David, 1981] which reports that sample sizes larger than 10 cause the efficiency of $\overline{R}$ with respect to s for estimating dispersion to decrease. One way to increase the efficiency of $\overline{R}$ when the sample size is larger than 10 is to divide the sample into subsamples [David, 1981]. For example, in Table 4-6, the sample of size 22 could be subdivided into 3 subsamples of size 8, 7, and 7. A range would be computed

for each subsample using equation (4-3). The corresponding values are 6.61, 10.40, and 14.26 mph. Finally, an average value would be calculated (10.42 mph) and used in equation (4-5) to compute n.

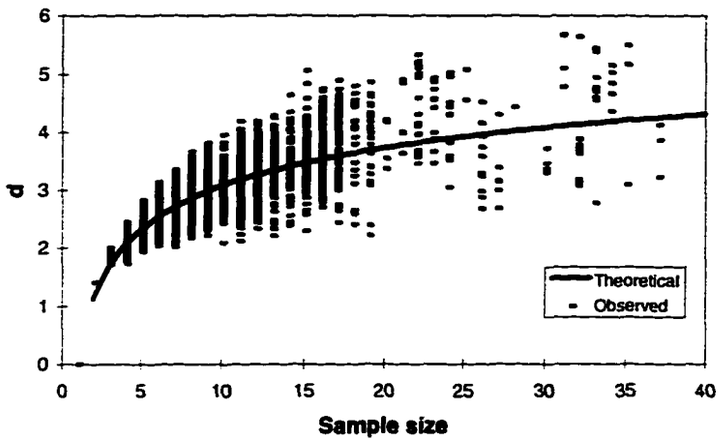

Figure 4-5: Theoretical and observed d values

Recommended Guidelines

This chapter revisited existing procedures to estimate minimum sample sizes for travel time studies. The work was motivated by the finding that the widely used guidelines included in the ITE Manual of Transportation Engineering Studies [Robertson, 1994] contained systematic numerical errors that resulted in lower than expected n values. A new formulation is proposed here (equation 4-5) which solves those shortcomings. The new formulation still maintains the use of $\overline{R}$ to estimate sample sizes because of its conceptual simplicity and ease of use.

One issue frequently addressed by traffic engineers in charge of planning and conducting travel time studies is that their budgetary constraints impose data collection

limitations. As a result, even with a methodology such as the one proposed in this chapter, chances are that the actual number of runs made will be much smaller than the required sample size computed using a pre-specified confidence level of, say, 95%. This means that the uncertainty associated with the computational procedure will be higher. One way to take this effect into consideration is by using confidence levels lower than 95%. For illustration purposes, Table 4-5 includes values of n for 99.73%, 95%, 85%, and 75% confidence levels. Notice that the required sample size decreases as the confidence level decreases. In practice, this means that traffic engineers should define confidence levels that are consistent with their specific needs and constraints. For example, if it is acceptable that up to 15% of future speed samples can be outside of a pre-specified interval of, say, 10 mph (which corresponds to $\varepsilon = 5$ mph), then an 85% confidence level is sufficient. This would be equivalent to say, if speed samples were collected every weekday, that up to 39 out of 260 speed samples would be allowed to exceed the specified 10 mph interval in any given year.

Because the ITE guidelines are so widely used, future editions of the ITE Manual of Transportation Engineering Studies should include tables similar to Table 4-5 that show required sample sizes for a wide range of confidence levels. For completeness, the ITE manual should discontinue the use of equation (4-2) to compute $\overline{R}$ and start using equation (4-3) for this purpose. The ITE manual should also consider including a comparison between the sample range approach and the standard deviation approach. This will allow traffic engineers to estimate required sample sizes and to validate results once the data are collected.

Chapter 5
DATABASE MANAGEMENT PROCEDURES

This chapter describes a geographic relational database developed to efficiently manage highway segment travel time data in a GIS environment. As discussed in Chapter 3, segments are assigned unique identification numbers in order to provide the capability to index data from travel time studies performed on different dates and times. This chapter describes both the structure or schema of the geographic database and procedures for building queries needed to derive specific information from the database including average speeds, travel times, and time delays.

Geographic Database Schema

As shown in Figure 5-1, the database is structured around six attribute tables: CORR_SEGMENTS, CORR_NAMES, FUNCT_TYPES, SEG_TYPES, SEG_TRAVEL_TIME, and WEEK_DAYS. A short description of these tables is given below. A summary of the associated attributes is given in Table 5-1. A sample of records is shown in Figure 5-2. The location of the segments is shown in Figure 3-3.

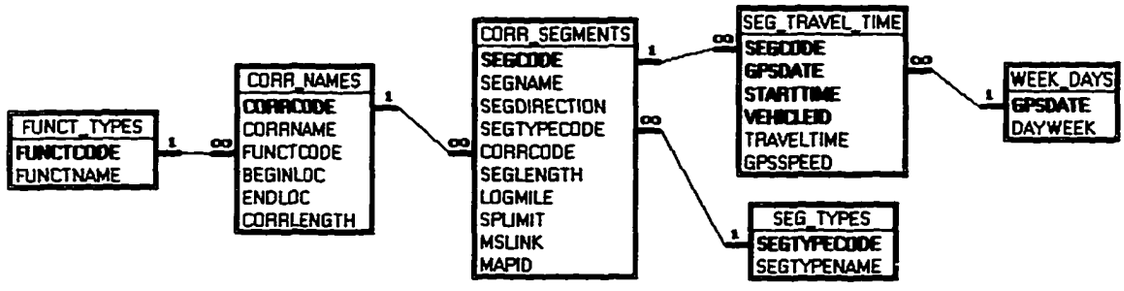

Figure 5-1: Geographic database schema

Table 5-1: Geographic database table attributes

Table Name	Attribute	Key	Description
CORR_SEGMENTS	SEGCODE	X	Segment code: has the same value as MSLINK
	SEGNAME		Segment name
	SEGDIRECTION		Segment direction: EB, WB, NB, SB
	SEGTYPECODE		Segment type code: 1, 2, 3, 4, 5, 6, or 7
	CORRCODE		Corridor code of corridor to which segment belongs
	SEGLENGTH		Segment length (mi)
	LOGMILE		Cumulative length along corridor
	SPLIMIT		Posted speed limit (mph)
	MSLINK		Linkage between graphical element and attribute table; created by MGE
	MAPID		Map identification number; created automatically by MGE
SEG_TYPES	SEGTYPECODE	X	Segment type code: 1, 2, 3, 4, 5, 6, or 7
	SEGTYPENAME		Segment type name equivalent to SEGTYPECODE
CORR_NAMES	CORRCODE	X	Corridor code
	CORRNAME		Corridor name
	FUNCTCODE		Corridor function class code: 1 or 2
	BEGINLOC		Location where corridor begins
	ENDLOC		Location where corridor ends
	CORRLENGTH		Corridor length
FUNCT_TYPES	FUNCTCODE	X	Corridor functional class code: 1 or 2
	FUNCTNAME		Corridor functional name equivalent to FUNCTCODE
SEG_TRAVEL_TIME	SEGCODE	X	Segment code
	GPSDATE	X	Date GPS data were collected
	STARTTIME	X	Time stamp at beginning of segment (in seconds UTC)
	VEHICLEID	X	Probe vehicle ID number
	TRAVELTIME		Time in seconds probe vehicle takes to traverse segment length
	GPSSPEED		Average speed of GPS speeds associated with segment (mph)
WEEK_DAYS	GPSDATE	X	Date
	DAYWEEK		Day of the week: MO, TU, WE, TH, FR, SA, SU

- **Table CORR_SEGMENTS:** This table contains basic data about each segment, including a unique segment code, name, direction, type code, corridor code, length, posted speed limit, and internal linkage to the database. Most of the attribute descriptions provided in Table 5-1 are self-explanatory. However, some additional information may be needed in the case of the segment type code attribute (SEGTYPECODE); the corridor code attribute (CORRCODE); and the internal database linkage attributes (MSLINK and MAPID). SEGTYPECODE is used to classify segments by function within the study route (main route, on-ramp, off-ramp, and so on), and provides a linkage to a lookup table (SEG_TYPES) that contains this information (Figure 5-2).

Table CORR_SEGMENTS

SEG CODE	SEG NAME	SEGDIRECTION	SEGTYPE CODE	CORR CODE	SEG LENGTH	LOG MILE	SP LIMIT	MSLINK	MAPID
12444	I-10	EB	1	1	0.200	10.07	55	12444	21
12453	I-10	EB	1	1	0.106	10.17	55	12453	21
12454	I-10	EB	1	1	0.106	10.28	55	12454	21
12455	I-10	EB	1	1	0.200	10.48	55	12455	21
12451	I-12	EB	1	3	0.104	0.10	55	12451	21
12450	I-12	EB	1	3	0.104	0.21	55	12450	21
12463	I-12	EB	1	3	0.200	0.41	55	12463	21
12464	I-12	EB	1	3	0.200	0.61	55	12464	21
12449	I-12	EB	1	3	0.200	0.81	55	12449	21
12478	I-12	EB	1	3	0.168	0.98	55	12478	21

Table SEG_TYPES

SEGTYPE CODE	SEGTYPE NAME
1	main
2	interchange
3	on-ramp
4	off-ramp
5	service road
6	short
7	other

Table CORR_NAMES

CORR CODE	CORR NAME	FUNCT CODE	BEGINLOC	ENDLOC	CORR LENGTH
1	I-10	1	2 mi West of LA 415	Ascension Parish line	19.06
2	I-110	1	I-10 & I-110 split	Scenic Hwy	8.71
3	I-12	1	I-10 & I-12 split	1.5 mi East of LA 47	17.59
4	LA 19	2	Scenic Hwy	Wimbush Lane	5.62
5	Plank Rd	2	Government St	LA 64	14.64
6	Airline Hwy	2	LA 1145	2 mi East of Highland Rd	22.87

Table FUNCT_TYPES

FUNCT CODE	FUNCTNAME
1	Interstate
2	Principal arterial

Table SEG_TRAVEL_TIME

SEGCODE	GPSDATE	STARTTIME	VEHICLEID	TRAVELTIME	GPSSPEED
12444	25-JUL-95	49556.75	2	11.5	56.50
12444	25-JUL-95	54032.75	2	13.0	55.31
12444	25-JUL-95	58441.25	2	12.5	57.37
12444	25-JUL-95	67426.25	2	13.5	55.75
12444	25-JUL-95	71770.75	2	12.0	58.84
12444	03-OCT-95	42272.75	1	13.5	52.99
12444	03-OCT-95	43916.25	1	13.5	52.03
12444	03-OCT-95	41698.75	2	11.5	57.09
12444	03-OCT-95	45649.25	2	17.5	39.24
12444	03-OCT-95	49830.25	2	13.0	55.05
12444	04-OCT-95	41880.25	1	14.5	50.18
12444	04-OCT-95	44806.75	1	14.5	47.93
12444	04-OCT-95	47708.75	1	13.0	53.96
12444	12-OCT-95	79991.91	2	17.3	38.31
12444	16-OCT-95	40680.76	2	11.5	61.05
12444	16-OCT-95	80109.75	1	23.0	31.27
12444	18-OCT-95	40177.75	2	14.5	52.55
12444	18-OCT-95	74936.75	1	21.0	35.35
12444	18-OCT-95	77962.25	1	24.0	33.09
12444	06-MAR-96	79564.25	1	16.0	44.33
12444	06-MAR-96	81056.25	1	13.0	53.81
12444	06-MAR-96	82539.25	1	14.5	51.72
12444	06-MAR-96	84020.75	1	13.0	50.49
12444	07-MAR-96	80533.78	1	17.0	37.99
12444	12-MAR-96	47677.75	2	12.5	59.11
12444	14-MAR-96	46769.75	2	12.5	58.20
12444	19-MAR-96	48796.25	2	11.5	59.50
12444	19-MAR-96	81453.75	1	14.0	50.60
12444	19-MAR-96	82949.25	1	19.0	37.31
12444	19-MAR-96	84437.75	1	19.5	36.91
12444	21-MAR-96	47083.25	1	10.0	62.43

Table WEEK_DAYS

GPSDATE	DAYWEEK
25-JUL-95	TU
03-OCT-95	TU
04-OCT-95	WE
12-OCT-95	TH
16-OCT-95	MO
18-OCT-95	WE
06-MAR-96	WE
07-MAR-96	TH
12-MAR-96	TU
14-MAR-96	TH
19-MAR-96	TU
21-MAR-96	TH

Figure 5-2: Sample of records from the Baton Rouge travel time database

CORRCODE is used to associate segments with routes or corridors, and provides a linkage to a lookup table (CORR_NAMES) that contains further information about each corridor. CORRCODE is extremely useful when roads having different names are part of the same de-facto corridor.

MSLINK and MAPID are used for internal linking purposes within the GIS. In this research, all maps were processed using Intergraph's Modular GIS Environment (MGE) package. MGE automatically generates the MSLINK and MAPID fields every time a graphical feature is linked to the database. Strictly speaking, MSLINK can be used to identify each segment uniquely. Unfortunately, not all of the querying and reporting interfaces in MGE display the MSLINK field explicitly on the screen. For this reason, a separate identification code (SEGCODE) having the same value as MSLINK was defined for visualization and querying purposes (Table 5-1). The remainder of this dissertation uses field SEGCODE for segment identification.

- **Table SEG_TYPES:** This table is a lookup table that contains the linkage between segment type codes included in table CORR_SEGMENTS and the corresponding segment type names. Seven segment types have been defined: main, interchange, on-ramp, off-ramp, service road, short link, and other. As shown in Chapter 6, approximately 76% of the segments considered in this research were main segments.
- **Table CORR_NAMES:** This table contains basic corridor information, including name, beginning and ending points, and length. It also contains a field for a corridor functional class (FUNCTCODE) which provides a linkage to a lookup table (FUNCT_TYPES) that contains functional class information. Length is actually a

derived field based on the average of the cumulative lengths of all segments on both directions of travel along the corridor.

- **Table FUNCT_TYPES:** This table is a lookup table that contains the linkage between the corridor functional class codes included in table CORR_NAMES and the corresponding functional classes. Two functional classes have been defined: Interstate, and Principal Arterial. If this study had included other functional classes such as Minor Arterial, this table would have been expanded accordingly.
- **Table SEG_TRAVEL_TIME:** This table contains summarized segment travel time and speed data. For each segment code, date, time, and vehicle ID, it stores travel time, and average speed. For convenience, time in this table is expressed in seconds universal coordinated time (UTC). This is the table containing the bulk of the data.
- **Table WEEK_DAYS:** This table is a lookup table that contains dates and text indicating the corresponding day of the week: MO, TU, WE, TH, FR, SA, and SU. Joining this table with table SEG_TRAVEL_TIME allows users to make queries by day of week.

Database Queries

Two types of queries can be made: spatial and non-spatial queries. Spatial queries depend on segment location and require GIS tools for creating and executing the queries. Examples of spatial queries are some of the queries needed to generate color coded maps. In contrast, non-spatial queries do not depend on the actual location of a segment and, as a result, they can be created and executed outside the GIS environment. Examples of non-spatial queries are queries used to determine number of records per segment, or average speed values per time period.

While the number of queries that can be generated from the database is enormous, a small number of queries seem to be needed quite frequently. Some of the queries that fall into this category are the following:

- Selection of records associated with a specific segment
- Computation of minimum, average, and maximum speed per date range and per time period
- Computation of median speed per date range and per time period
- Determination of free flow speeds
- Computation of segment travel time delay
- Computation of speed and travel time at the corridor level

These queries are described in Appendix B. For the sake of brevity, only a few example queries are included. However, the database query building procedure is general enough to allow for the inclusion of additional and more complex queries.

Once the specific database information has been retrieved, the next step is to include the information in meaningful reports. Chapter 6 describes the reporting procedures developed during the study.

Chapter 6
IMPLEMENTATION PROCEDURES

This chapter describes a set of procedures developed to implement the travel time GPS-GIS methodology described in Chapters 3 and 5. Three procedures are described in the following sections: data collection, data reduction, and data reporting procedures. These procedures are the same as those followed in the Congestion Management System (CMS) project [Bullock and Quiroga, 1996]. For completeness, this chapter also summarizes the application of these procedures to three metropolitan areas in Louisiana included in the CMS project: Baton Rouge, Shreveport, and New Orleans.

Like other large research projects, the CMS project involved the work of many individuals and agencies. More than anything else in the CMS project, the procedures described in this chapter were the result of a collaborative work, including that of this author. They are included here both for completeness and because they are essential to understand fully the new GPS-GIS methodology.

Data Collection Procedure

In the case of Baton Rouge and New Orleans, a Trimble Placer 400 GPS receiver was used with an RDS 3000 differential correction unit and a laptop computer (Figure 6-1, Figure 6-2). The RDS 3000 unit collected differential correction data through a commercial FM subcarrier and provided the capability for doing differential corrections on a real-time basis. The positional accuracy of the resulting DGPS data were 2-5 m (7-16 ft) spherical error probability (SEP) [Trimble, 1993]. These data were stored in an ASCII file following Trimble's proprietary format in the laptop computer.

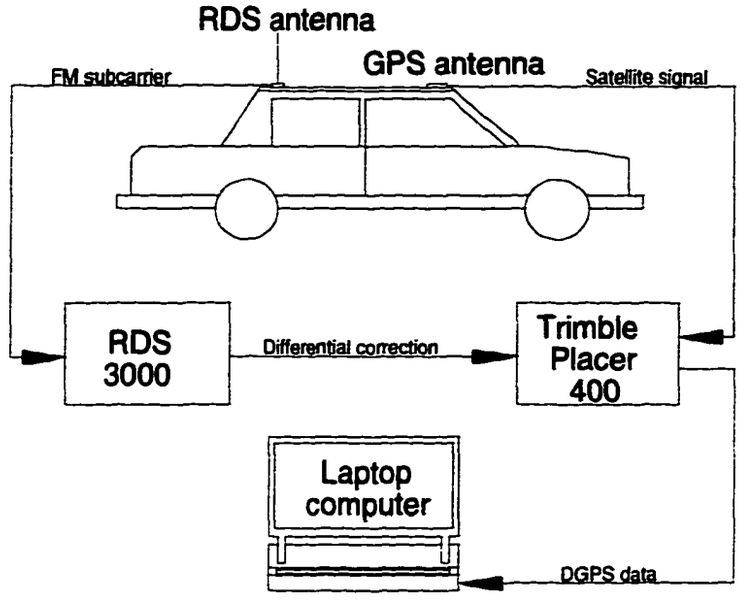

Figure 6-1: GPS receiver, laptop computer, and probe vehicle configuration used in Baton Rouge and New Orleans

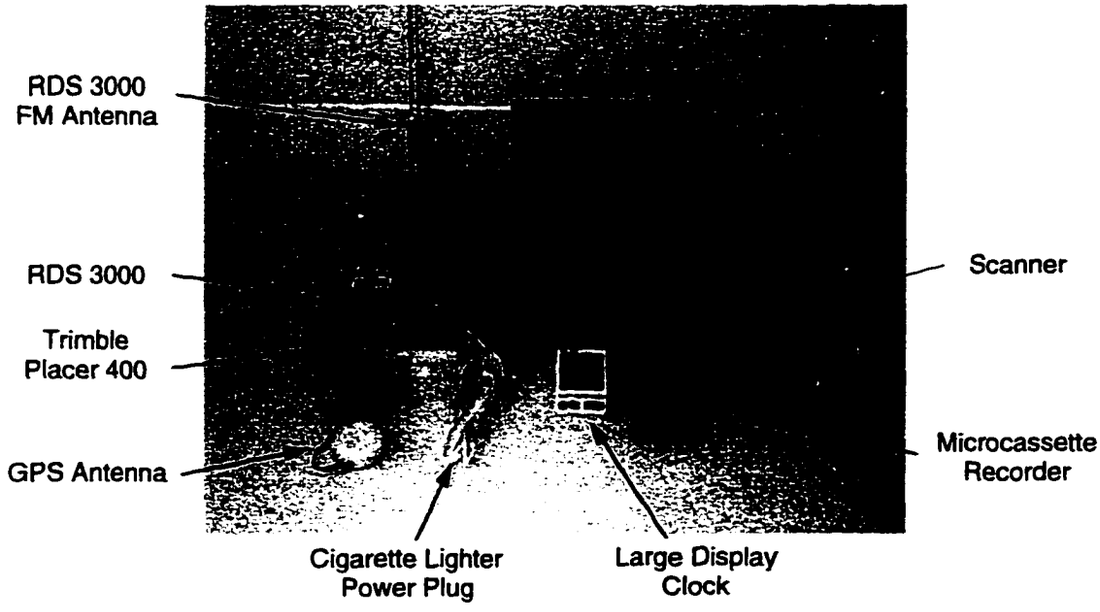

Figure 6-2: GPS equipment used in Baton Rouge and New Orleans (the scanner, the clock, and the microcassette recorder were not used in New Orleans)

In addition to position fixes, the Placer 400 GPS receiver also recorded time and speed. The receiver computed speed based on pseudorange (distance from satellite to receiver) and pseudorange rate data, i.e. independently from position fix computations. The resulting speed accuracy was 0.2 mph (1 sigma) with selective availability (SA) disabled under steady state conditions. When SA is enabled, speed accuracy decreases to perhaps 1 mph - 1 sigma (based on a telephone conversation with Trimble officials).

In the case of Shreveport, a rover/base station configuration was used for data collection [Petro, 1996]. The GPS rover receiver was a Pathfinder ProXL Trimble unit, equipped with a TDC1 datalogger. The base station was a 4000 SSE geodetic surveyor receiver. Differential correction was made by postprocessing the raw GPS data from the rover unit with the GPS data from the base station. This system configuration provided a submeter positional accuracy.

Also part of the equipment in Baton Rouge was a microcassette audio tape recorder to document changing weather conditions, disruptive traffic incidents, and queues at major intersections. The use of the device eliminated the need to make written notes while driving. Incidents on highways other than the one being driven were also recorded by using a scanner to monitor the Police band and by listening to the traffic reports produced by one of the local radio stations.

In each of the three metropolitan areas, a set of runs was scheduled to collect travel time and speed data. In general, runs were made during the AM peak and PM peak periods. For completeness, additional runs were scheduled during off peak and other specific traffic conditions. Details of the specific data collection schedules for each metropolitan area are included in the Case Studies section of this chapter.

Data Reduction Procedure

To efficiently transform GPS point travel time data into segment travel times and average speeds, a procedure was developed to filter and reduce these data so that only summary information could be written to the database. First, short filtering programs in C++ were written to filter out data that were not strictly geographic coordinates, time, speed, and differential correction status. Examples of data filtered out included satellite navigational data, communication status, and other messages. Second, an application was written in Microstation Developing Language (MDL) to interactively link each segment with the filtered GPS data in a GIS environment. When the user loads the application, a data reduction form appears on the screen (Figure 6-3a). The user selects an input GPS data file, and the application displays all GPS points on the screen. The user then clicks on segments (Figure 6-3b), and the application determines entrance and exit times and average speeds. For example, when the user clicks on segment 12444, the corresponding travel time and average speed are computed and shown in the data reduction form (Figure 6-3a). The application also displays a number of points ahead so that the user knows that the vehicle traveled on I-12 and that the next segment to click on is 12451 (Figure 6-3b). Selection of successive segments proceeds in a similar fashion.

Figure 6-4 shows a short sequence of screen captures of the actual data reduction process on six segments located near the I-10 & I-12 split in Baton Rouge. For clarity, a thumbnail sketch showing the location of the segment being processed is also included in the upper right corner of each screen. Notice in each case two circles indicating the segment end points. The larger circle indicates the end of the segment and can be made

larger or smaller to allow users to modify the criteria with which GPS points can be linked to a segment. The smaller circle denotes the beginning of the segment.

(a) GPS data reduction form

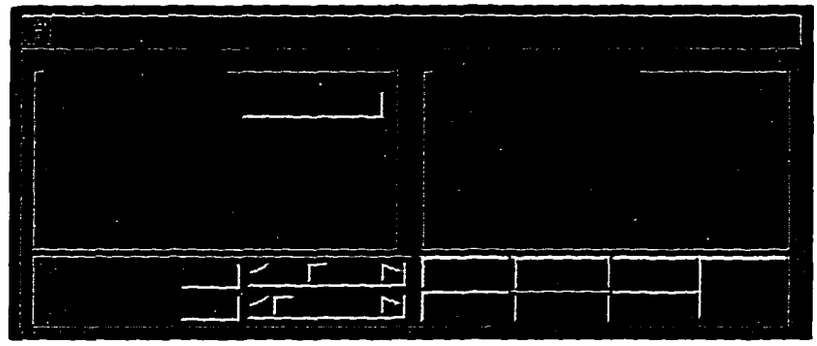

(b) Assignment of GPS points to segment 12444

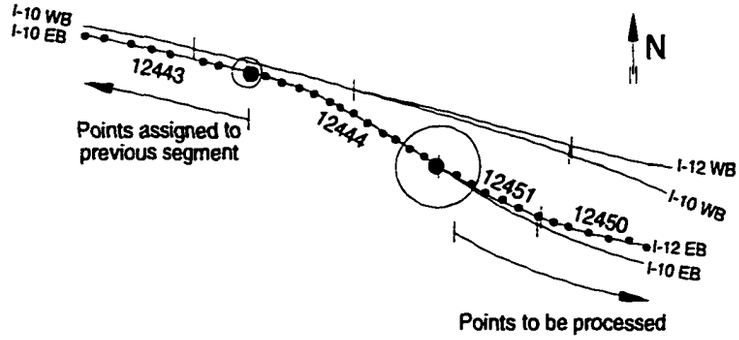

Figure 6-3: Graphical interface used for data reduction

Between June 1995 and July 1996, several undergraduate students used this data reduction application to process travel time runs totaling nearly 30,000 miles on 329 miles of urban highways in Baton Rouge, Shreveport, and New Orleans. They generated 183,000 segment travel time records from 2.9 million GPS data points collected. In a typical application, they were able to process two hours worth of data (a total of 7,200 GPS data points) in 15-20 minutes, i.e. about eight times faster than the actual driving in the field. Operators were typically trained in one to two hours, and became proficient

within 10 hours. More automation could reduce processing times even more. Eventually, the application might be able to select segments automatically without any user assistance. Data reduction would then take only a few seconds.

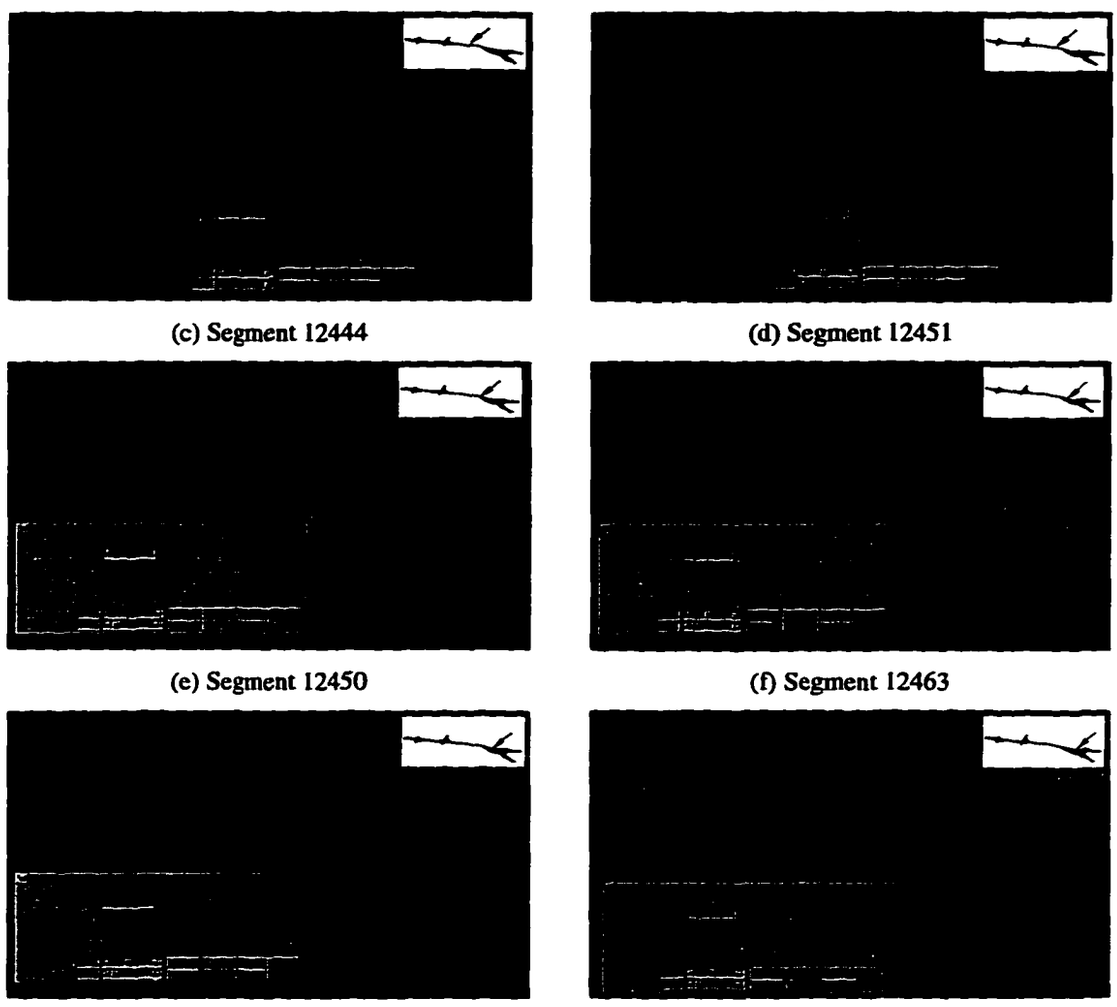

Figure 6-4: Example of the data reduction process on I-10 & I-12 in Baton Rouge

Data Reporting Procedure

After the segment travel time and speed data are imported into the database, the next step is to construct reports summarizing the data collected. An obvious approach,

which is traditional in travel time studies, is to draw speed-distance or speed-time profiles along the corridor of interest (Figure 2-4). However, this output information could be greatly enhanced with the use of GIS and database querying and reporting tools. Three reporting options are discussed here: Maps; archival tabular reports; and World Wide Web (WWW) reports.

Maps

Figure 6-5 and Figure 6-6 show sample color coded maps that contain average observed speeds in Baton Rouge from September 1995 to May 1996 during the AM peak (7:00-8:00 am) and PM peak (4:30-5:30 pm) time periods. Figure 6-5 shows a copy of an actual production map. Figure 6-6a and Figure 6-6b show more detailed views of the study area core. As a guide to readers who do not have access to color copiers to reproduce Figure 6-5 and Figure 6-6 faithfully, a gray scale version of these figures is included in Figure 6-7 and Figure 6-8.

Maps such as those shown in Figure 6-5 through Figure 6-8 are very powerful because the location of problem areas becomes readily apparent. For example, Figure 6-6a and Figure 6-8a clearly show AM peak congestion problems on I-12 west bound (WB) between Sherwood Forest Boulevard and Jefferson Highway, and Florida Boulevard WB between McGehee and Monterey Boulevard. Likewise, Figure 6-6b and Figure 6-8b clearly show PM peak congestion problems on I-10 east bound (EB) from the Mississippi River bridge to the I-10 & I-12 split, and Airline Highway south bound (SB) between Goodwood Avenue and Old Hammond Highway. Notice, however, that the color coded maps of Figure 6-6 are much more powerful visually than the gray scale maps of Figure 6-8 because the color coded maps also show clearly those segments in the Baton Rouge

network that experience high speeds. This characteristic makes color coded maps such as those in Figure 6-6 extremely effective for explaining traffic characteristics and performance at public meetings.

The color sequence used in Figure 6-5 and Figure 6-6 is not usually recommended in traditional cartographic practice because of the difficulty frequently encountered with a saturated yellow in the middle of the sequence [Brewer, 1994]. In general, sequential lightness steps with a transition from light yellow to dark purple-blue through green, or from yellow to dark red through orange, are preferred. However, in traffic engineering the use of a red-yellow-green sequence is common practice. Red normally denotes zero to very low speeds, e.g. through the use of stop signs or red lights at signalized intersections. In contrast, green normally denotes vehicle movement, e.g. through the use of green lights at signalized intersections. Because a red-yellow-green sequence is a common language understood by both the traffic engineering community and the traveling public, it makes sense to maintain the same sequence when constructing maps that show the spatial variability of speeds on the network. This approach is common practice as evidenced by the growing number of cities having web sites which display maps showing near real-time travel time and speed data on their networks.

The queries used to generate maps such as those shown in Figure 6-5 through Figure 6-8 could be modified to display other traffic indicators like coefficients of variation (see Chapter 7). The queries could also be modified to conform to classification schemes other than the 0-20, >20-30, >30-40, >40-50, and > 50 mph scheme adopted here. For example, depending on the highway functional class, one of the classification schemes included in the Highway Capacity Manual [TRB, 1994] might be used.

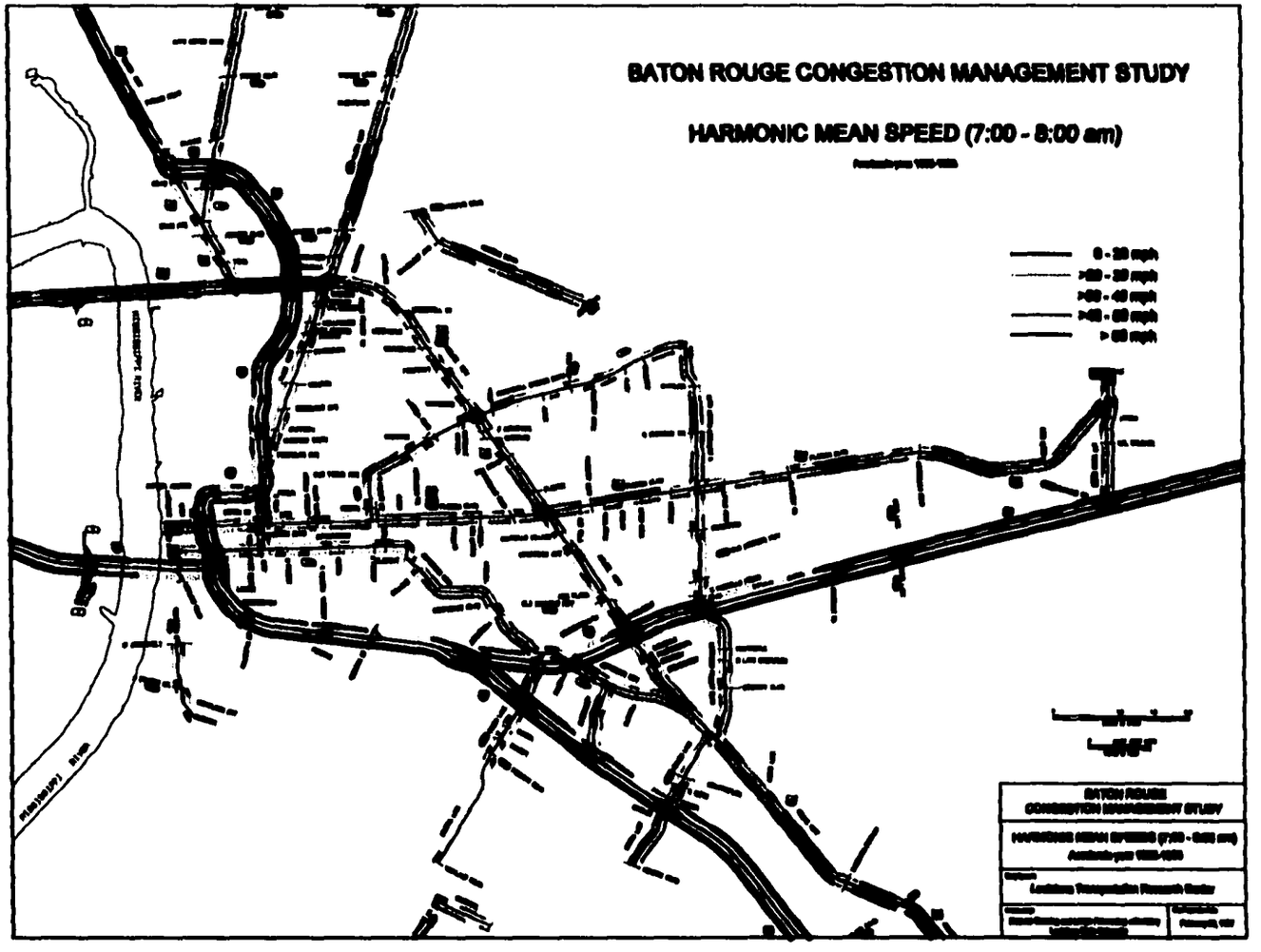

Figure 6-5: Average (harmonic mean) speeds observed in Baton Rouge from September 1995 to May 1996 (AM peak: 7:00-8:00 am) - color coded map

(a) AM peak (7:00-8:00 am)

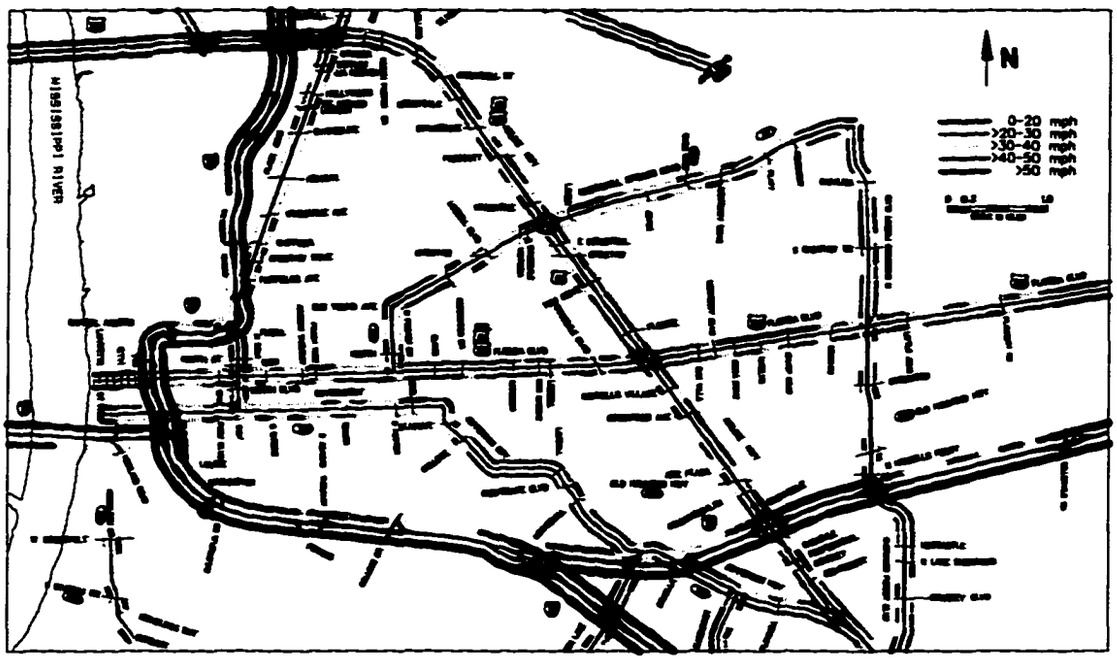

(b) PM peak (4:30-5:30 pm)

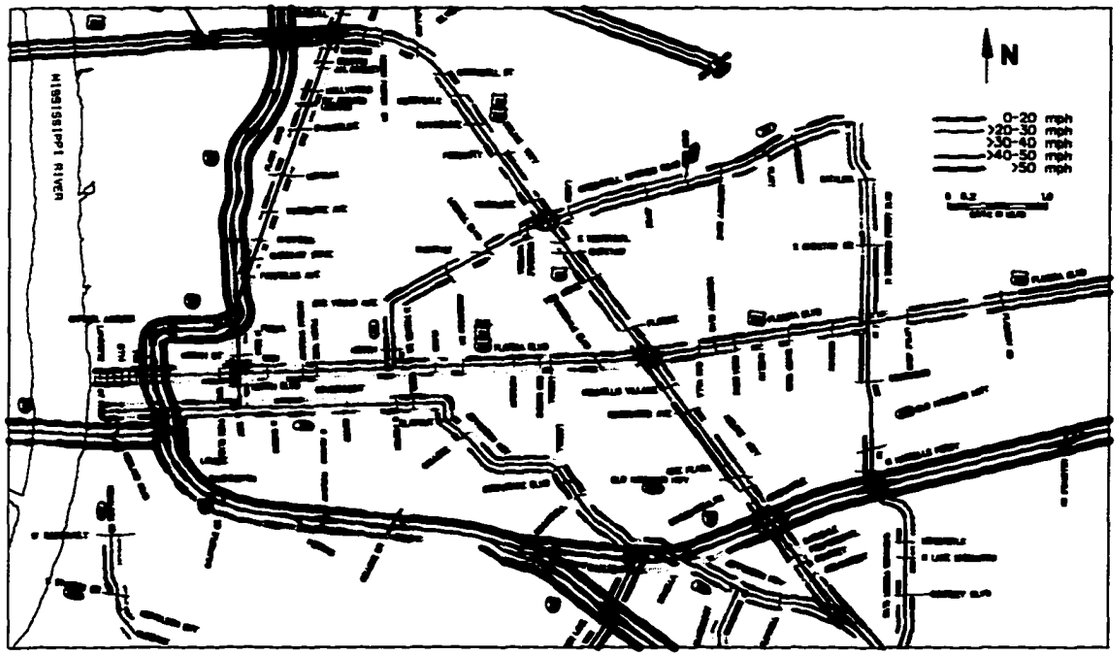

Figure 6-6: Average (harmonic mean) speeds observed in Baton Rouge from September 1995 to May 1996 (detail of study area core) - color coded maps

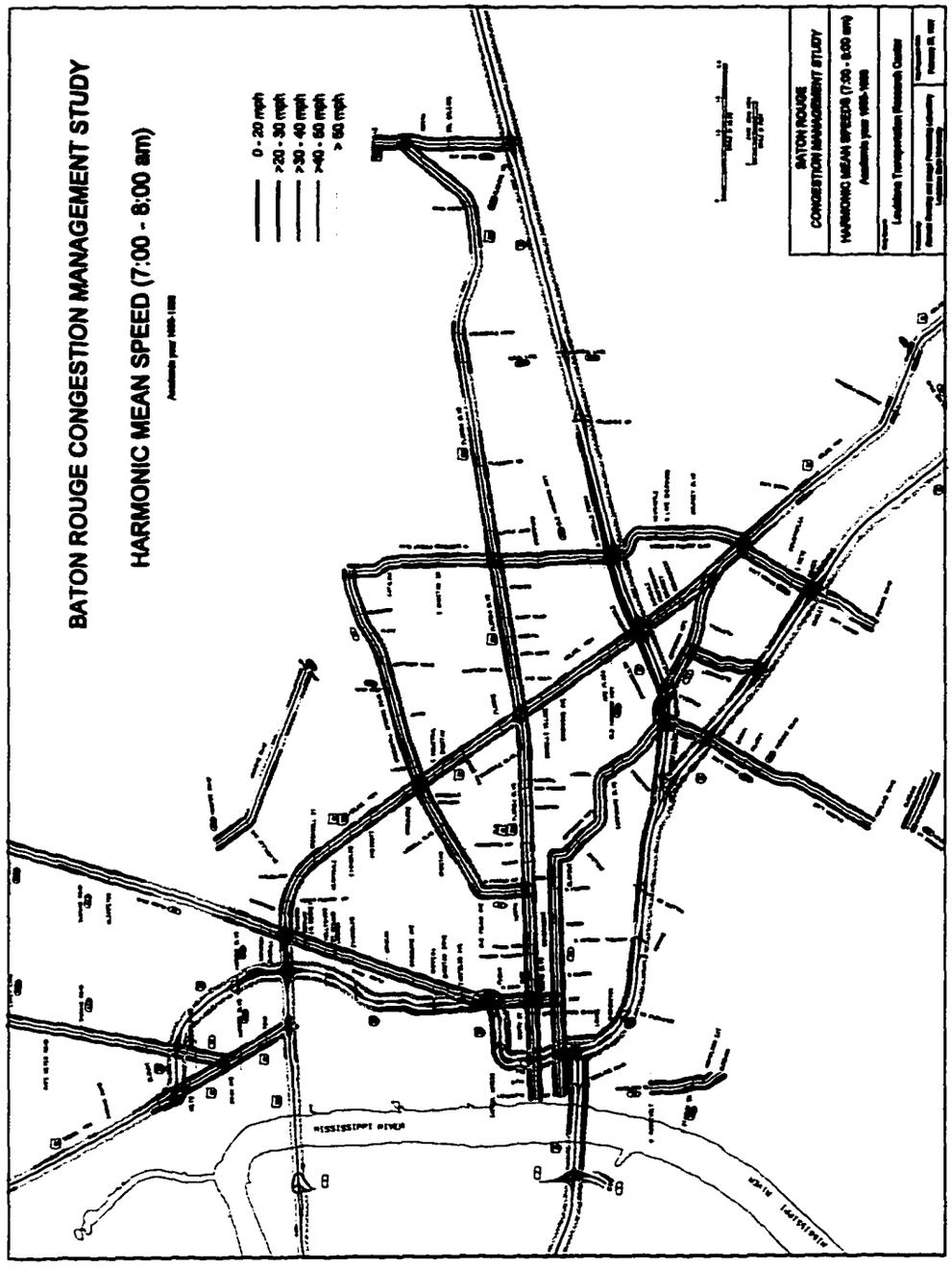

Figure 6-7: Average (harmonic mean) speeds observed in Baton Rouge from September 1995 to May 1996 (AM peak: 7:00-8:00 am) - gray scale map

(a) AM peak (7:00-8:00 am)

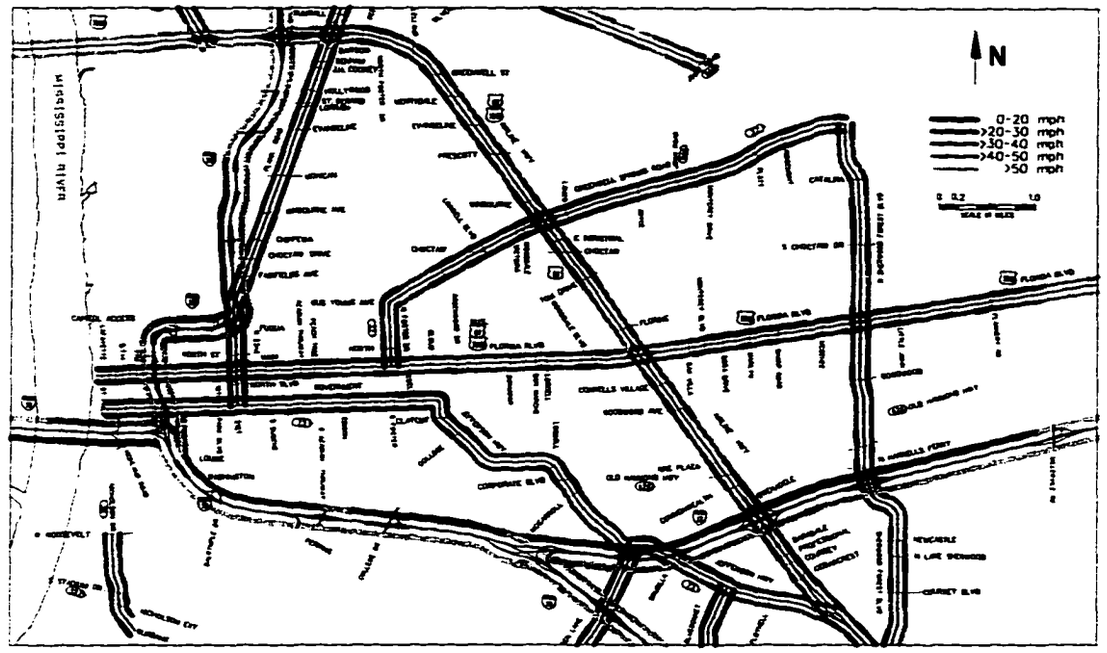

(b) PM peak (4:30-5:30 pm)

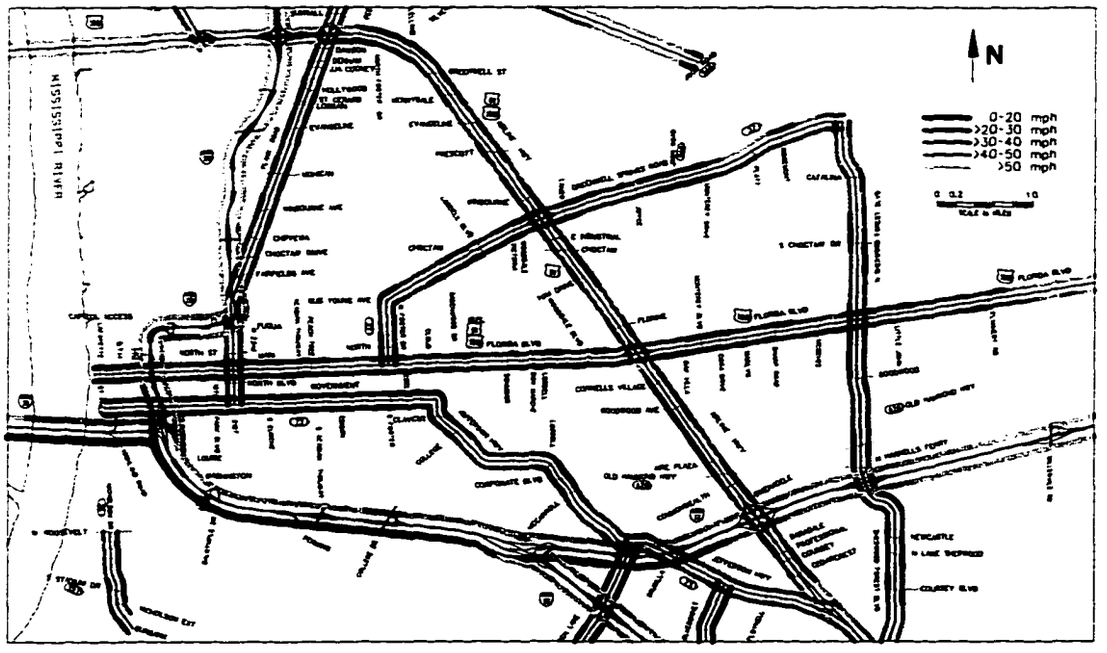

Figure 6-8: Average (harmonic mean) speeds observed in Baton Rouge from September 1995 to May 1996 (detail of study area core) - gray scale maps

Archival Tabular Reports

Maps are not very efficient for archiving travel time and speed data. For archiving and analysis, reports similar to those used to document highway features like sign posts and culverts were implemented. These reports are produced on 11x17 paper and cover 20 highway segments in each direction of travel. For production purposes, the highway network was divided into sections, as shown in Figure 6-9. Figure 6-10 shows two sample report pages for Sections 11 and 12 in Baton Rouge. Section numbers are shown in the lower right corner of each report. For each segment, these reports show average speeds and average cumulative travel time during the AM peak, off peak, and PM peak periods. The shading next to the average speed values is related to the ratio of observed speed to posted speed limit. As the ratio decreases, i.e. as the observed speed decreases with respect to the posted speed limit, the shading becomes darker. This scheme makes the visual identification of problem areas easy.

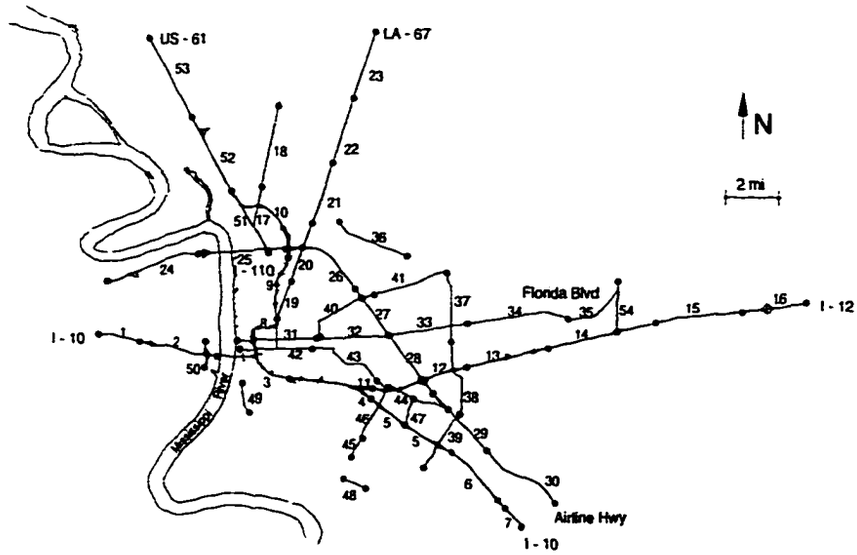

Figure 6-9: Sections for the production of tabular reports in Baton Rouge

(a) I-10 & I-12 corridor between Acadian and the I-10 & I-12 split

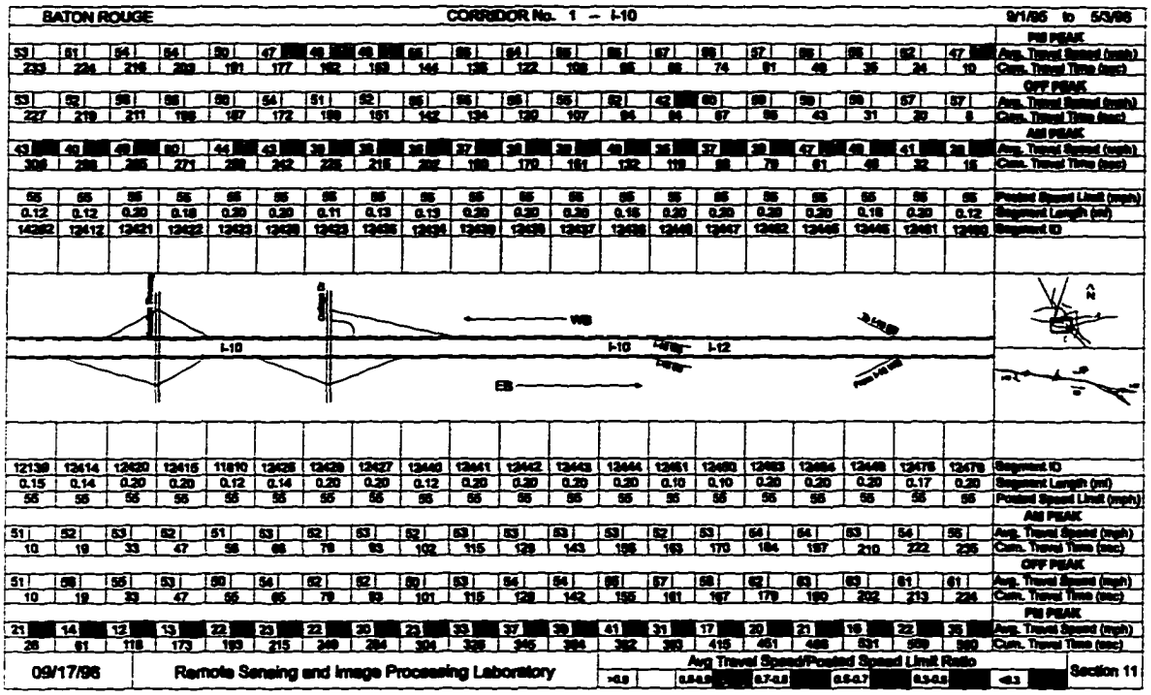

(b) I-10 & I-12 corridor between the I-10 & I-12 split and Sherwood Forest Blvd

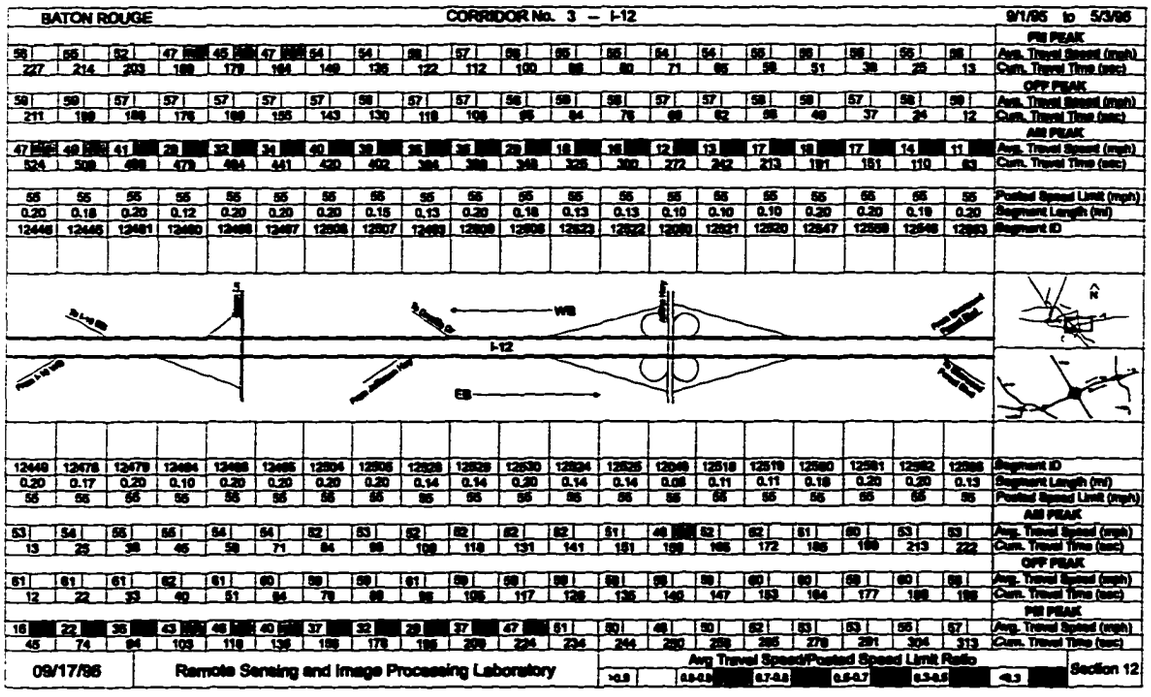

Figure 6-10: Example report pages for the I-10 & I-12 corridor during the PM peak hour (4:30 to 5:30 pm) from September 1995 to May 1996 in Baton Rouge

WWW Reports

A number of organizations in Baton Rouge such as local consultants, transit operators, and media became interested in the travel time and speed data that had been collected. There were also government agencies throughout the country, particularly MPOs, that were interested in obtaining general information about the GPS-GIS methodology that was being developed. To address these information reporting needs a series of web pages was constructed to allow users working from remote computers to retrieve general information about the project, as well as detailed travel time and speed data in such a way that technical support to interpret the data was not required [Quiroga, Bullock, and Schwehm, 1997]. The web page that contains general information about the project is located at http://rsip.lsu.edu/projects/cms/cmshome.html. This page also contains links to other web pages that display specific travel time information.

Of interest here is the web page that allows remote users to execute queries by segment and download the corresponding data into their computers. This web page is located at http://www.rsip.lsu.edu/cms/cmsbtr/cms-query.html. Currently, the system allows users to make queries by segment in the Baton Rouge network either by clicking on a set of sensitive maps until finding the specific segment of interest (Figure 6-11) or by typing in the segment code in a text field. The system then displays all existing records associated with that segment and produces hourly summary speed data. Currently the sensitive maps are image files that represent specific areas of the vector GIS map. This is obviously inefficient. With the recent introduction of Internet-oriented GIS publishing tools such as Intergraph's Geomedia Web Map, it will be possible to modify the web page so that the original vector GIS map can be used directly in its native format.

(a) Congestion network sensitive map

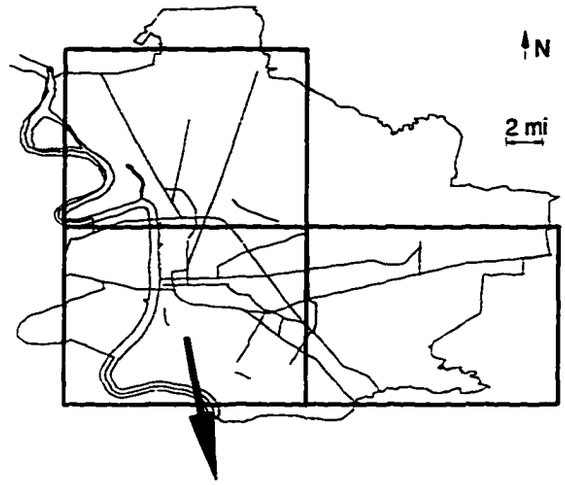

(b) Southwest quadrant sensitive map

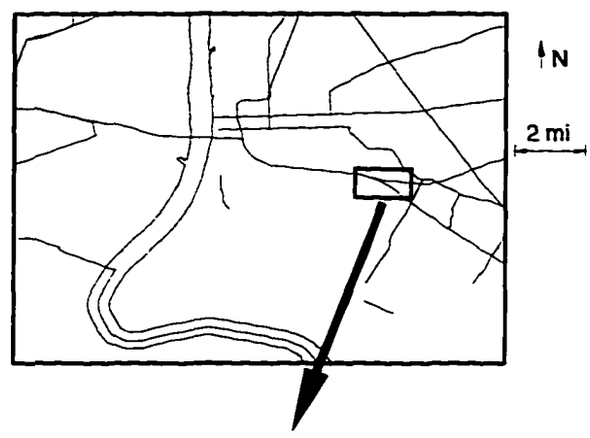

c) I-10 & I-12 split sensitive map

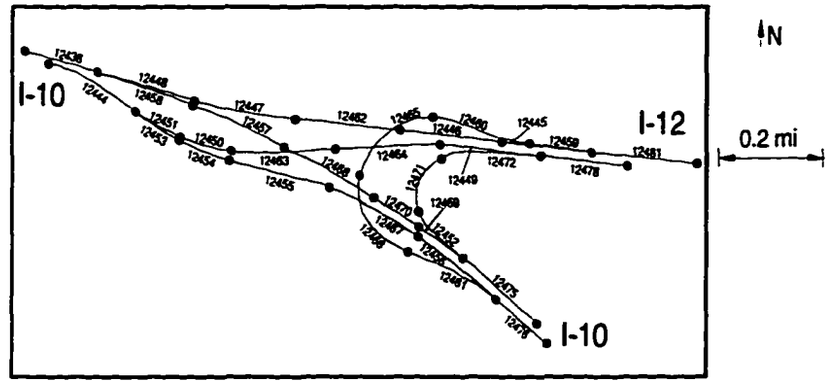

Figure 6-11: Congestion network and segmentation at the I-10 & I-12 split in Baton Rouge. Rectangles delineate clickable areas on the CMS WWW home page

Case Studies

This section summarizes the application of the GPS/GIS methodology to three metropolitan areas in Louisiana: Baton Rouge, Shreveport, and New Orleans.

Baton Rouge

The Baton Rouge MPO, the Capital Region Planning Commission (CRPC), defined a congestion corridor network composed of 22 corridors covering 151 mi (Figure 6-12). As shown in Table 6-1, three of the 22 corridors were located on the Interstate highway system and covered 45 mi. The remaining 19 corridors were located on principal arterials and covered 106 mi. Including both directions of travel, on-ramps, off-ramps, and interchanges, the total network length was 369 mi.

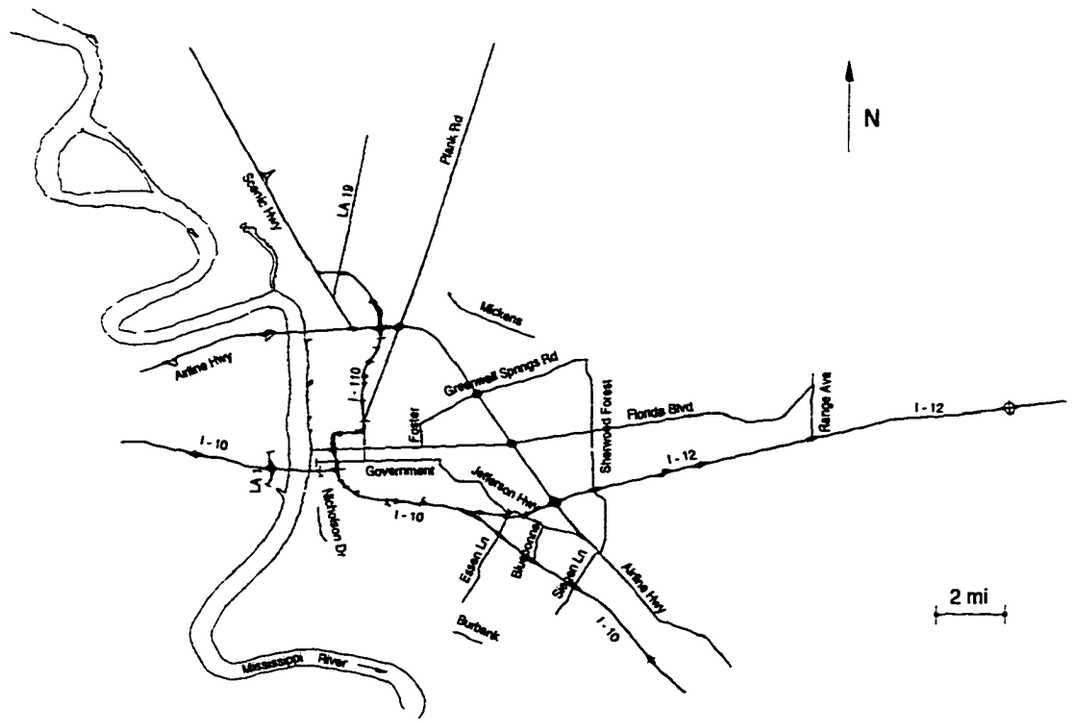

Figure 6-12: Congestion corridor network in Baton Rouge

Table 6-1: Congestion corridor network in Baton Rouge

ID	Name	From	To	Length (mi)	
				Interstate Highway	Principal Arterial
1	I-10	2 mi West Of LA 415	Ascension Parish line	19.06	
2	I-110	I-10 & I-110 Split	Scenic Hwy	8.71	
3	I-12	I-10 &-12 Split	1.5 mi East of LA 447	17.59	
4	La 19	Scenic Hwy	Wimbush Lane		5.62
5	Plank Rd	Government St	LA 64		14.64
6	Airline Hwy	LA 1145	2 mi East of Highland Rd		22.87
7	Florida Blvd	River Front	Range Ave		14.69
8	Mickens Rd	Hooper Rd	Joor Rd		3.01
9	Sherwood Forest Blvd	Greenwell Springs Rd	Airline Hwy		6.75
10	Siegen Lane	Airline Hwy	Perkins Rd		2.47
11	N Foster Dr	Florida Blvd	Greenwell Springs Rd		0.78
12	Government St	River Front	Jefferson Hwy		3.44
13	Jefferson Hwy	Airline Hwy	Government St		5.41
14	Staring Lane	Perkins Rd	Highland Rd		1.99
15	Essen Lane	Perkins Rd	Jefferson Hwy		1.86
16	Bluebonnet Rd	Jefferson Hwy	I-10		1.31
17	Burbank Dr	Gardere Ln	Bluebonnet Rd		0.92
18	Nicholson Dr	Roosevelt St	Burbank Dr		1.25
19	LA 1	I-10	ICWW		0.42
20	Greenwell Springs Rd	N Foster Dr	Sherwood Forest Blvd		5.24
21	Scenic Hwy	Airline Hwy	LA 64		10.67
22	Range Ave	Florida Blvd	I-12		2.29
			TOTAL	**45.36**	**105.63**

The map shown in Figure 6-12 was generated with DGPS point data, following the procedure described in Chapter 3. Both directions of travel on all 22 corridors, as well as physical discontinuities, were surveyed to construct corridor directional centerlines. Each directional centerline was then partitioned using 0.2-mi segments. This procedure resulted in a total of 2,397 segments Of these, 1,852 segments were located along the main routes. The remaining 545 segments were located on interchanges, on-ramps, off-ramps and intersecting streets.

Once the corridor network was surveyed and the directional centerline base map developed, a set of runs was scheduled to measure travel time and speed. Runs began in May 1995 and continued through July 1996. As a result, records for the Summer season of 1995, academic year 1995-1996, and Summer 1996 were gathered. Because the objective was to measure typical traffic congestion conditions, runs were not made for

three weeks at the beginning of the academic year to allow the network to stabilize. For a similar reason, runs were not scheduled during academic breaks such as the Christmas-New Year break or the Spring break. Runs were made during three traffic time periods: weekday morning (6:00 to 9:00 am), weekday afternoon (3:00 to 6:00 pm), and off peak (9:00 am to 3:00 pm). Off peak runs also included runs on selected Sunday mornings to obtain free flow speeds.

A total of 25,000 mi of travel runs on the 151-mi highway network were made, resulting in 428 GPS data files and 2.5 million GPS point records. The data reduction GIS application described previously was used to process these records, resulting in 155,300 segment records. On average, there were about 65 records per segment. Obviously, some corridors and segments ended up with more records than others, as shown in Table 6-2. Between May 1995 and May 1996, runs were made on all corridors, although efforts were concentrated on routes that were perceived to have the most severe congestion problems.

Shreveport

The Shreveport MPO, the Northwest Louisiana Council of Governments (NLCOG), defined a congestion corridor network composed of 10 corridors covering 93 mi (Figure 6-13). As shown in Table 6-3, of the 10 corridors, two were located on the Interstate highway system and covered 19 mi. The remaining seven corridors were located on principal arterials and covered 74 mi.

As in Baton Rouge, DGPS point data were used to construct the directional centerline base map shown in Figure 6-13. Each corridor directional centerline was then partitioned using 0.2-mi segments. This procedure resulted in a total of 1,473 segments.

covering 238 mi of directional centerlines. Of these, 1,092 segments were located along the main routes. The remaining 381 segments were located on interchanges, on-ramps, off-ramps and intersecting streets.

Table 6-2: Segment record summary by corridor and time period in Baton Rouge

Corridor			Summer 1995			Academic year 1995-1996			Summer 1996			Total
ID	Name	# segm.	6-9 am	Off peak	3-6 pm	6-9 am	Off peak	3-6 pm	6-9 am	Off peak	3-6 pm	
	Main route:											
1	I-10	219	2,314	3,614	2,507	7,101	1,937	6,036	2,404	1,019	2,286	**29,218**
2	I-110	115	2,695	4,710	3,540	3,431	501	2,456	132	517	9	**17,991**
3	I-12	194	2,127	3,238	2,518	4,532	1,343	3,037	3,117	601	2,256	**22,769**
4	LA 19	68	268	424	388	939	267	474				**2,760**
5	Plank Rd	181	949	1,297	1,126	1,647	570	544				**6,133**
6	Airline Hwy	277	2,392	4,369	2,832	6,013	2,278	3,738			2	**21,624**
7	Florida Blvd	190	1,913	1,933	1,645	4,148	2,423	3,226		159	158	**15,605**
8	Mickens Rd	34	170	187	221	235	121	245				**1,179**
9	Sherwood Forest	86	707	1,192	817	1,264	472	569				**5,021**
10	Siegen Lane	32	332	525	372	551	148	249				**2,177**
11	N Foster Dr	12	63	49	58	68	41	69				**348**
12	Government St	52	390	765	582	612	190	395		2	9	**2,945**
13	Jefferson Hwy	70	528	1,121	679	1,191	389	677				**4,585**
14	Staring Lane	20	220	251	232	493	204	270				**1,670**
15	Essen Lane	28	268	354	298	679	293	369				**2,261**
16	Bluebonnet Rd	18	88	96	94	315	160	193				**946**
17	Burbank Dr	10	104	130	109	217	83	131				**774**
18	Nicholson Dr	15				229	108	156	5	35	13	**546**
19	LA 1	6	13	45	49	68	20	34				**229**
20	Greenwell Springs	70	500	435	554	565	236	599				**2,889**
21	Scenic Hwy	125	426	635	568	1,287	248	842		4		**4,010**
22	Range Ave	30	139	114	148	523	383	300	26	2	19	**1,654**
	Subtotal	**1,852**	**16,606**	**25,484**	**19,337**	**36,108**	**12,415**	**24,609**	**5,684**	**2,339**	**4,752**	**147,334**
	Non-main route:	545	1,010	1,651	1,211	1,793	485	1,180	233	163	240	**7,966**
	Total	**2,397**	**17,616**	**27,135**	**20,548**	**37,901**	**12,900**	**25,789**	**5,917**	**2,502**	**4,992**	**155,300**

NLCOG made all runs between July 1995 and August 1996. They scheduled two runs per direction and per time period on each CMS corridor. Runs included four traffic time periods: AM peak (7:30 to 8:30 am), noon peak (12:00 to 12:30 pm), PM peak (4:30 to 5:30 pm), and off peak. The noon runs were made on the Kings Highway corridor, which was reported to exhibit congestion problems during the lunch hours. NLCOG made most off peak runs late at night, between 9:00 pm to 3:00 am.

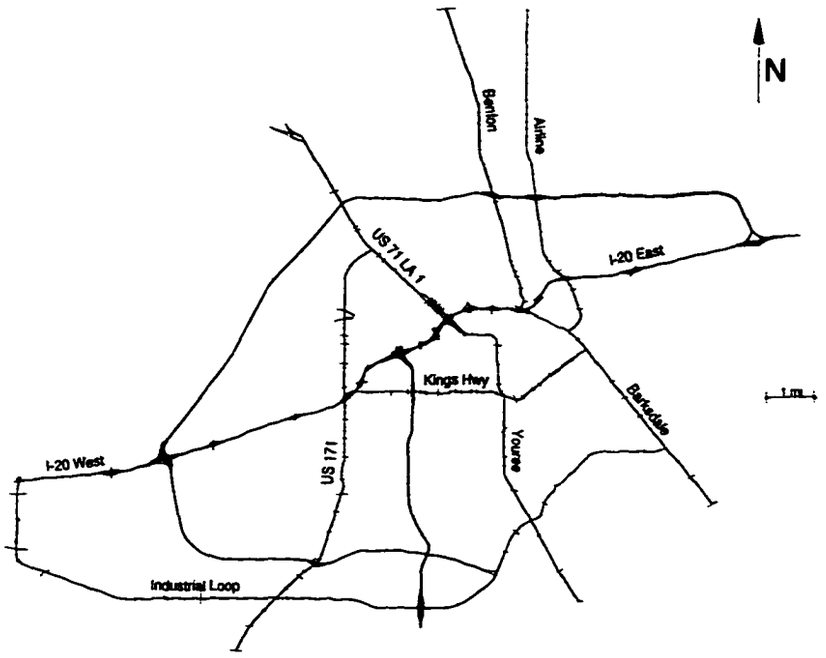

Figure 6-13: Congestion corridor network in Shreveport

Table 6-3: Congestion corridor network in Shreveport

ID	Name	From	To	Length (mi)	
				Interstate Highway	Principal Arterial
1	I-20 West	LA 526	Spring St	10.69	
2	I-20 East	Spring St	I-220	8.20	
3	US 71 LA 1	I-20	US 71 LA 1 Split		7.04
4	Youree	I-20	Flournoy Lucas		8.58
5	US 171	Williamson Way	Market St		11.57
6	Industrial Loop	I-20	Barksdale Blvd		18.58
7	Kings Hwy	Hearne Ave	Barksdale Blvd		5.76
8	Benton	Old Minden Rd	Kingston Rd		8.22
9	Airline	Barksdale Blvd	Kingston Rd		8.60
10	Barksdale Blvd	Airline Dr	Curtis Sligo Rd		5.54
			TOTAL	**18.89**	**73.89**

A total of 844 mi of travel runs on the 93-mi highway network were made, resulting in 100 GPS data files and 85,000 GPS point records. The data reduction GIS application described previously was used to process these records, resulting in 5,048 segment records. On average, there were about 3.4 records per segment. Obviously, some corridors and segments had more records than others, as shown in Table 6-4.

Table 6-4: Segment record summary by corridor and time period in Shreveport

Corridor			Time period				Total
ID	Name	# segm.	AM peak	Noon peak	PM peak	Off peak	
	Main route:						
1	I-20 West	122	203		202	64	469
2	I-20 East	95	173		169	88	430
3	US 71 LA 1	87	169		204	104	477
4	Youree	105	213		217	112	542
5	US 171	144	288		288	142	718
6	Industrial Loop	211	256		207	134	597
7	Kings Hwy	78		153	156	78	387
8	Benton	90	180		183	90	453
9	Airline	96	190		239	96	525
10	Barksdale Blvd	64	133	2	137	71	343
	Subtotal	1,092	1,805	155	2,002	979	4,941
	Non-main route:	381	42	0	49	16	107
	Total	1,473	1,847	155	2,051	995	5,048

New Orleans

The New Orleans MPO, the Regional Planning Commission (RPC), defined a congestion corridor network composed of 31 corridors covering 248 mi. For this study, data collection, data reduction, and data reporting was limited to seven corridors, covering 86 mi (Figure 6-14). As shown in Table 6-5, of the 7 corridors 3 were located on the Interstate highway system and covered 31 mi. The remaining 4 corridors were located on principal arterials and covered 54 mi.

RPC made all GPS runs with a GPS equipment configuration similar to that used in Baton Rouge (Figure 6-2). RPC staff made the runs for identifying both directions of travel and physical discontinuities on all 31 corridors. Actual travel time runs on the reduced seven-corridor network were made by a consultant to RPC.

As in Baton Rouge, DGPS point data were used to construct the centerline base map shown in Figure 6-14. Each corridor directional centerline was then partitioned using 0.2-mi segments. This procedure resulted in a total of 3,794 segments, covering 581 mi of directional centerlines. For the reduced network composed of corridors No. 1

to 7 (Table 6-5), the result was 1,338 segments and covered 214 mi of directional centerlines. 1,039 of these segments were located along the main routes. The remaining 299 segments were located on interchanges, on-ramps, off-ramps and intersecting streets.

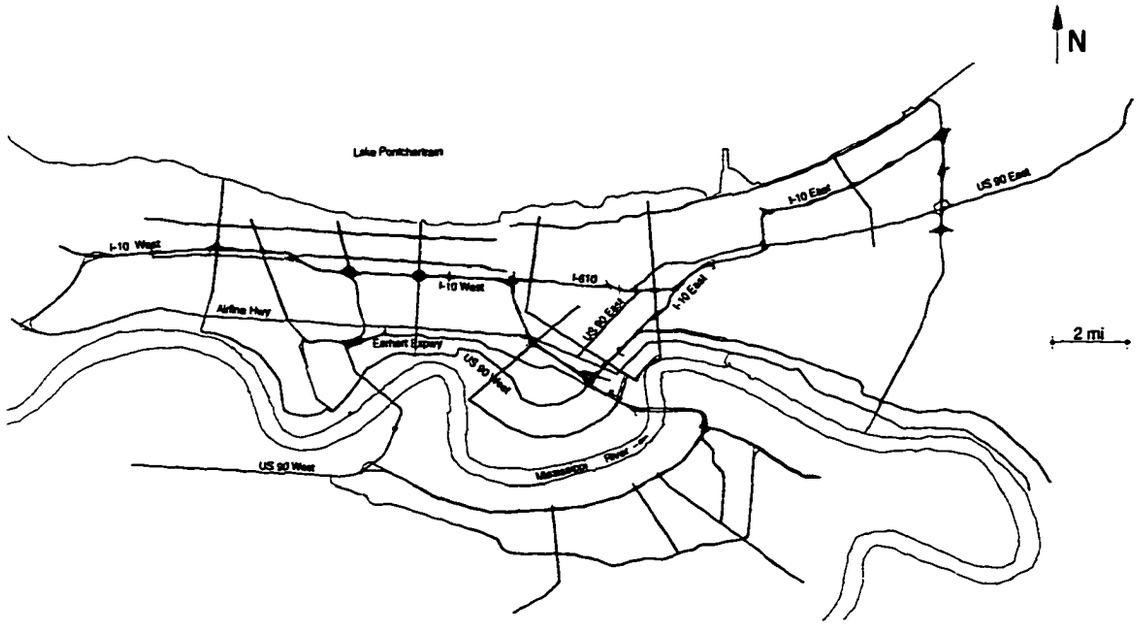

Figure 6-14: Congestion corridor network in New Orleans

Table 6-5: Congestion corridor network in New Orleans

ID	Name	From	To	Length (mi)	
				Interstate Highway	Principal Arterial
1	I-10 West	I-310	Poydras St at Camp	10.35	
2	I-10 East	Poydras St at Camp	I-510	16.30	
3	I-610	I-10 West	I-10 East	4.68	
4	Airline Hwy	Jefferson Parish line	Tulane at Loyola		15.37
5	US 90 East	Claiborne at Tulane	US 11 at US 90		16.71
6	Earhart Expwy	Hickory	Poydras at Loyola		5.22
7	US 90 West	Jefferson Parish line	Claiborne at Tulane		16.90
			TOTAL	**31.33**	**54.20**

RPC began making runs on June 1996. Since then, RPC has been collecting GPS data on a continuous basis, and it intends to continue doing so until the end of 1997. For

this research, data collected on corridors No. 1 to 7 between June and July 1996 were made available. In general, these runs were conducted during the AM peak (6-9 am) and PM peak (3-6 pm) time periods. A few GPS data points were collected outside these time periods, mainly after 9 am. For the most part, however, these extra points were collected during extremely heavy traffic conditions, possibly due to incidents. As a result, these data should not be considered representative of off peak traffic conditions.

A total of 3,805 mi of travel runs were made, resulting in 68 GPS data files and 322,000 GPS point records. The data reduction GIS application described previously was used to process these records, resulting in 22,613 segment records. On average, there were about six records per segment. Obviously, some corridors and segments ended up with more records than others, as shown in Table 6-6.

Table 6-6: Segment record summary by corridor and time period in New Orleans

Corridor			Time period			Total
ID	Name	# segm.	6-9 am	3-6 pm	Other	
	Main route:					
1	I-10 West	115	2,027	1,643	359	**4,029**
2	I-10 East	194	3,093	2,741	711	**6,545**
3	I-610	56	3,330	1,967	178	**5,475**
4	Airline Hwy	186	419	348	92	**859**
5	US 90 East	201	796	863	127	**1,786**
6	Earhart Expwy	58	457	261		**718**
7	US 90 West	229	658	566	21	**1,245**
	Subtotal	**1,039**	**10,780**	**8,389**	**1,488**	**20,657**
	Non-main route:	299	669	412	54	**1,135**
	Other corridors:	2,456	379	346	96	**821**
	Total	**3,794**	**11,828**	**9,147**	**1,638**	**22,613**

Chapter 7
ANALYSIS

The preceding chapters described the development and implementation of a methodology using GPS receivers and GIS technology for conducting travel time studies. As mentioned in Chapter 6, implementation of the methodology was carried out as part of the Congestion Management System (CMS) project [Bullock and Quiroga, 1996] which included three metropolitan areas in Louisiana: Baton Rouge, Shreveport, and New Orleans. During the implementation phase, several decisions based upon engineering judgment were made, including the use of 0.2-mi segments and 1-Hz GPS sampling rates. Unfortunately, some of these decisions could not be tested before the full project implementation was undertaken because of tight deadlines imposed by the project schedule. Now that large amounts of travel time data have been collected, this dissertation research provided the opportunity to go back and analyze some of the important parameters of the new GPS-GIS methodology.

The analysis in this chapter focuses on four areas: aggregation levels, sampling rates, central tendency, and dispersion. The aggregation level analysis examines the effect of using different highway segment lengths. The sampling rate analysis addresses the effect of collecting GPS data at different time intervals. The central tendency analysis compares harmonic mean speeds and median speeds. The dispersion analysis examines variations and reliability of the central tendency estimators.

Aggregation Levels

Examples 1, 2, and 3 described in Chapter 3 were based on a nominal 0.2-mile segmentation scheme. With this scheme, 0.2-mi segments were used throughout the network, except where shorter segments were required because of lack of space for a 0.2-mi segment. For consistency, these shorter segments were always placed immediately after physical discontinuities. This explains the lengths associated with segments 12453, 12454, 12451, and 12450, located immediately after the I-10&I-12 split in Baton Rouge (Figure 3-3, Table 3-3). However, segmentation schemes based on nominal segment lengths other than 0.2 mi are also possible. Shorter segments require a larger number of segments but the corresponding aggregated speeds tend to be closer to the original GPS point speeds. Conversely, longer segments require a fewer number of segments but the corresponding aggregated speeds tend to deviate from the original GPS point speeds.

How close or how far aggregated speeds are with respect to the original GPS speeds is a function of traffic characteristics. To illustrate this point, consider the four groups of speed-distance profiles of Figure 7-1. Each group contains from five to eight profiles that represent the variation of GPS speeds along the route considered. Each profile is associated with a single travel time run. Dates, starting times, ending times, and total travel times associated with each run are summarized in Table 7-1. For completeness, Figure 7-1 also shows median speeds for each route. These median speeds were obtained from all runs made from September 1995 to May 1996 and represent a measure of central tendency. A more detailed discussion on the use of median speeds is provided in the central tendency section of this chapter.

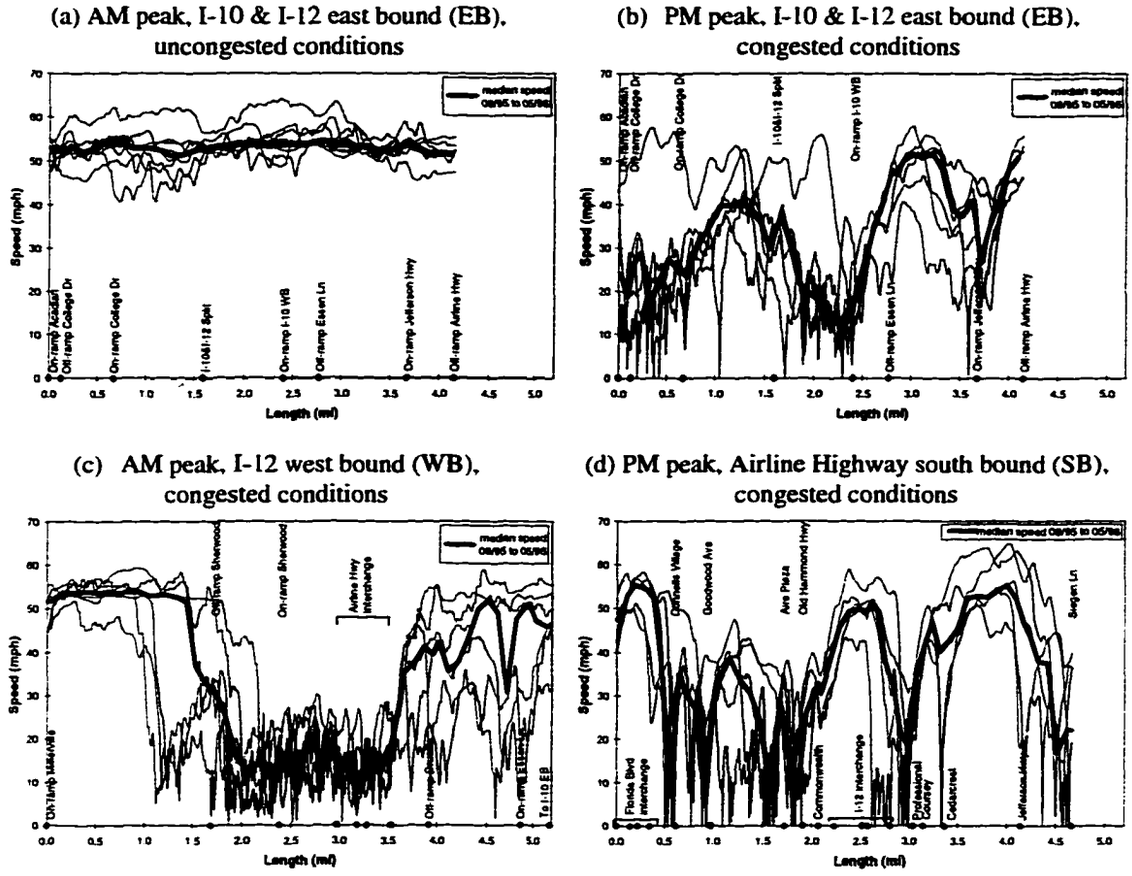

Figure 7-1: Speed-distance profiles using GPS on selected corridors in Baton Rouge, Louisiana

Figure 7-1a shows that AM peak traffic flow on the I-10 & I-12 corridor (EB) is fairly uniform, with median speeds slightly above 50 mph. As a result, it may be reasonable to assume that relatively long segments (1 mile long or longer) could be used to aggregate AM peak GPS speeds without causing a significant loss in data quality. In contrast, Figure 7-1b shows that PM peak traffic flow on the same corridor is highly variable, with actual speeds ranging from 0 to 60 mph and median speeds ranging from 10 to 50 mph. In this case, relatively long segments (1 mile long or longer) would result in a significant loss in data quality and, therefore, shorter segments would be required.

Figure 7-1c and Figure 7-1d further illustrate this point. Figure 7-1c is an interesting case because it shows two distinct changes in traffic behavior at about 1/3 and 2/3 of the total 5.18-mi distance. The middle 1/3 seems to indicate a need for relatively long segments, whereas the first 1/3 and the last 1/3 seem to indicate a need for shorter segments.

Table 7-1: Dates and time periods associated with the runs shown in Figure 7-1

(a) AM peak, I-10&I-12 EB, uncongested conditions

Date	Start Time	End Time	Total Travel Time (min)
09/28/95	7:21:57 am	7:26:33 am	4:36
10/02/95	7:40:19 am	7:44:53 am	4:34
10/03/95	7:10:12 am	7:15:13 am	5:01
10/04/95	7:25:00 am	7:29:56 am	4:56
01/08/96	7:18:29 am	7:23:09 am	4:40
01/23/96	7:09:25 am	7:13:41 am	4:16
02/01/96	7:15:16 am	7:19:59 am	4:43
02/12/96	7:30:20 am	7:35:01 am	4:41

(b) PM peak, I-10&I-12 EB, congested conditions

Date	Start Time	End Time	Total Travel Time (min)
10/16/95	5:11:51 pm	5:21:33 pm	9:42
10/18/95	4:36:25 pm	4:46:11 pm	9:46
10/23/95	4:58:59 pm	5:10:10 pm	11:11
01/11/96	4:56:18 pm	5:09:39 pm	13:21
03/25/96	4:55:12 pm	5:03:16 pm	8:04
03/28/96	5:05:33 pm	5:11:43 pm	6:10

(c) PM peak, I-12 WB, congested conditions

Date	Start Time	End Time	Total Travel Time (min)
09/28/95	7:02:19 am	7:15:02 am	12:43
10/02/95	7:21:13 am	7:35:01 am	13:48
10/03/95	7:06:54 am	7:28:42 am	21:48
10/04/95	7:07:57 am	7:19:28 am	11:31
01/23/96	7:40:15 am	7:54:00 am	13:45
02/01/96	7:33:53 am	7:52:49 am	18:56
02/12/96	8:11:48 am	8:22:45 am	10:57

(d) PM peak, Airline Highway SB, congested conditions

Date	Start Time	End Time	Total Travel Time (min)
11/28/95	4:47:00 pm	5:00:56 pm	13:56
02/06/96	5:11:18 pm	5:26:20 pm	15:02
03/07/96	4:54:03 pm	5:03:44 pm	9:41
03/26/96	4:44:40 pm	4:58:45 pm	14:05
04/26/96	4:39:20 pm	4:54:15 pm	14:55

In theory, the sampling theorem discussed in Chapter 3 [Tobler, 1987] could be used to estimate required segment lengths depending on the need to detect specific traffic flow effects. For example, Figure 7-1b shows that the I-10 & I-12 split has some effect on the traffic behavior on the I-10 & I-12 corridor (EB). Since the total length of the disturbance generated by this physical discontinuity is around 0.3 miles, the longest segment that could be used to detect its effect would have to be 0.15 miles. Obviously, in order to apply the sampling theorem in this context, it would be necessary to have a fairly

good idea of the size of the disturbance. One way to accomplish this would be by using fairly short segments for the data reduction process and then aggregating the resulting segment data as needed, following the mathematical model described in Chapter 3. Another way would be by using dynamic segmentation techniques, which is discussed in Chapter 8.

Evaluation of Alternative Aggregation Levels

To evaluate the effect of using different segment lengths, seven segmentation schemes were considered for each of the conditions shown in Figure 7-1. These segmentation schemes are summarized in Table 7-2.

Table 7-2: Summary of segmentation schemes

Corridor	Length (mi)	Item	Segmentation scheme						
			1	2	3	4	5	6	7
I-10 & I-12 EB		No. of segments	42	21	10	6	3	2	1
	4.15	Segment length (mi)	0.099	0.197	0.415	0.691	1.38	2.07	4.15
I-12 WB		No. of segments	52	26	13	6	3	2	1
	5.18	Segment length (mi)	0.100	0.199	0.398	0.863	1.73	2.59	5.18
Airline Hwy SB		No. of segments	48	24	12	6	3	2	1
	4.66	Segment length (mi)	0.097	0.194	0.388	0.777	1.55	2.33	4.66

To cover a wide range of segment lengths, the seven segmentation schemes were structured so that each segment length was approximately twice as long as the next lower segment length, beginning with approximately 0.1 mi. Each segmentation scheme was structured so that the total length considered was divided into segments of equal length. For example, for the 4.15-mi section of the I-10&I-12 corridor EB, segmentation scheme No. 4 implied the use of 6 segments of 0.691-mi each. By having segments of equal length, it became easier to determine whether the specific segmentation scheme was capable of detecting the effect of physical discontinuities.

The data reduction procedure was then applied to each of the seven segmentation schemes in order to obtain segment speed using data from the GPS runs described in Table 7-1. As an illustration, Figure 7-2 shows the corresponding speed-distance profiles for each of the seven segmentation schemes on the I-10 & I-12 corridor EB (Table 7-2) using data from the six PM peak runs described in Table 7-1b. For visualization purposes, each profile was constructed by drawing straight lines connecting points located half way along the segments.

A comparison between the profiles of Figure 7-1b and those of Figure 7-2 clearly indicates that using segments longer than 1.38 mi long resulted in an almost complete loss of data compared to the original GPS speed data (Figure 7-2e through Figure 7-2g). Using 0.415-mi to 0.691-mi segments (Figure 7-2c and Figure 7-2d) resulted in a better fit between GPS speed data and aggregated segment speed data because the effects of the I-10 WB on-ramp and the Jefferson Highway on-ramp became apparent. These observations turned out to be consistent with the sampling theory concepts discussed previously because both 0.415 mi and 0.691 mi not only were smaller than 1.38 mi but also smaller than half the total length of the disturbances generated by the I-10 WB on-ramp and the Jefferson Highway on-ramp (around 2 mi and 1.5 mi, respectively). Using 0.099-mi to 0.197-mi segments (Figure 7-2a and Figure 7-2b) resulted in an even better fit between the original GPS speed data and the aggregated segment speed data because the effects of practically all physical discontinuities became visible. Only the effects of microscopic acceleration-deceleration patterns were not replicated. To replicate these effects, segment lengths much shorter than 0.1 miles would have been required.

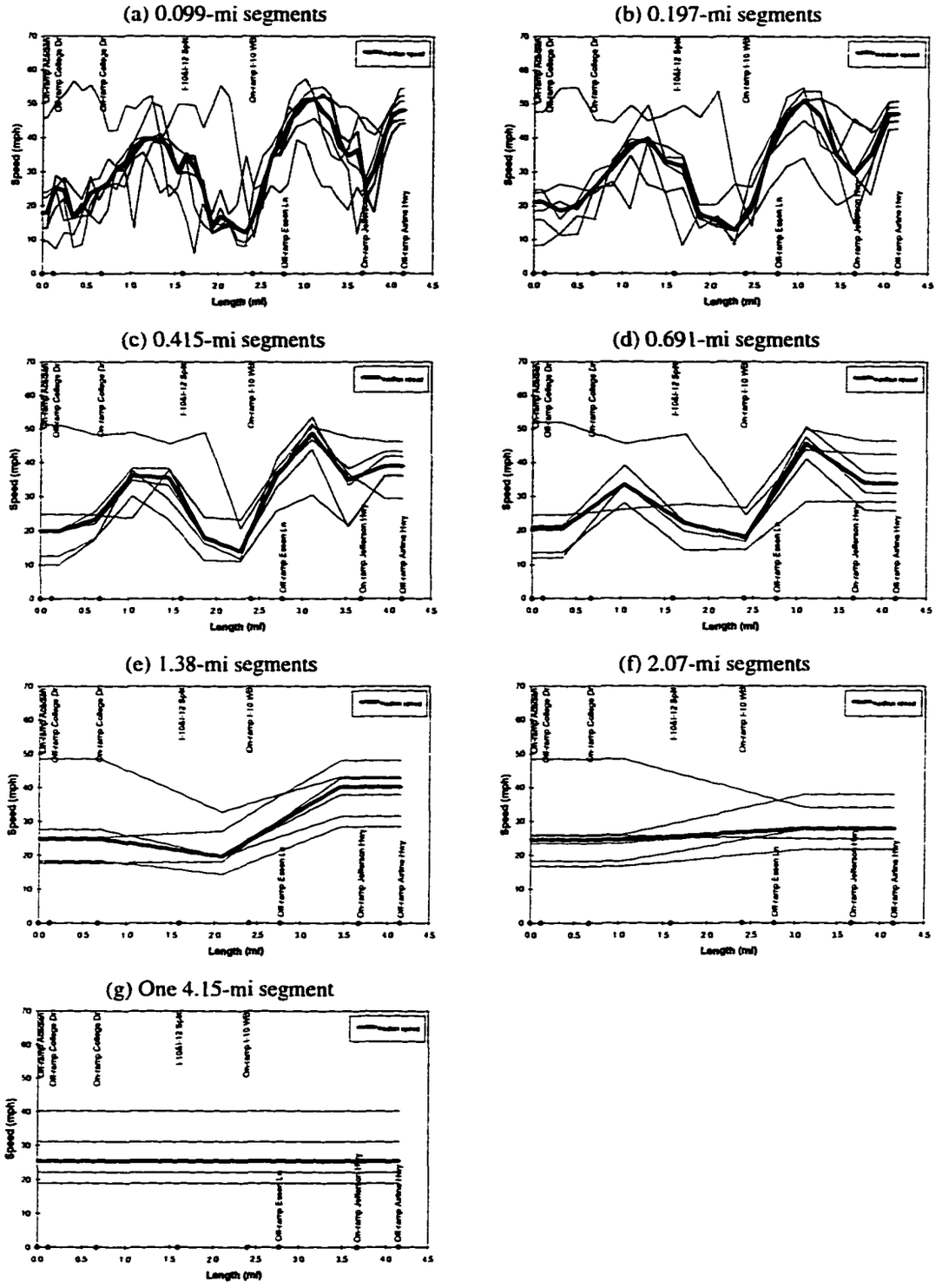

Figure 7-2: PM peak speeds on the I-10 & I-12 corridor using various segment lengths for GPS speed data aggregation

It may be interesting to compare the speed-distance profiles of Figure 7-2 with those resulting from the use of single links connecting physical discontinuities. The reason is that links are normally the shortest spatial units used for computing speeds and travel times [Robertson, 1994] [TRB, 1994], and also represent what many drivers perceive to be the minimum useful lengths for trip planning purposes. The speed-distance profiles for the link-based segmentation scheme are shown in Figure 7-3. For consistency with the profiles of Figure 7-2, the profiles of Figure 7-3 were also constructed by drawing straight lines connecting points located half way along the segments. Notice that with the link segmentation scheme, only the effect of the I-10 WB on-ramp was evident. The effect of other physical discontinuities, particularly the Jefferson Highway on-ramp, were hinted at but not clearly demonstrated. This is an indication that link-based travel time studies are not sufficient and that finer levels of resolution are needed to characterize localized effects properly.

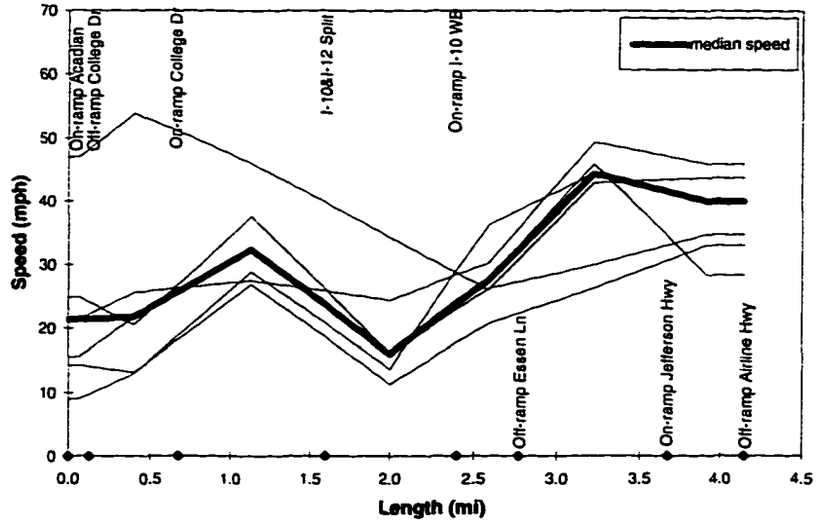

Figure 7-3: PM peak speeds on the I-10 & I-12 corridor using single links between physical discontinuities for GPS speed data aggregation

Speed-distance profiles like those included in Figure 7-2 only provide a rough, qualitative way of determining segment lengths. However, it is also necessary to provide a quantitative measure to evaluate alternative segment lengths. The procedure to compute such a measure is explained below.

Speed Residual Distributions

In order to provide a quantitative measure of the improvement in fit for smaller segment lengths, an analysis was made of the distributions of differences between original GPS speeds and aggregated speeds (or speed residuals). As shown in Figure 7-4, each GPS speed had a residual with respect to its corresponding aggregated speed.

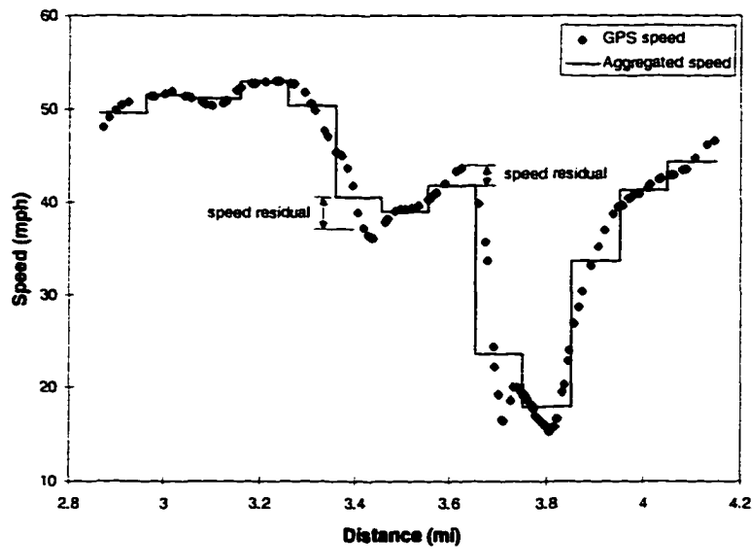

Figure 7-4: Comparison between original GPS speeds and aggregated speeds (using 0.099-mi segments)

Initially, it was expected that residuals would be normally distributed around a mean of zero. However, as shown in Figure 7-5, for segments smaller than 0.5 miles, the distributions of residuals tended to be more peaked, i.e. they had a positive kurtosis

[Duncan, 1986], than the corresponding theoretical normal distribution (zero kurtosis). For segments larger than 0.5 miles, the distributions of residuals did flatten considerably (in several cases the kurtosis became negative) but, still, they did not fit a normal distribution. In most cases, regardless of segment length, the distributions of residuals tended to be symmetric around zero. When checked for normality using the Kolmogorov-Smirnov test (see page 105 for a more complete description on the use of this test), the corresponding D values were larger than 6.3. For example, for the distributions shown in Figure 7-5, the D values for 0.099-mi and 0.197-mi segments were 8.08 and 8.30, respectively. Since these values were larger than 6.3, there was statistical evidence that the distributions of residuals did not fit a normal distribution.

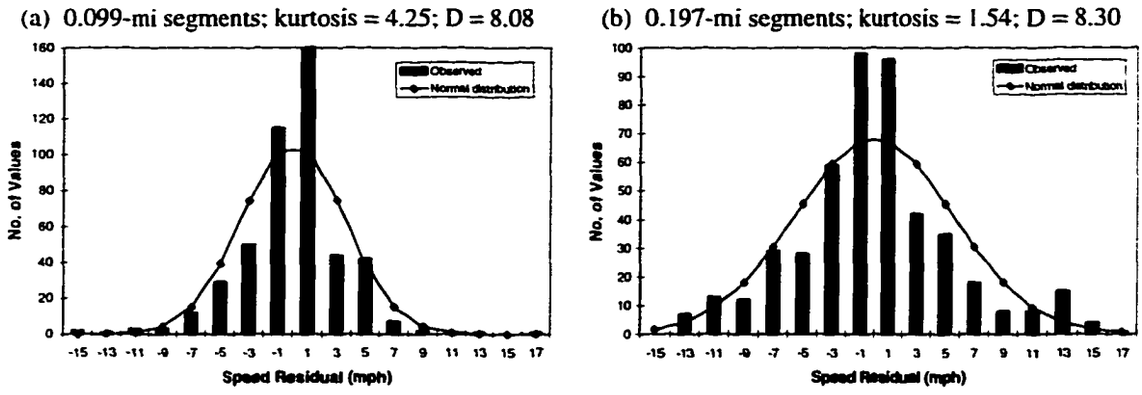

Figure 7-5: Comparison between speed residual distributions and the normal distribution (PM peak run made on I-10 & I-12 EB on October 16, 1995)

The distributions of residuals seemed to suggest a double exponential distribution, also known as the Laplace distribution [Hahn and Meeker, 1991]. The probability density function of the double exponential distribution of speed residuals r, assuming a mean of zero and a standard deviation σ, is of the form

$$f(r,\sigma)=\frac{1}{2\sigma}\exp(-|r|/\sigma) \tag{7-1}$$

This function has a continuous first derivative except at the peak center at r = 0. This discontinuity causes a difficulty when testing whether the distributions of residuals fit the double exponential distribution because negative r values must be analyzed separately from positive r values. However, since distributions of speed residuals were symmetric, the difficulty mentioned above was solved by reducing speed residuals to absolute speed residuals and by analyzing the corresponding distributions of absolute speed residuals.

The analysis of the distributions of absolute speed residuals was made using cumulative probability dot plots like those shown in Figure 7-6 [Meeker and Escobar, 1997]. Figure 7-6 shows that absolute speed residuals had a tendency to follow straight lines on semi-log paper (arithmetic scale for residuals and logarithmic scale for probabilities) for segment lengths smaller than 0.5 miles and probability values larger than 10% (actually 5% for segment lengths smaller than 0.2 miles). Figure 7-6 indicates the probability that an individual absolute speed residual will be larger than the absolute speed residual shown. For example, in Figure 7-6b, the probability that an absolute speed residual will be larger than 6 mph is about 9% when using 0.099-mi segments; 22% when using 0.197-mi segments; 32% when using 0.415-mi segments, and so on.

To construct the dot plots shown in Figure 7-6, the series of individual absolute speed residuals associated with a single travel time run were ordered in descending order. A plotting position value, which represents the probability that a speed residual value can be exceeded, was then assigned to each speed residual. The formulation used to calculate plotting position values was [Meeker and Escobar, 1997]

$$P_o = \frac{i-0.5}{n} 100\% \qquad (7\text{-}2)$$

where P_o is the cumulative probability associated with a speed residual located in the i position, assuming a descending sequence composed of n speed residuals.

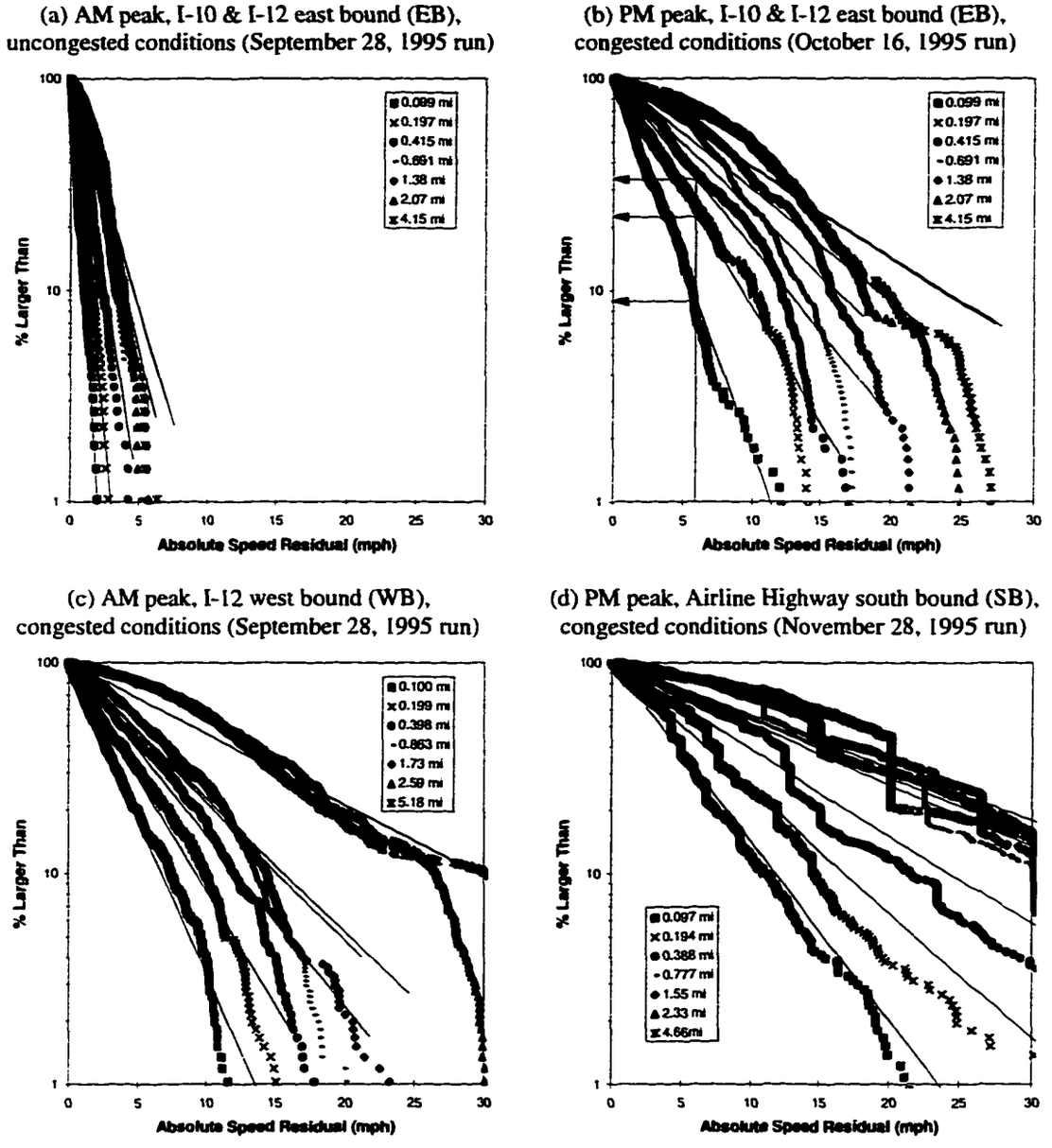

Figure 7-6: Exponential probability plots for selected runs in Baton Rouge, Louisiana (dots represent individual speed residuals; solid lines represent theoretical values)

To construct the solid lines in Figure 7-6, theoretical negative exponential distributions were plotted. The mathematical formulation of the cumulative negative exponential distribution is given by

$$P_t = \left[\exp\left(-|r|/\bar{r}\right)\right]100\% = \left[\exp\left(-|r|/\sigma_{|r|}\right)\right]100\% \qquad (7\text{-}3)$$

where P_t is theoretical probability; $\bar{r}$ is average absolute speed residual; and $\sigma_{|r|}$ is standard deviation of the series of absolute speed residuals. In the case of the negative exponential distribution, $\sigma_{|r|}$ is equal to $\bar{r}$.

An example of the procedure to compute observed and theoretical probabilities is included in Table 7-3. The GPS data used correspond to the PM peak travel time run conducted on the I-10 & I-12 corridor (EB) on October 16, 1995. The aggregated speeds are those resulting from the use of 0.099-mi segments. Both observed and theoretical probabilities are shown in Figure 7-6b.

Table 7-3: Observed and theoretical probabilities for the October 16, 1995 PM peak run on I-10 & I-12 EB (segment length: 0.099 mi; n = 473; $\bar{r}$ = 2.46 mph)

i[1]	GPS point time stamp (hh:mm:ss)	GPS point location (mi)	GPS speed (mph)	Aggregated speed[2] (mph)	Absolute speed residual r (mph)	Observed cum. prob. P_o Eqn. (7-2) (%)	Theoretical cum. prob. P_t Eqn. (7-3) (%)
1	5:20:31 pm	3.66	39.90	23.58	16.32	0.11	0.13
2	5:13:19 pm	0.493	5.30	20.55	15.25	0.32	0.21
3	5:13:18 pm	0.491	5.60	20.55	14.95	0.53	0.23
:		:	:	:	:	:	:
106	5:16:06 pm	1.87	23.50	27.39	3.89	22.30	20.61
107	5:16:40 pm	1.98	10.00	13.87	3.87	22.52	20.75
108	5:12:20 pm	0.114	25.30	29.02	3.72	22.73	22.10
:		:	:	:	:	:	:
471	5:17:03 pm	2.08	14.80	14.78	0.022	99.47	99.10
472	5:15:25 pm	1.53	29.40	29.41	0.010	99.68	99.59
473	5:17:57 pm	2.28	12.30	12.29	0.009	99.89	99.65

[1] Table ordered in descending order of absolute speed residual

[2] Aggregated speed is the arithmetic average of all GPS speeds associated with a segment (Figure 7-4)

The Kolmogorov-Smirnov test [Massey, 1951] [Ostle and Mensing, 1975] was used to test quantitatively whether the observed probability distributions actually fitted an exponential distribution. With this test, the maximum absolute difference D between corresponding P_o and P_t values is computed. If the observed D value is smaller than a critical D value at a specified significance level, the hypothesis that the observed distribution fits the theoretical distribution cannot be rejected. As a reference for the reader, a sample of critical D values is shown in Table 7-4.

Table 7-4: Critical D(%) values used for the Kolmogorov-Smirnov test (adapted from Massey [1951])

	Level of significance α				
n	0.20	0.15	0.10	0.05	0.01
1	90	92	95	98	99
2	68	73	78	84	93
3	56	60	64	71	83
:	:	:	:	:	:
25	21	22	24	27	32
30	19	20	22	24	29
35	18	19	21	23	27
>35	$107/\sqrt{n}$	$114/\sqrt{n}$	$122/\sqrt{n}$	$136/\sqrt{n}$	$163/\sqrt{n}$

Table 7-5 shows both critical and observed D values for the travel time runs shown in Figure 7-6. For simplicity, only the critical D values for a 0.05 significance level α are included. Table 7-5 shows in bold the observed D values that turned out to be smaller than the corresponding critical D values. In these cases, the hypothesis that the observed distributions fitted an exponential distribution could not be rejected at the 0.05 significance level.

The general trend was that observed D values were smaller than critical D values for segment lengths smaller than 0.5 miles. The exceptions were the 0.415-mi segmentation scheme for the PM peak run on I-10 & I-12 EB and all segmentation

schemes for the PM peak run on Airline Highway. In these two cases, there was evidence to reject the hypothesis that the observed distributions fitted an exponential distribution. In the case of the Airline Highway plots, there were jumps that became more evident as the segment length increased. These jumps were due to those periods of time when the probe vehicle was actually stopped at a signalized intersection. While the GPS speeds were zero, the segment aggregated speeds were not. As a result, the corresponding speed residuals were larger than zero and equal in magnitude to the segment aggregated speeds. In general, however, a closer examination of the trends shown in Figure 7-6b (for 0.415-mi segments) and Figure 7-6d (for segments shorter than 0.5 mi) reveals that the difference between the observed distribution of residuals and the theoretical distribution of residuals was not too large. This is an indication that the exponential distribution could still be used reasonably well to describe the corresponding distributions of absolute speed residuals.

Table 7-5: Comparison between critical and observed D values for the travel time runs shown in Figure 7-6

Travel time run	n	Critical D (%) for α=0.05	Item	Segmentation scheme (Table 7-2)						
				1	2	3	4	5	6	7
AM peak, I-10 & I-12 EB (September 28, 1995 run) (Figure 7-6a)	243	8.7	Segment length (mi)	0.099	0.197	0.415	0.691	1.38	2.07	4.15
			$\bar{r}$ (mph)	0.43	0.64	1.10	1.61	1.70	2.00	2.01
			Actual D (%)	4.5	3.3	7.8	9.5	8.9	18.2	13.3
PM peak, I-10 & I-12 EB (October 16, 1995 run) (Figure 7-6b)	473	6.3	Segment length (mi)	0.099	0.197	0.415	0.691	1.38	2.07	4.15
			$\bar{r}$ (mph)	2.46	4.00	5.42	6.98	8.26	10.30	10.19
			Actual D (%)	3.2	3.2	8.0	14.9	13.8	18.9	15.8
AM peak, I-12 WB (September 28, 1995 run) (Figure 7-6c)	632	5.4	Segment length (mi)	0.100	0.199	0.398	0.863	1.73	2.59	5.18
			$\bar{r}$ (mph)	2.96	4.03	5.33	6.59	6.80	12.84	12.88
			Actual D (%)	3.3	3.9	5.2	8.9	8.4	16.8	15.2
PM peak, Airline Hwy SB (November 28, 1995) (Figure 7-6d)	736	5.0	Segment length (mi)	0.097	0.194	0.388	0.777	1.55	2.33	4.66
			$\bar{r}$ (mph)	5.12	7.31	10.55	15.00	16.60	16.02	17.41
			Actual D (%)	11.4	11.3	11.5	16.1	17.1	16.4	20.1

Prior to selecting the Kolmogorov-Smirnov test for determining goodness of fit in this dissertation, another commonly used test, the χ^2 test [May, 1990], was tried. To

apply this test, absolute residuals were grouped into intervals and the total number of observations within each interval was compared with theoretical negative exponential distribution values. Unfortunately, the χ^2 test tended to produce inconsistent results. For example, there were cases of observed distributions having different shapes which ended up with very similar χ^2 values. Figure 7-7 clearly shows this situation. There were also cases of observed distributions having seemingly similar shapes which ended up with very different χ^2 values. Finally, many χ^2 values turned out to be very sensitive to the number of intervals and interval size used. These inconsistencies agree with reports in the literature [Massey, 1951] [Ostle and Mensing, 1975]. These reports indicate that one of the weaknesses of the χ^2 test is that the grouping procedure results in a significant loss of information, particularly for large sample sizes. By comparison, with the Kolmogorov-Smirnov test individual observations can be treated separately which means that no loss of information occurs.

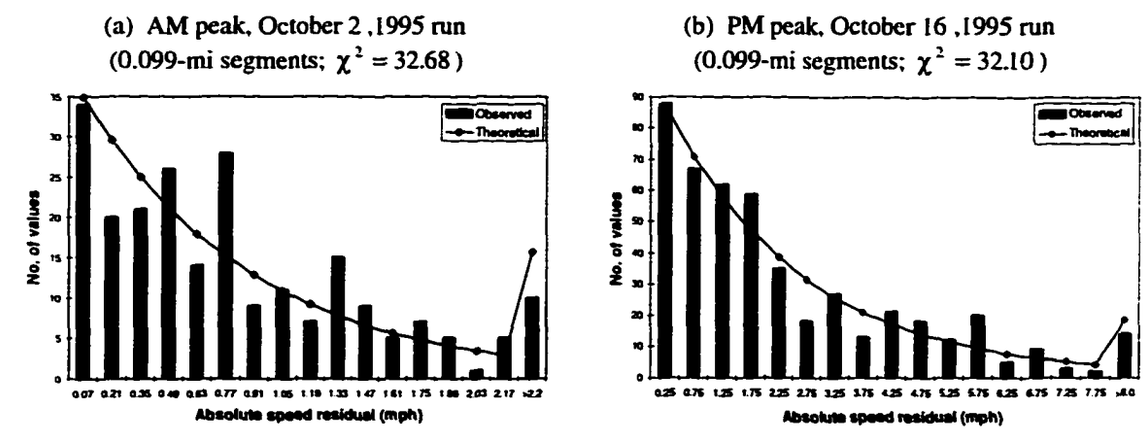

Figure 7-7: Comparison between distribution of average absolute speed residuals and the exponential distribution (travel time runs made on I-10 & I-12 EB)

Effect of Segment Length on Speed Residuals

In the previous section, speed residuals were reduced to absolute speed residuals as an artifact to demonstrate the feasibility of using the double exponential distribution to fit the distributions of residuals. The analysis then focused on testing whether the distributions of absolute speed residuals fitted a negative exponential distribution. This analysis showed that for segments smaller than 0.5 mi, the negative exponential distribution was indeed appropriate to model the distributions of absolute speed residuals. Only one parameter, $\bar{r}$ (or $\sigma_{|r|}$), was used to characterize absolute speed residuals. This was possible only because in a negative exponential distribution the mean and the standard deviation are the same. However, since standard deviation measures dispersion with respect to the mean, and since the mean of the actual distributions of residuals is zero, not $\bar{r}$, the conclusion is that $\sigma_{|r|}$ has to be less than the standard deviation σ of the actual distribution of residuals. This means that using $\bar{r}$ or $\sigma_{|r|}$ to characterize the actual distributions of residuals would have the effect of underestimating the actual dispersion of the GPS speeds with respect to the corresponding aggregated speeds.

Like $\sigma_{|r|}$, σ varies with segment length, as shown in Figure 7-8. Each curve represents the relationship between segment length and σ for each of the travel time runs described in Table 7-1. Notice that the effect of segment length on σ is particularly significant for segment lengths smaller than 0.5 mi. For larger segment lengths, that effect tends to decrease until, eventually, it becomes negligible for segment lengths larger than 1.5 mi. Obviously, there are numerical differences between plots, particularly between the AM and PM plots for the I-10&I-12 section (Figure 7-8a and Figure 7-8b).

However, plots associated with congested conditions tend to exhibit a similar behavior, particularly for segment lengths shorter than 1 mi. For example, the PM plots for the Interstate highway sections (Figure 7-8b and Figure 7-8c) suggest σ values of about 3 mph for 0.1-mi segments, and 5 mph for 0.2-mi segments.

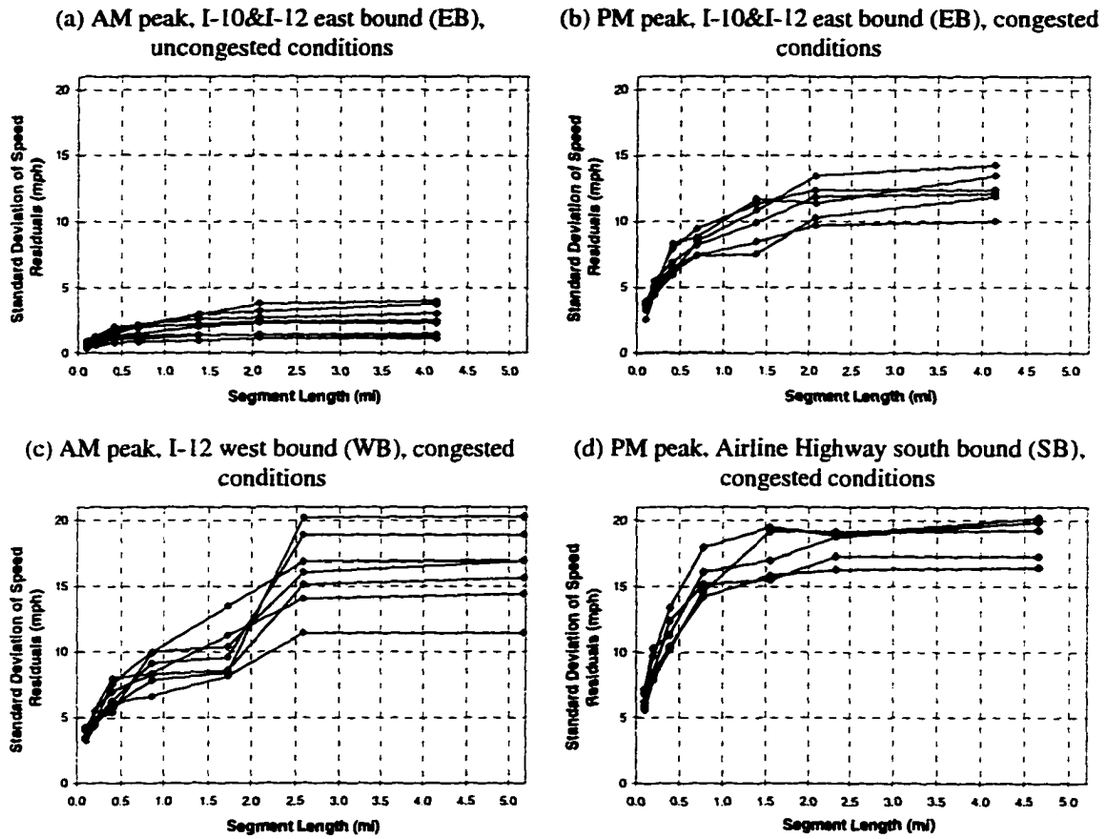

Figure 7-8: Effect of segment length on standard deviations of speed residuals

The plots for the Airline Highway runs (Figure 7-8d) show larger σ values for the same segment lengths (7 mph and 9 mph, respectively). The Airline Highway section considered is a signalized highway, as opposed to I-10 and I-12 which are controlled access facilities. This is a clear indication that data collected on signalized highways

need shorter segment lengths than controlled access facilities in order to achieve similar speed residual levels.

Some I-12 WB plots (Figure 7-8c) show a large jump in σ values when moving from 1.73-mi to 2.59-mi segments. As shown in Figure 7-1c, this phenomenon is closely related to sharp changes in traffic behavior at about 1.6 mi and 3.6 mi, i.e. at about 1/3 and 2/3 of the total 5.18-mi distance. As a result, it is reasonable to expect relatively modest increases in speed residuals when moving from 6 segments 0.86-mi long to 3 segments 1.73-mi long, but then large jumps in speed residuals when moving from 3 segments 1.73-mi long to 2 segments 2.59 mi long.

Probability values associated with individual speed residuals can be obtained by integrating equation (7-1). For example, the probability that a speed residual will be larger than a specified value is given by

$$P = \left[\exp\left(-|r|/\sigma\right)\right]100\% \tag{7-4}$$

As an illustration, assume σ = 5 mph (value obtained for 0.2-mi segments on I-10 and I-12). The probability that a speed residual will be larger than 5 mph is about 37%; the probability that a speed residual will be larger than 10 mph is about 14%; and the probability that a speed residual will be larger than 15 mph is about 5%.

Sampling Rates

As described in Chapter 3, GPS receiver sampling rates play an important role in defining the number of GPS points that can be associated with a segment. As an illustration, Table 3-1 (page 27) showed the maximum number of GPS points that could be associated with a segment for various combinations of segment length and speed,

assuming a sampling rate of 1 Hz (maximum sampling rate of the GPS equipment used in this research). Lower sampling rates would obviously result in a lower number of GPS points per segment. From sampling theory [Tobler, 1987], the minimum sampling rate should be such that there are at least two GPS points per segment. As shown in Table 3-2a (page 28), this means that the time interval between consecutive GPS points should be at most half the segment travel time values included in Table 3-1.

Because of their role in defining the number of GPS points per segment, sampling rates also have an effect on average segment speeds. If the speeds of the GPS points associated with a segment are relatively uniform, the effect of a varying sampling rate on the corresponding average segment speeds should be minor. In general, though, variations in average segment speed are expected to grow as the sampling rate decreases (i.e., the time interval increases) because of the uncertainty associated with a lower number of GPS points per segment.

Sampling Rate Schemes

To determine the effect of sampling rate variations on the number of GPS points per segment and the uncertainty of segment speeds, six subsets were generated from the data associated with each of the GPS runs described in Table 7-1. The six subsets were the result of assuming six different sampling rates as follows:

- 1 Hz (time interval of 1 second)
- 0.5 Hz (time interval of 2 seconds)
- 0.2 Hz (time interval of 5 seconds)
- 0.1 Hz (time interval of 10 seconds)

- 0.06667 Hz (time interval of 15 seconds)
- 0.05 Hz (time interval of 20 seconds).

Each subset was then applied to the conditions described in Figure 7-1 (I-10 & I-12 EB AM and PM peaks; I-12 WB PM peak; and Airline Highway PM peak). For simplicity, only one segmentation scheme was considered (0.197-mi segments for I-10 & I-12 EB; 0.199-mi segments for I-12 WB; and 0.194-mi segments for Airline Highway SB).

For each condition and travel time run subset, the corresponding number of GPS points and average speed per segment were obtained. As an illustration, Table 7-6 shows the number of GPS points per segment and segment speed for the six sampling intervals evaluated for the PM peak run of October 16, 1995 on the 4.15-mi section of I-10 & I-12 EB (Figure 7-1b). For example, for the first 0.197-mi segment (i.e. from 0 to 0.197 mi), assuming a time interval of 1 second, the number of GPS points were 34 and the segment speed was 18.46 mph. Likewise, for the same segment, assuming a time interval of 20 seconds, the number of GPS points was 2 and the segment speed was 10.60 mph. Notice that as the sampling rate decreased (i.e., as the time interval increased), the number of GPS points per segment decreased and the variation in segment speed with respect to the 1-second speed increased. Notice also that for time intervals of 15 seconds and 20 seconds, some of the segments were left without any GPS points and that some other segments were left with just 1 GPS point.

The pairs of number of GPS points-segment speed values for each condition and travel time run subset were then used to generate the plots shown in Figure 7-9. Each plot represents a composite figure which summarizes the relationship between the number of GPS points per segment, segment speed, and time interval for all runs

associated with a specific corridor. For example, Figure 7-9b contains all pairs of GPS points - segment speed values obtained for the 36 subsets obtained from the 6 runs (6 subsets for each run) made on I-10 & I-12 EB (PM peak). For completeness, Figure 7-9 also shows the numerical percentage of segments that ended up with GPS points associated with them, as well as a theoretical curve (dotted line) and a best fit curve (solid line) for each group of points. This is discussed in the following section.

Table 7-6: Number of GPS points per segment and segment speed on I-10 & I-12 EB (PM peak run of October 16, 1995; segment length = 0.197 mi)

Cumulative Distance (mi)		Number of GPS points per segment for a time interval of						Segment speed (mph) for a time interval of					
From	To	1 sec	2 sec	5 sec	10 sec	15 sec	20 sec	1 sec	2 sec	5 sec	10 sec	15 sec	20 sec
0	0.197	34	17	7	4	3	2	18.46	17.90	17.23	17.03	15.97	10.60
0.197	0.395	26	13	5	2	1	1	21.25	21.39	21.44	17.85	15.90	25.20
0.395	0.592	32	16	7	4	3	2	18.85	18.66	19.41	21.13	18.63	22.10
0.592	0.790	25	13	5	2	1	1	25.78	25.77	26.40	27.30	23.70	25.90
0.790	0.987	19	9	4	2	2	1	30.68	30.80	31.00	30.20	30.55	29.80
0.987	1.185	14	7	2	1	0	1	36.60	36.26	36.90	35.30	-	35.30
1.185	1.38	10	5	2	1	1	0	40.27	40.30	40.25	41.50	41.50	-
1.38	1.58	19	10	4	2	1	1	32.18	32.27	33.08	33.00	35.30	37.60
1.58	1.78	17	8	4	2	2	1	29.41	29.61	29.13	28.50	29.05	28.40
1.78	1.97	37	19	7	4	2	2	16.02	16.20	15.03	16.08	13.35	19.45
1.97	2.17	33	16	7	3	2	2	14.37	14.63	14.26	15.03	15.35	12.40
2.17	2.37	47	24	9	5	3	2	12.68	12.68	12.66	14.40	12.37	13.85
2.37	2.57	33	16	7	3	3	2	20.85	20.83	21.59	21.27	21.80	21.50
2.57	2.76	15	8	3	2	1	1	34.89	34.80	35.47	35.35	35.40	35.40
2.76	2.96	13	6	2	1	0	0	44.99	45.10	46.20	49.10	-	-
2.96	3.16	13	7	3	1	1	1	51.22	51.20	51.37	50.70	51.40	50.70
3.16	3.36	12	6	2	1	1	0	51.37	51.17	51.80	53.00	53.00	-
3.36	3.55	15	7	3	2	1	1	39.81	39.57	40.20	42.10	36.40	45.00
3.55	3.75	19	10	4	2	1	1	29.35	29.54	29.95	30.00	39.90	39.90
3.75	3.95	25	12	5	2	2	1	23.06	22.92	23.02	21.65	22.50	16.40
3.95	4.15	15	8	3	2	1	1	42.70	42.75	42.70	42.75	42.60	40.80

Sampling Rate Model

The theoretical curves shown in Figure 7-9 resulted from applying the following expression:

$$N = \frac{3{,}600L}{u\Delta t} \tag{7-5}$$

where N is number of GPS points per segment; L is segment length in miles: u is segment speed in mph; and Δt is time interval in seconds.

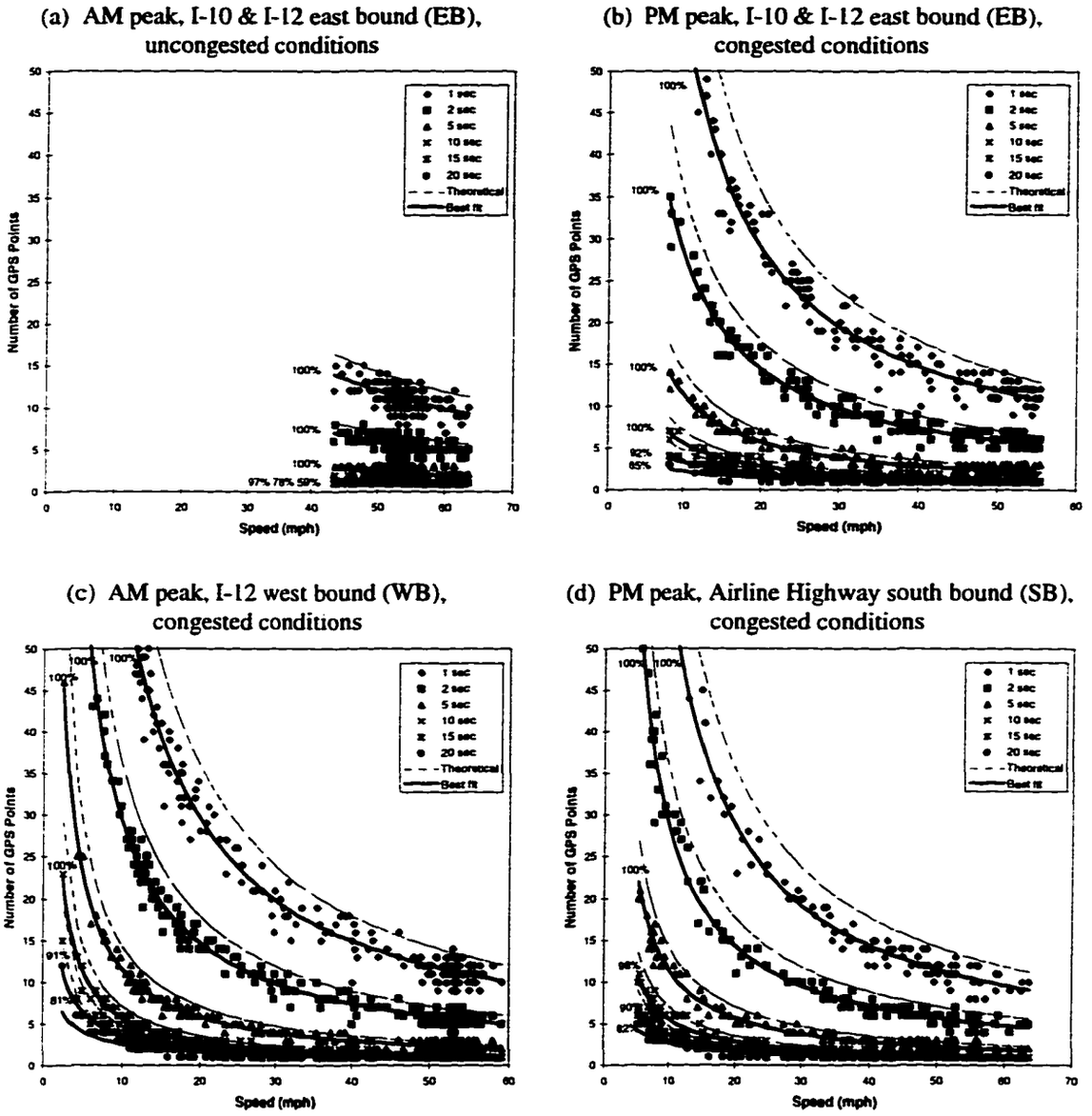

Figure 7-9: Number of GPS points per segment as a function of time interval and vehicle speed

As an illustration, Table 7-7 shows the theoretical equations for the six Δt values considered here, assuming L = 0.197 mi. For comparison purposes, Table 7-7 also

includes the best fit equations obtained for each group of points shown in Figure 7-9b (I-10 & I-12 EB, PM peak conditions). Figure 7-9b shows that the theoretical curves represented an upper bound for the number of GPS points per segment. A comparison between the coefficients of the equations in Table 7-7 indicates that the actual number of GPS points per segment was about 25% lower than what the theoretical equation suggests. This means that the actual time interval was about 30% longer than the nominal time interval. For example, if the nominal time interval was 1 second, the effective average time interval was about 1.3 seconds. This larger value was due to occasional gaps in the GPS data (bridges, tree canopy, and signal losses), perhaps to imperfections in the way the GPS receiver collected and processed the data, and to the fact that the actual number of GPS points per segment N was an integer. Figure 7-9b also shows that the best fit curves were essentially parallel to the theoretical curves. The value of the exponent (very close to one) of the best fit equations in Table 7-7 confirms this assessment.

Table 7-7: Number of GPS points per segment and segment speed assuming 0.197-mi segments on I-10 & I-12 EB (PM peak plots shown in Figure 7-9b)

Time interval (sec)	Theoretical equation	Best fit equation	R^2
1	$N=\frac{709}{u}$	$N=\frac{528}{u^{0.970}}$	0.952
2	$N=\frac{355}{u}$	$N=\frac{264}{u^{0.970}}$	0.938
5	$N=\frac{142}{u}$	$N=\frac{110}{u^{0.985}}$	0.861
10	$N=\frac{70.9}{u}$	$N=\frac{53.8}{u^{0.980}}$	0.780
15	$N=\frac{47.3}{u}$	$N=\frac{20.4}{u^{0.785}}$	0.764
20	$N=\frac{35.5}{u}$	$N=\frac{8.40}{u^{0.570}}$	0.619

For time intervals up to 5 seconds, 100% of the segments ended up with GPS points. For time intervals larger than or equal to 10 seconds, the percentage of segments with GPS points started to decrease as the time interval increased. This trend was consistent with sampling theory concepts. For example, for a time interval of 10 seconds, a few segments were left without any GPS data if the vehicle was traveling at around 55 mph. At this speed, the travel time was almost 13 seconds. From sampling theory (Table (3-2a) on page 28), the time interval had to be at most 6 seconds (assuming a time interval of 1/2 the segment travel time). A time interval larger than 6 seconds would almost inevitably result in some segments not having any GPS data. The results obtained for a time interval of 5 seconds vs. those obtained for a time interval of 10 seconds confirm this assessment.

The fact that no segment was left without GPS data for a time interval of 5 seconds indicates that the traditional sampling theory requirement that the largest time interval be at most half the travel time is sufficient for travel time studies with GPS. This information can be used in practice in order to define acceptable polling intervals when using data communication media such as radio or cellular phones.

As shown in Table 7-6, segment speeds varied increasingly with respect to the 1-second segment speed as sampling rates decreased (i.e., as time intervals increased). To observe this effect, the relative variation in speed with respect to the 1-second segment speed was computed for each value of speed and then plotted against the corresponding time interval (Figure 7-10). For example, for the first 0.197-mi segment (from 0 to 0.197 mi) shown in Table 7-6, the 1-second segment speed was 18.46 mph. Likewise, the 20-second segment speed was 10.60 mph. The corresponding relative variation in speed was

-42.6%. This value was plotted in Figure 7-10b under the 20-second time interval category.

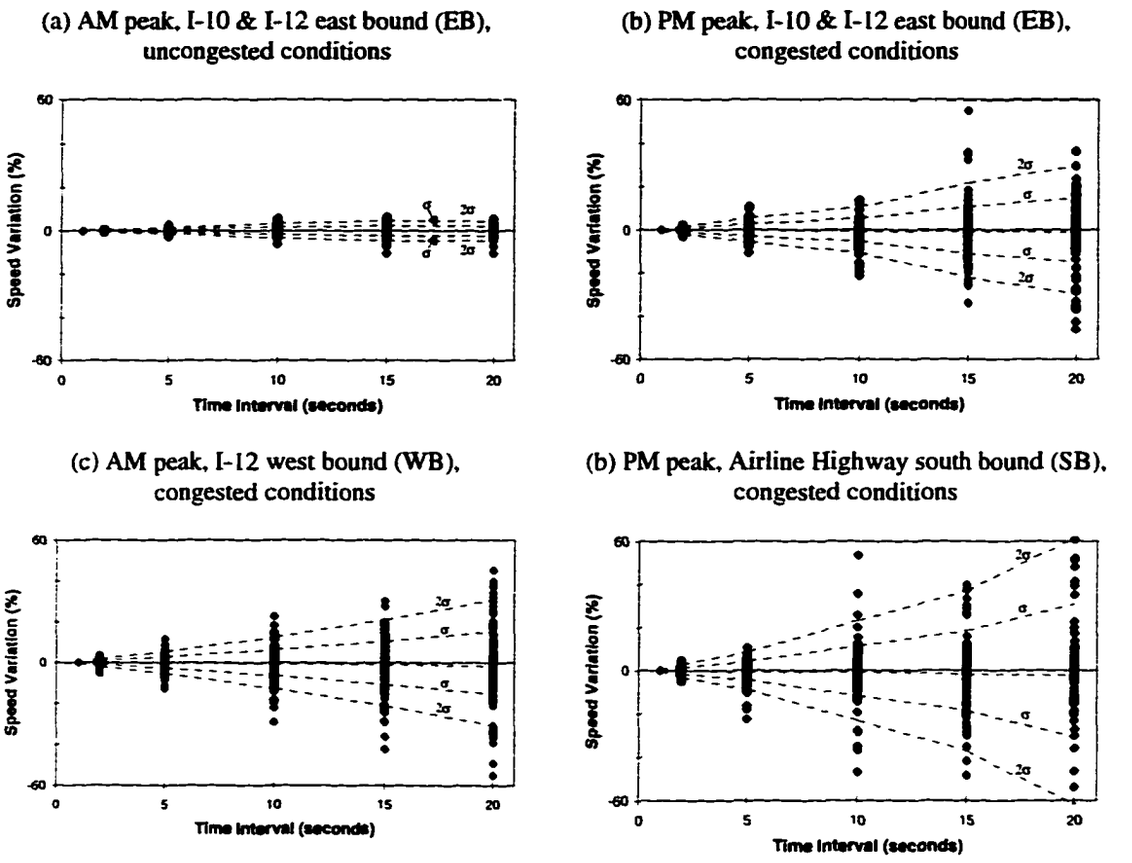

Figure 7-10: Relative variation of segment speed with respect to the 1-second segment speed as a function of time interval

Figure 7-10 shows relative variations in speed for all runs associated with a specific corridor. For completeness, it also shows dotted lines depicting average relative variations (almost horizontal lines), as well as 1-σ and 2-σ bands. Notice that as the time interval increases, the 1-σ and 2-σ bands tend to spread. This is a clear indication of the increasing uncertainty associated with the computed segment speed as the time interval increases. Notice also the difference in behavior between plots according to traffic

condition. Of particular interest is the larger spread observed for the Airline Highway plot (Figure 7-10d). This is an indication that for signalized highways such as Airline Highway the time interval between GPS points has to be shorter than that for a controlled access highway such as I-10 or I-12 in order to achieve the same level of certainty associated with the computed segment speeds. For example, if it is desired to limit the 2-σ speed variation at 5%, the largest time interval that could be accepted for a controlled access highway such as I-10 or I-12 would be around 10 seconds. In contrast, the largest time interval that could be accepted for a signalized highway such as Airline Highway would have to be only 5 seconds.

Central Tendency

Chapter 3 described a general procedure to obtain average speeds from a set of individual segment speed records. The procedure was made general enough so that the resulting formulation (equation (3-10)) could be applied to one or several segments, and to one or several records per segment. The formulation was based on the computation of arithmetic mean travel times for individual segments (equation (3-6)); a total length by adding individual segment lengths (equation (3-7)); a total travel time by adding arithmetic mean travel times for all segments (equation (3-8)); and an average speed resulting from dividing the total length over the total travel time (equation (3-9) and equation (3-10)). Because travel times were expressed in terms of individual segment speeds, the resulting formulation (equation (3-10)) ended up having the form of a weighted harmonic mean in which individual speeds were located in the denominator of the denominator.

One disadvantage of this configuration was that the resulting formulation was very sensitive to individual speeds which were much lower than the rest in the series. As a result, outlying low speeds, which tend to occur during atypically adverse traffic conditions, could result in very small average speeds. Since the objective of using a formulation such as equation (3-10) was to obtain a solid, robust estimator of central tendency, the question then was how appropriate the harmonic mean speed formulation was for estimating central tendency. After all, the central tendency estimator did not necessarily have to be the harmonic mean speed for the application considered.

One possible modification to the harmonic mean formulation would be to manually filter out records that are "atypical". However, this does not appear to be feasible in an environment in which large amounts of data are being collected. One solution, which does not involve manually filtering out the data, would be to compute the arithmetic mean of all speeds associated with a segment. Unfortunately, arithmetic mean speeds are based on the use of a central tendency estimator of travel time (harmonic mean travel time) that is very difficult to conceptualize (Figure 7-11).

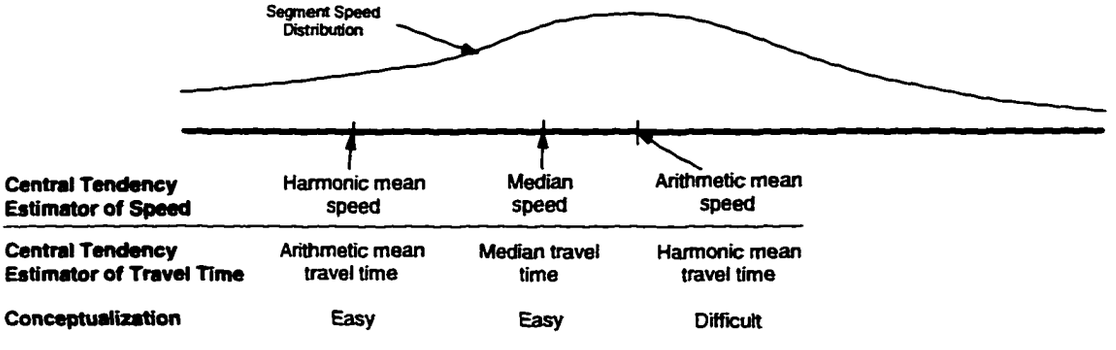

Figure 7-11: Physical interpretation of harmonic mean speeds, median speeds and arithmetic mean speeds

A second possible modification would be to convert equation (3-6) so that median segment travel times are calculated instead of arithmetic mean segment travel times (Figure 7-11). Like the first solution, computing median segment travel times does not involve filtering out the data. The median is known for not being seriously affected by outliers and in many cases it is preferred by statisticians as a measure of central tendency [Duncan, 1986]. Since speeds are used to compute segment travel times, median travel times for individual segments would be obtained from median speed values for that segment. The end result would be a formulation similar to equation (3-10), but that uses segment median speeds instead of segment harmonic mean speeds. The median speed formulation would be

$$\bar{u}_L = \frac{1}{\sum_{i=1}^{n}\left[\frac{L_i}{L_T}\frac{1}{u_{m_i}}\right]} \tag{7-6}$$

where u_{m_i} is median speed associated with segment i during the time period being studied.

In order to test the effect of using equation (7-6) instead of equation (3-10), both harmonic mean speed and median speed formulations were used to obtain average speeds for nearly 1,900 segments in the Baton Rouge network, using 26,000 segment records collected from September 1995 to May 1996 during the AM peak (7:00-8:00 am) and PM peak (4:30-5:30 pm) periods. Differences between the harmonic mean speed and median speed formulations for individual segments were obtained and then the distribution of all differences was defined and plotted, as shown in Figure 7-12. The shape of the AM peak and PM peak distributions was very similar. Only a few values were negative, showing

that for most segments median speeds were larger than harmonic mean speeds. However, most differences were smaller than 2 mph. In fact, the mean difference for the AM and PM periods was very small: 2.11 and 1.59 mph, respectively. This means that, for most segments, median speeds could be used instead of harmonic mean speeds and still produce essentially the same results.

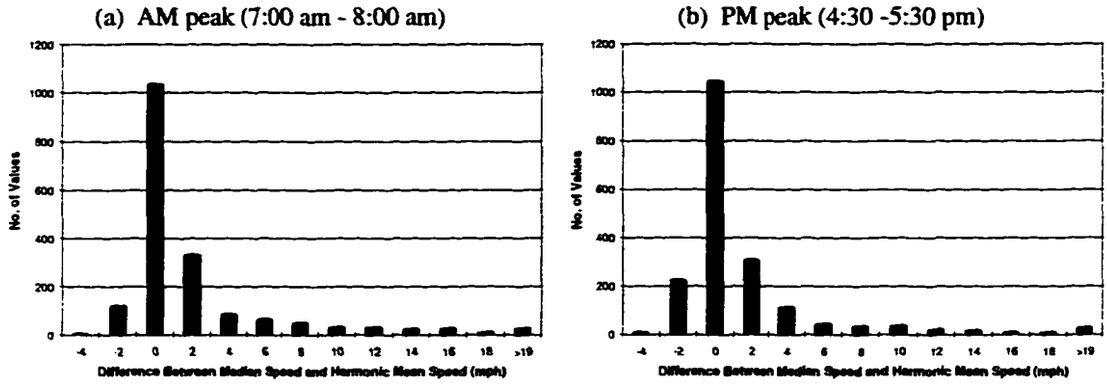

Figure 7-12: Distribution of differences between median speed and harmonic mean speed (September 1995 - May 1996)

In some cases, however, differences between median speeds and harmonic mean speeds were just too large and could not be ignored. As an illustration, Table 7-8 shows the largest differences observed for the PM peak (4:30-5:30 pm) period. For the most part, incidents like stalled vehicles, accidents, or extremely heavy rain were responsible for the low harmonic mean speeds. Such incidents were responsible for the big difference between median and harmonic mean speeds. After removing speeds associated with incidents, most harmonic mean speeds increased sharply, while median speeds barely changed at all. As a result, differences between median speeds and harmonic mean speeds decreased.

Table 7-8: Largest differences between median speeds and harmonic mean speeds in Baton Rouge, Louisiana (September 1995 - May 1996, 4:30-5:30 pm time period)

Segment	Functional Class	All records				After removing records associated with incidents			
		No. of records	Median speed (mph)	Harm. mean speed (mph)	Diff. (mph)	No. of records	Median speed (mph)	Harm. mean speed (mph)	Diff. (mph)
13275	Principal Arterial	7	51.33	23.57	27.76	7	51.33	23.57	27.76
12300	Interstate	17	52.84	24.81	28.03	15	53.88	48.57	5.32
12270	Interstate	17	44.34	16.00	28.34	12	52.18	48.11	4.07
13564	Principal Arterial	5	42.24	13.76	28.48	4	43.09	43.57	-0.49
12269	Interstate	15	49.18	20.08	29.10	11	50.29	48.07	2.22
12198	Interstate	13	49.63	19.61	30.02	10	50.96	50.48	0.49
12199	Interstate	13	52.06	21.73	30.33	11	53.07	53.73	-0.66
12271	Interstate	17	46.47	15.84	30.63	13	49.54	28.36	21.18
12268	Interstate	17	49.70	18.94	30.76	14	50.53	49.33	1.20

The only segments that did not exhibit a significant reduction in speed difference were segments 13275 and 12271. Segment 13275 is located on Florida Boulevard WB (inbound), just before the O'Neal Lane signalized intersection. Florida Boulevard WB is not usually congested during the PM peak. Only two of the seven times that the probe vehicle was going west and crossed O'Neal Lane, the stop light was on red and caused the vehicle to stop. Since the effect of the signalized intersection on WB traffic appears to be low, it can be argued that a relatively high median speed represents average traffic conditions much better than a low harmonic mean speed. Segment 12271 is located on I-10 EB on the Mississippi River bridge (Figure 6-5b). Its location is near the upstream limit of the congestion caused by the I-10&I-110 merge. As a result, traffic on segment 12271 tends to be unstable and unpredictable. In this case, choosing between the median and the harmonic mean does not really make any difference. However, differences between median speeds and harmonic mean speeds for neighboring segments tend to be much smaller. Consequently, it can be argued that median speed approach is still better for segment 12271 because it does not involve executing a separate query to compute the harmonic mean speed for just one segment.

Dispersion Estimators

The various speed-distance profiles included in Figure 7-1 and Figure 7-2 clearly show a picture of traffic flow variability both in space and time. This issue is very much related to that of traffic flow reliability, which has received a great deal of attention in recent years. There is an increasing body of evidence that supports the notion that traffic flow variability results in uncertainties which affect the way travelers perceive travel time and, therefore, their choice of one route/mode over another [Senna, 1994]. As a result, reducing traffic flow variability is increasingly being considered an important objective when defining highway traffic operation strategies such as ramp metering and signal coordination to improve traffic flow [OECD, 1994].

Previously, an analysis was made of the variability of individual GPS speeds with respect to their corresponding aggregated segment speeds. In this section, the analysis focuses on the variability of segment speeds with respect to the central tendency estimators (harmonic mean speeds and median speed) described in the previous section.

Dispersion Formulations

A measure of dispersion of segment speeds u is given by the standard deviation s_u. By definition [Dowdy and Wearden, 1985], s_u is given by

$$s_u = \sqrt{\frac{\sum [u - E(u)]^2}{m - 1}} \tag{7-7}$$

where E(u) is the expected value of u, and m is the sample size per segment. For simplicity, the subscript i, as used in equation (7-6), is dropped. A measure of relative dispersion is given by the coefficient of variation CV. This coefficient can be expressed as

$$CV = \frac{s_u}{E(u)} \tag{7-8}$$

Combining equation (7-7) and equation (7-8) yields

$$CV = \frac{1}{E(u)}\sqrt{\frac{\sum[u - E(u)]^2}{m-1}} \tag{7-9}$$

Normally, expected values of central tendency are estimated using the arithmetic mean. This is the implementation usually found in calculators, electronic spreadsheets, and database packages. However, from the previous section, either the harmonic mean speed or the median speed are used as central tendency estimators of segment speeds. As a result, it is necessary to adapt equations (7-7) through (7-9) so that they reflect the central tendency estimator that is actually being used.

In practice, it is possible to derive an expression to determine s_u, assuming any E(u), in terms of E(u), the arithmetic mean $\overline{u}$, and the standard deviation $s_{\overline{u}}$ associated with $\overline{u}$. Expanding equation (7-7),

$$(m-1)s_u^2 = \sum u^2 - 2mE(u)\overline{u} + mE(u)^2 \tag{7-10}$$

Following a similar procedure, it can be proved that

$$(m-1)s_{\overline{u}}^2 = \sum u^2 - m\overline{u}^2 \tag{7-11}$$

Subtracting equation (7-11) from equation (7-10) yields

$$s_u^2 = s_{\overline{u}}^2 + \frac{m}{m-1}[\overline{u} - E(u)]^2 \tag{7-12}$$

or

$$s_u = \sqrt{s_{\overline{u}}^2 + \frac{m}{m-1}[\overline{u} - E(u)]^2} \tag{7-13}$$

Equation (7-13) shows that s_u for any E(u) is larger than the standard deviation $s_{\bar{u}}$ associated with the arithmetic mean $\bar{u}$. Obviously, if E(u) happens to be the same as $\bar{u}$, then s_u will in turn be same as $s_{\bar{u}}$. For example, assume that E(u) is the median speed u_m. Equation (7-13) then becomes

$$s_{u_m} = \sqrt{s_{\bar{u}}^2 + \frac{m}{m-1}\left[\bar{u} - u_m\right]^2} \qquad (7\text{-}14)$$

where s_{u_m} is the standard deviation associated with u_m.

Table 7-9 shows a sample of s_u and CV values for selected segments in Baton Rouge. The s_u values for most segments were similar, regardless of which E(u) was used. This was logical because harmonic mean speeds were very similar to median speeds, as described in the previous section. In most cases, arithmetic mean speeds were similar to both harmonic mean speeds and median speeds. The two segments for which there were big differences in s_u values, 12271 and 13275, were also the segments for which the differences between harmonic mean speeds and median speeds were large, as described in the previous section.

Table 7-9: s_u and CV values for selected segments in Baton Rouge, Louisiana (September 1995 - May 1996, 4:30-5:30 pm time period)

Segment	No. of records	Harmonic mean speed			Median speed			Arithmetic mean speed		
		E(u) (mph)	s_u (mph)	CV	E(u) (mph)	s_u (mph)	CV	E(u) (mph)	s_u (mph)	CV
11765	4	54.11	2.36	0.044	54.07	2.37	0.044	54.19	2.36	0.044
11769	4	55.96	5.48	0.098	56.27	5.46	0.097	56.36	5.46	0.097
11770	4	46.33	3.97	0.086	46.09	4.00	0.087	46.58	3.96	0.085
11771	4	14.96	18.57	1.241	13.53	19.26	1.423	21.01	17.21	0.819
11773	2	47.72	1.52	0.032	47.75	1.52	0.032	47.75	1.52	0.032
12271	17	15.84	27.79	1.754	46.47	25.42	0.547	33.09	21.35	0.645
12440	27	23.37	10.12	0.433	25.20	9.71	0.385	26.42	9.63	0.365
12441	28	32.64	8.22	0.252	33.61	8.05	0.239	34.54	7.99	0.231
12442	30	36.55	11.29	0.309	44.59	11.53	0.259	40.24	10.65	0.265
12443	30	38.65	10.86	0.281	44.12	10.64	0.241	41.80	10.38	0.248
12444	30	40.76	9.32	0.229	42.54	9.07	0.213	42.89	9.06	0.211
13275	7	23.57	27.48	1.166	51.33	23.86	0.465	40.31	20.69	0.513

Figure 7-13 and Figure 7-14 show differences between standard deviations for nearly 1,900 segments in Baton Rouge. Figure 7-13a and Figure 7-14a show differences in standard deviation between harmonic mean speeds and arithmetic mean speeds. Figure 7-13b and Figure 7-14b show differences in standard deviation between median speeds and arithmetic mean speeds.

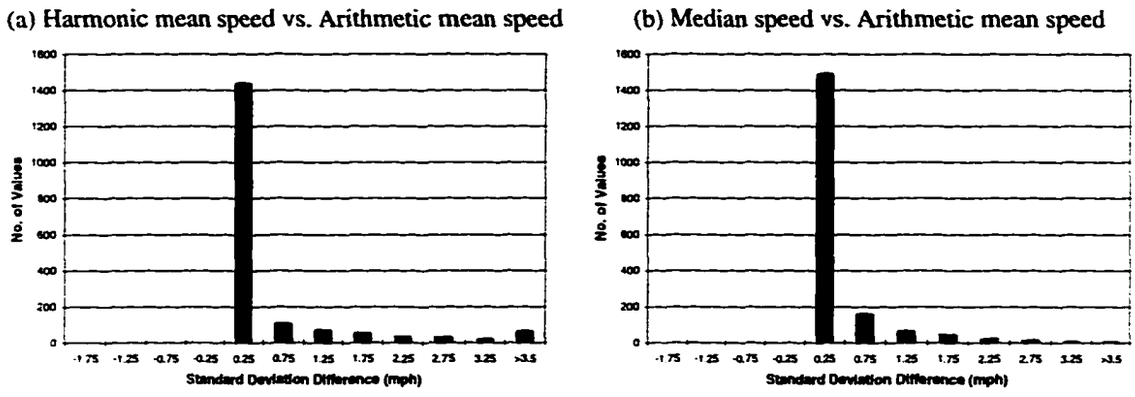

Figure 7-13: Standard deviation differences for harmonic mean speeds and median speeds with respect to arithmetic mean speeds (based on runs made in Baton Rouge from September 1995 to May 1996 during the AM peak - 7:00-8:00 am)

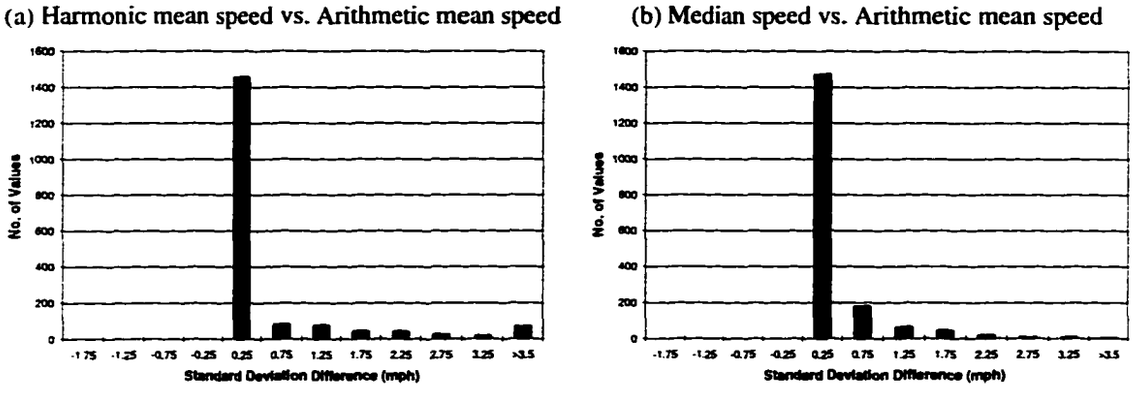

Figure 7-14: Standard deviation differences for harmonic mean speeds and median speeds with respect to arithmetic mean speeds (based on runs made in Baton Rouge from September 1995 to May 1996 during the PM peak - 4:30-5:30 pm)

All differences were positive, indicating that the standard deviations based on arithmetic mean speeds were smaller than those based on harmonic mean speeds or median speeds. This is a clear validation of the trend suggested by equation (7-13). Most differences were smaller than 0.5 mph. This indicates that as a first cut approximation the standard deviations based on arithmetic mean speeds could be used to estimate the standard deviations for both harmonic mean speeds and median speeds. However, for increased accuracy, equation (7-13) should be used to calculate the actual standard deviation values.

Spatial Distribution of Coefficients of Variation

As shown in Table 7-9, CV values tend to follow similar trends as s_u, even though differences between CV values are more pronounced because they are affected by the specific E(u) used in their computation. In practice, it would be of interest to develop the capability to locate on a map where CV values are high and where they are low in order to determine problem areas and define the need for specific actions.

As shown in Chapter 6, GIS tools can be effectively used to produce color coded maps in which each color represents a specific condition. When this concept is used to map the location of CV values, the results are maps like those shown in Figure 7-15. As in Chapter 6, a gray scale of these maps is provided in Figure 7-16 as a guide to readers who do not have access to color copies to reproduce Figure 7-15 faithfully. In these maps, the following classification scheme was used: 0-0.05, >0.05-0.10, >0.10-0.15, >0.15-0.20; and > 0.20. Obviously, different visualization effects could be obtained by modifying this classification scheme.

(a) AM peak (7:00-8:00 am)

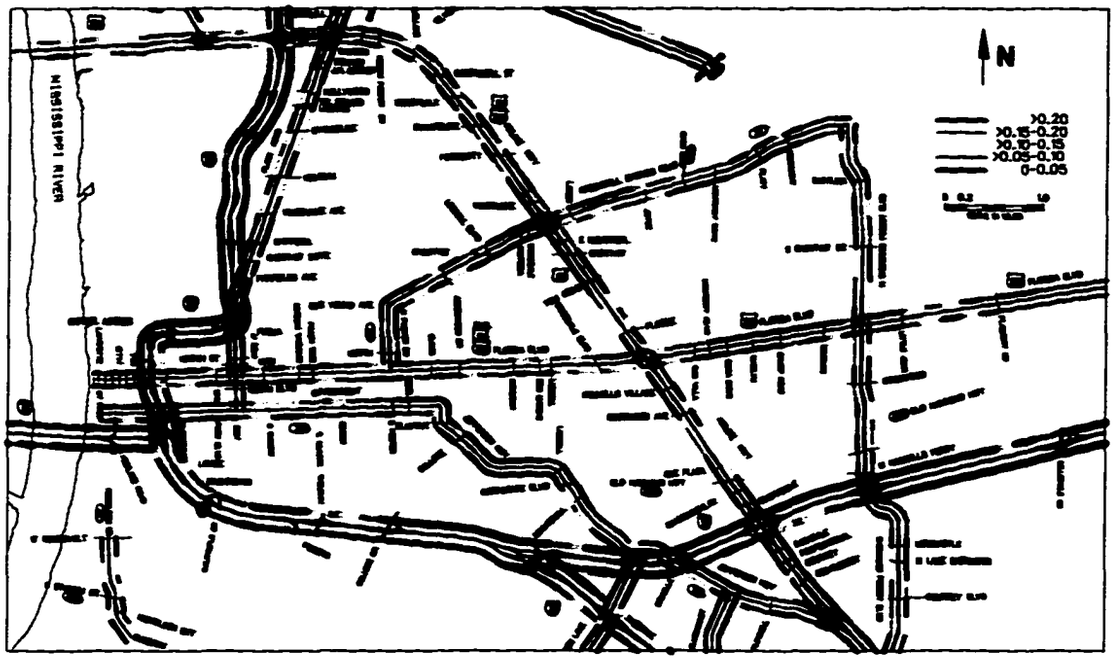

(b) PM peak (4:30-5:30 pm)

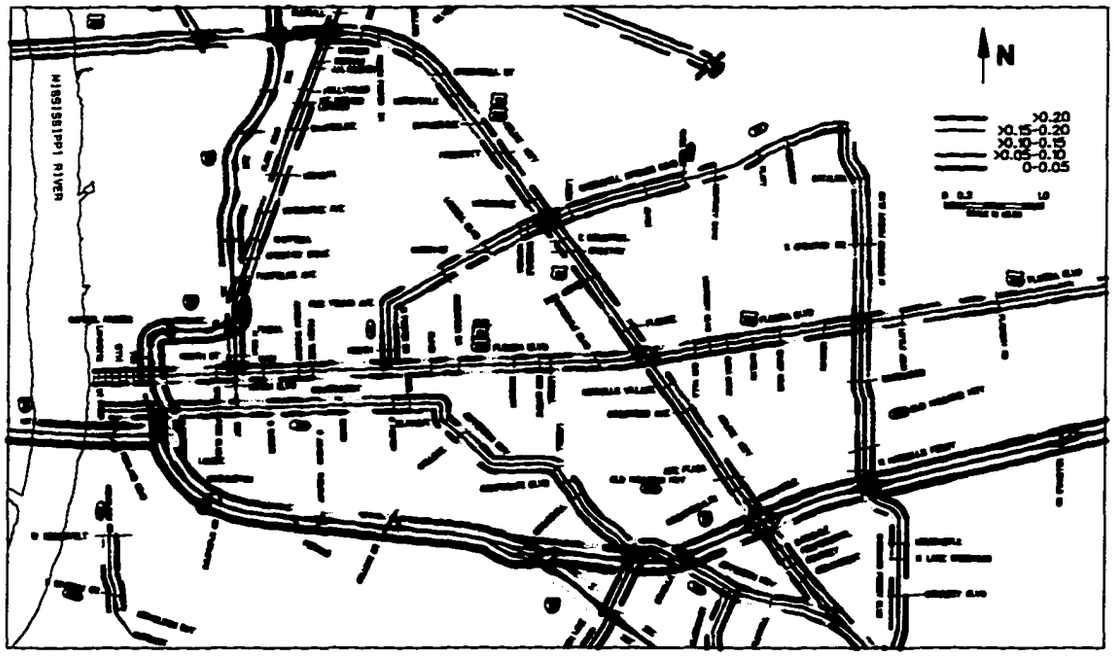

Figure 7-15: Coefficients of variation for median speeds in Baton Rouge (based on data collected from September 1995 to May 1996) - color coded maps

(a) AM peak (7:00-8:00 am)

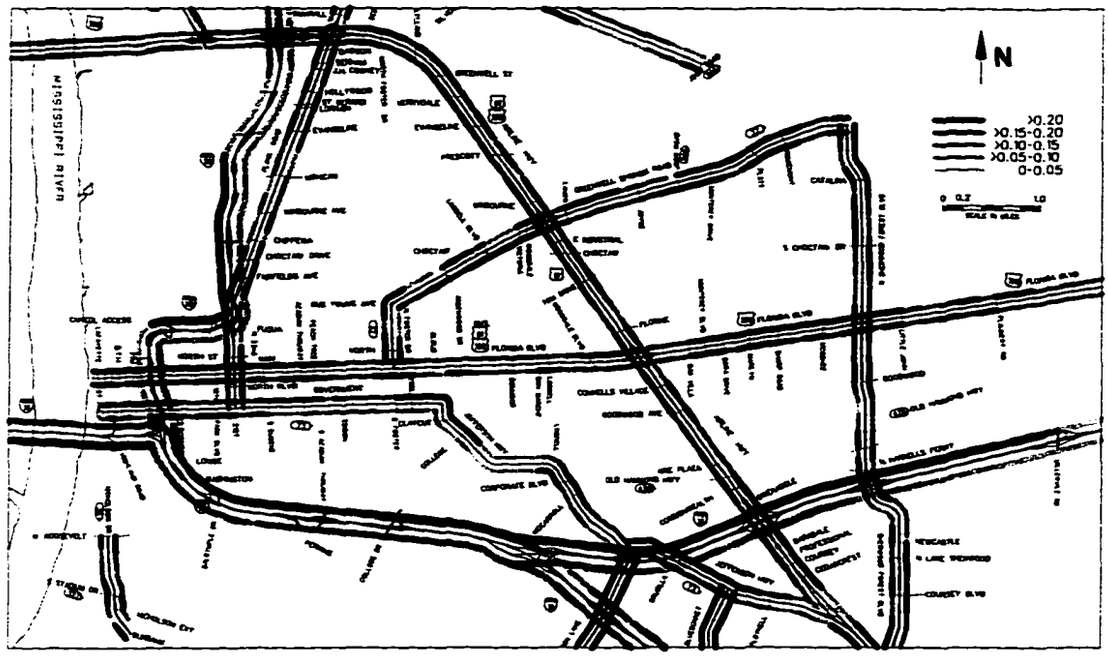

(b) PM peak (4:30-5:30 pm)

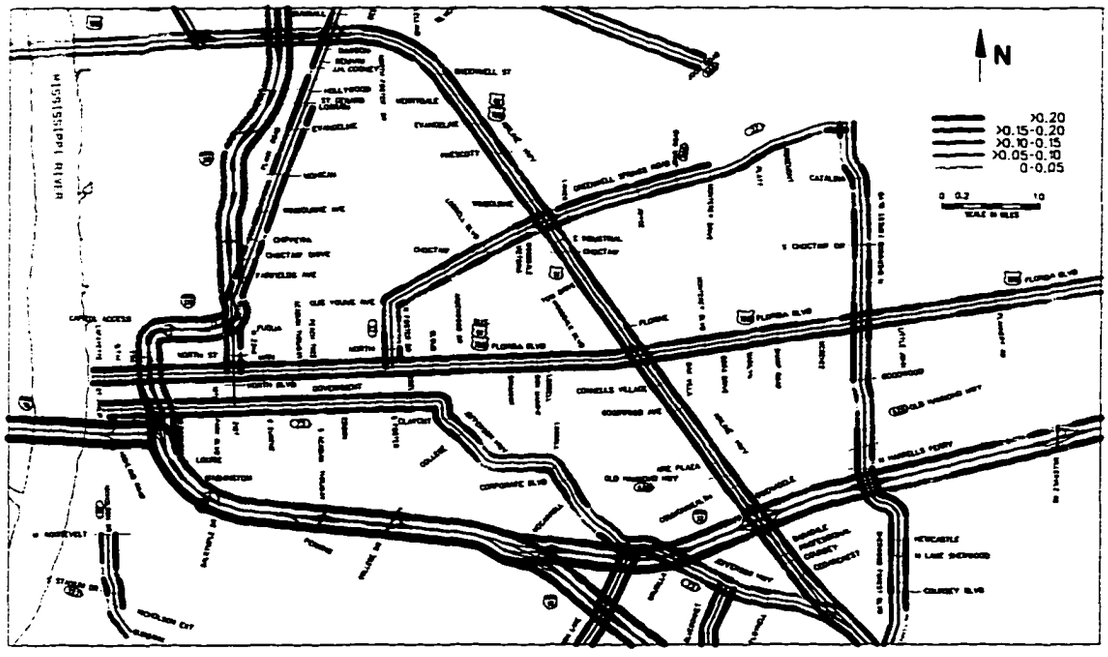

Figure 7-16: Coefficients of variation for median speeds in Baton Rouge (based on data collected from September 1995 to May 1996) - gray scale maps

Following May [1990], CV values normally range from 0.08 to 0.17. This makes traffic flow with CV values larger than 0.17 highly variable. In Figure 7-15 (or Figure 7-16), highly variable traffic flow is essentially defined by the location and number of segments falling in the >0.20 CV category. Notice that practically entire corridors in the Baton Rouge network fall into this category. Examples include the I-10 & I-12 corridor WB between Millerville and Louise during the AM peak (Figure 7-15a or Figure 7-16a), and the I-10 & I-12 corridor EB west of Airline Highway during the PM peak (Figure 7-15b or Figure 7-16b). This picture of the traffic flow situation in Baton Rouge looks definitely more critical than that obtained with the average speed maps of Figure 6-6. The reason is that CV values represent the combined effect of a standard deviation in the numerator (which tends to increase for smaller speeds, as shown in Table 7-9) and an average speed in the denominator (which decreases for smaller speeds).

This amplifying effect might eventually be used to define powerful performance measures based on CV values. For example, it could be used to help characterize unstable regions of the speed-flow curve (Figure 7-17). For example, on the I-10 & I-12 corridor EB west of Airline Highway during the PM peak period, speeds typically range from less than 20 mph to around 50 mph. Based on some count data collected on the I-10 corridor, flow rates larger than 1,800 vehicles per hour per lane during the PM peak hour are not unusual. This means that traffic flow tends to operate in the unstable region of the speed-flow curve (Figure 7-17). This instability can be characterized by large CV values (larger than 0.2) as shown in Figure 7-15.

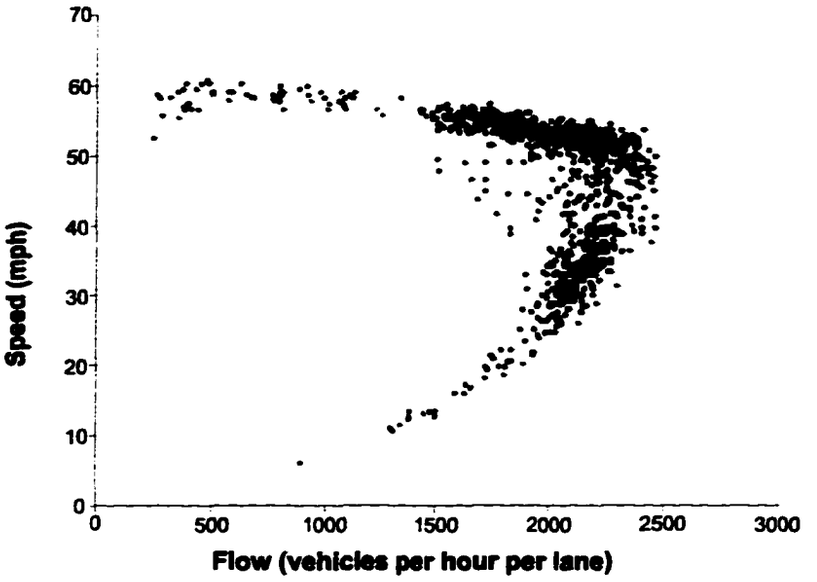

Figure 7-17: Observed speed-flow relationship on I-8 in San Diego, California (adapted from TRB [1994])

Chapter 8
CONCLUSIONS AND FUTURE WORK

Chapters 1 through 7 describe a new methodology for conducting travel time studies based on GPS receivers and GIS technology. Compared to traditional approaches, the new methodology provides consistency, automation, finer resolution levels, and better accuracy in measuring travel time and speed data on highway networks. These combined characteristics enable the accurate detection of localized traffic flow characteristics (Figure 6-6, Figure 6-10) which, with the use of traditional approaches, would be extremely difficult (Figure 2-4). The new methodology automates the data collection and data reduction procedures, and provides improved procedures for documenting and analyzing measured travel times and speeds on highway networks. As a result, large amounts of reliable travel time and speed data can be collected and processed.

This chapter summarizes the contributions documented in this dissertation; examines advantages and disadvantages of the new methodology; and describes areas that warrant further research.

Summary and Conclusions

The new GPS-GIS methodology includes a spatial model that handles GPS data in a GIS environment, data management procedures, data collection procedures, data reduction procedures, and data reporting procedures. It also includes the development of a new methodology for estimating sample size requirements, and procedures to analyze the significance of the speed and travel time data obtained.

GPS-GIS Methodology Procedures

The spatial model aggregates GPS travel time and speed data into highway segment travel time and speed data (Figure 3-4). The study cases considered here used highway segments which were nominally 0.2 mi in length. However, the model is sufficiently general so that other segment sizes can be easily accommodated. The spatial model can be used to obtain travel time and speed for a variety of scenarios ranging from a single segment to an entire corridor; from a single run to a complete set of runs; from a single time period to several time periods during the day; and from one season to several seasons throughout the year.

The database management procedures describe a geographic relational database schema and associated queries developed to efficiently manage highway segment travel time data in a GIS environment. The database schema (Figure 5-1) was composed of six attribute tables which store data relative to segments, corridors, and segment travel time and speeds. Examples of spatial and non-spatial queries were also included. Spatial queries depend on segment location and require GIS tools for creating and executing the queries. In this dissertation, spatial queries were used to generate color coded average speed maps and coefficient of variation maps. However, they can also be used to generate other maps such as travel delay maps or travel time contour maps. Non-spatial queries do not depend on the actual location of a segment and, as a result, they can be created and executed outside the GIS environment. In this dissertation, non-spatial queries were used to compute minimum, average, and maximum speeds by time period for individual segments; free flow speeds; segment travel time delay; average speed and

travel time at the corridor level; and differences between central tendency estimators of speed.

The data collection, data reduction, and data reporting procedures described in this dissertation were developed in the Baton Rouge Congestion Management System (CMS) project [Bullock and Quiroga, 1996]. The data collection procedure uses GPS receivers to automatically record time, local coordinates, and speed every one second. To efficiently perform the aggregation from GPS point to highway segments, an interactive data reduction application with a convenient user interface was developed within the GIS (Figure 6-3). This application plays back the GPS data file and automatically computes segment travel time and speed data. These travel time and speed data are then imported into the geographic database where they can be used for the production of reports.

The data reporting procedure uses graphical and tabular reports including color coded maps (Figure 6-6), archival tabular reports (Figure 6-10), and dynamic World Wide Web (WWW) reports (Figure 6-11). These graphical and tabular reports constitute an improvement over traditional reporting procedures like speed-distance profiles and speed-time profiles. Color coded maps show the spatial variation of items such as speed and travel time, and are particularly suitable for explaining travel time delays and congestion issues at public meetings. Tabular reports offer a very compact way of archiving travel time and speed data along highway segments. This makes them suitable for archival and analytical purposes. WWW reports allow users with access to the Internet to select highway segments and retrieve all records associated with these segments. These reports are useful for making the travel time and speed data accessible to a wide audience without having to provide technical support to interpret the data.

The GPS-GIS methodology was applied to three metropolitan areas in Louisiana: Baton Rouge, Shreveport, and New Orleans. These metropolitan areas are using the travel time and speed data collected for developing their congestion management systems. A synopsis of congestion corridor characteristics, travel time data, and reporting procedures is included in Table 8-1. It may be worth noting that other metropolitan areas like San Antonio, TX; Lafayette, LA; and Albuquerque, NM, are using or have expressed an interest in using approaches similar to the GPS-GIS approach described here.

Table 8-1: Summary corridor, travel time, and reporting data for Baton Rouge, Shreveport and New Orleans

Description	Baton Rouge	Shreveport	New Orleans
Congestion Corridor Network Information:			
Number of corridors:			
Interstate highways	3	2	3
Principal arterials	19	8	4
Total	22	10	7
Length			
Interstate highways (miles)	45.4	18.9	31.3
Principal arterials (miles)	105.6	73.9	54.2
Total	151.0	92.8	85.5
Segments:			
Number of segments			
Main routes	1,852	1,092	1,039
Interchanges, ramps, etc.	545	381	299
Total	2,397	1,473	1,338
Total length (miles)	368.6	237.9	213.8
Average segment length (miles)	0.15	0.16	0.16
Travel Time Data:			
Number of GPS data files	428	100	68
Number of GPS data points (in thousands)	2,500	85	322
Segment data:			
On main routes:			
6-9 am	58,398	1,805	10,780
Noon peak		155	
3-6 pm	48,698	2,002	8,389
Off-peak	40,238	979	1,488
Total	147,334	4,941	20,657
On non-main routes:	7,966	107	1,135
On other corridors			821
Total	155,300	5,048	22,613
Data Reporting:			
Color coded maps	yes	yes	yes
Archival tabular reports	yes	yes	yes
CMS WWW query interface	yes	no	no

As shown in Table 8-1, an extremely large number of segment travel time and speed records (more than 180,000) were collected in Baton Rouge, Shreveport, and New Orleans. Collecting these records with traditional approaches would have been extremely difficult, if not impossible, primarily because of the difficulty in working with fine resolution levels and because of significant accuracy limitations (Figure 2-4). The GPS-GIS methodology described in this dissertation overcame these difficulties. A finer resolution level meant that with the new methodology it became possible to detect localized effects, which has become crucial for the design and implementation of appropriate engineering solutions to traffic problems. Better accuracy meant that with the new methodology it became possible to obtain reliable, consistent data, which has become crucial for the definition of adequate traffic performance measures.

Sampling Size Requirements

This dissertation included the development of an updated methodology for estimating minimum sample sizes. For the past 20 years, many travel time studies have been planned and executed following guidelines included in the ITE manuals of traffic and transportation engineering studies. However, this dissertation showed that the ITE guidelines seriously underestimate sample size requirements (or alternatively, it overestimates confidence levels associated with specified sample sizes). First, the ITE methodology uses the normal distribution Z statistic instead of the t-distribution t statistic, even though the methodology assumes the use of small sample sizes. Second, it uses a moving-range procedure to estimate average sample ranges which tends to produce lower values than true average ranges. Third, the tables included in the ITE methodology, which were intended to be used instead of the iterative mathematical formulation, contain

numerical errors that systematically produce lower sample sizes than those resulting from the equations.

To correct the shortcomings of the ITE methodology, a new methodology was developed (equation (4-5)). The new methodology uses t-distribution parameters and a more reliable procedure to estimate average sample ranges (equation (4-3)). The new methodology was compared to a commonly used and accepted sample standard deviation formulation, and was found to provide similar sample sizes. The sample range was chosen for the new methodology instead of the sample standard deviation because field personnel tend to understand and calculate sample ranges much more easily than standard deviations. Realizing that budgetary capabilities of agencies nationwide vary widely, the new methodology includes tables summarizing sample size requirements for a wide range of confidence levels (75% to 99.73%) (Table 4-5) instead of just one (95%) that is included in the current ITE guidelines. Such a wide range of confidence levels should help traffic engineers to make decisions regarding sample sizes which are consistent with their specific needs and constraints.

Analysis of Key Parameters of the GPS-GIS Methodology

For analyses were included in this dissertation: aggregation levels, sampling rates, central tendency, and dispersion. The aggregation level analysis examined the effect of using different segment lengths for the aggregation process. Seven segmentation schemes ranging from 0.1-mi to 5-mi segments were considered. In general, the observed trend was that segments longer than 1 mile resulted in an almost complete loss of data compared to the original GPS data. Segments shorter than 1 mile, and more specifically segments shorter than 0.5 miles, resulted in a better fit between original GPS speed data

and aggregated speed data (Figure 7-2). These observations were consistent with sampling theory concepts because localized effects became visible only when the segment lengths used in the aggregation process were at most half the length of the disturbances generated by the localized effects.

The analysis also showed that use of links (i.e. segments connecting physical discontinuities) for the aggregation process resulted in a very coarse level of resolution which masked the effect of most physical discontinuities (Figure 7-3). This is a clear indication that link-based travel time studies are not sufficient and that finer levels of resolution are needed to characterize localized effects properly. It must be noted that finer segments are needed mostly for analysis purposes. For other purposes like trip planning, longer segments might still be used, depending on the users' requirements and perception. Data for these longer segments can be easily generated by aggregating the data from the finer resolution level.

In order to provide a quantitative measure of the improvement in fit for smaller segment lengths, an analysis was made of the distributions of differences between original GPS speeds and aggregated speeds (or speed residuals). The analysis showed that standard deviations of speed residuals began to decrease noticeably only for segments shorter than 0.5 miles (Figure 7-8). The analysis also showed differences in behavior between controlled-access highways and signalized highways. Signalized highways show larger standard deviations for the same segment length than controlled-access highways. For example, for a 0.2-mi segmentation scheme, the standard deviation was around 5 mph on the I-10 & I-12 corridor EB, which is a controlled access facility. In contrast, the standard deviation was around 9 mph on Airline Highway SB, which is a signalized

highway. This is a confirmation that traffic flow is more erratic on signalized highways, and that signalized highways require shorter segments than freeways in order to achieve similar standard deviation levels.

Speed residuals, particularly those for segments shorter than 0.5 miles in length, had a tendency to follow a double exponential distribution (or Laplace distribution). This knowledge can be used to better characterize the relationship between original GPS speeds and aggregated speeds, and to provide a probabilistic framework to the definition of segment lengths (Figure 7-6). For example, using the 5-mph σ value obtained for the I-10 & I-12 EB corridor, it can be shown that the probabilities that a speed residual will be larger than 5 mph, 10 mph, and 15 mph are 37%, 14%, and 5%, respectively. With this kind of information it can be inferred that if 0.2-mi segments are used in a freeway such as I-10 or I-12 in Baton Rouge, the difference between GPS speeds and aggregated speeds will be less than 5 mph 63% of the time; less than 10 mph 86% of the time; and less than 15 mph 95% of the time.

The sampling rate analysis examined the effect of using different time intervals between consecutive GPS data points on the number of GPS points that could be associated with a segment and the variability of the resulting aggregated segment speeds. Seven sampling rate schemes were considered, ranging from 1 Hz (time interval of 1 second) to 0.05 Hz (time interval of 20 seconds) (Figure 7-9). For simplicity, only one segment length was used (around 0.2 miles). In agreement with sampling theory concepts, it was observed that the time interval between consecutive GPS points could not exceed half the shortest segment travel time in order to achieve a 100% segment

coverage, i.e. 100% of the segments having GPS data associated with them. Using larger time intervals (or lower sampling rates) resulted in some segments not having GPS data.

The actual number of GPS points per segment turned out be about 25% lower than theoretical values. As a result, actual time intervals turned out to be about 30% longer than nominal time intervals. These larger values were likely due to occasional gaps in the GPS data (bridges, tree canopy, and signal losses), to imperfections in the way the GPS receiver collected and processed the data, and to the fact that the number of GPS points per segments was always an integer.

Sampling rates also have an effect on the value and variability of segment speeds. The observed trend was that aggregated segment speeds varied increasingly as the sampling rate decreased (time interval increased) (Figure 7-10). For example, for the I-10 & I-12 EB corridor during congested conditions, using 5-second time intervals resulted in 95% of the segments having speeds which varied less than 5% with respect to their 1-second segment speeds. In contrast, using 20-second time intervals resulted in less than 50% of the segments having speeds which varied less than 5% with respect to their 1-second segment speeds. This is an indication of the increasing uncertainty and, therefore, lower reliability, associated with aggregated segment speeds as time intervals increase.

The central tendency analysis compared harmonic mean speeds and median speeds. The original procedure included in this dissertation to compute average segment speeds was based on the computation of arithmetic means of travel times. This resulted in a harmonic mean formulation for average segment speeds. Harmonic mean speeds are very sensitive to outlying low speeds, which tend to occur during atypically adverse traffic conditions. Because manually filtering out data in an environment in which large

amounts of data are being collected is not feasible, an alternative procedure, using median speeds, was implemented. For most segments, median speeds and harmonic mean speeds turned out to be very similar (Figure 7-12). In some cases, however, the two values differed considerably. For the cases evaluated in this dissertation, median speeds represented typical traffic flow conditions better than harmonic mean speeds. If the median is used instead of the harmonic mean to estimate average segment speeds, equation (7-6) should be used instead of equation (3-10).

The dispersion analysis examined the variability of segment speeds with respect to central tendency estimators of speed. Two measures of dispersion were used: the standard deviation of segment speeds, which provides an absolute measure of dispersion around the central tendency estimator used; and the coefficient of variation, which provides a relative measure of dispersion with respect to the central tendency estimator used. A formulation was developed to compute standard deviations for harmonic mean speeds and median speeds based on the traditional standard deviation formulation normally found in calculators, electronic spreadsheets, and database packages (equation (7-14)).

The analysis on the coefficients of variation focused on their spatial variability. As mentioned previously, GIS tools can be effectively used to produce color coded maps in which each color represents a specific condition. This concept was used to map the location of coefficients of variation associated with AM and PM peak conditions in Baton Rouge (Figure 7-15). The maps show that a substantial proportion of highway segments in Baton Rouge have coefficients of variation much higher than what is considered typical in urban areas. Practically entire corridors fall into this category. This shows that

an urban area like Baton Rouge is in urgent need to implement highway traffic operation strategies such as ramp metering and signal coordination to reduce variability and, hence, to improve traffic flow. Actually, since high coefficients of variation tend to be associated with low speeds, and since low speeds indicate congested conditions, it may be reasonable to assume that by reducing congestion in general, speeds should increase, and consequently, traffic variability should decrease. This means that additional strategies that focus on demand reduction, for example, should prove beneficial.

Coefficient of variation maps tend to portray a picture of traffic flow more critical than that obtained with average speed maps. The reason is that coefficients of variation represent the combined effect of a standard deviation in the numerator (which tends to increase for smaller speeds) and an average speed in the denominator (which decreases for smaller speeds). This amplifying effect might eventually be used to define powerful performance measures that could be used to help characterize unstable regions of the speed-flow curve.

In defining such performance measures, resolution level issues must be taken into consideration. In this dissertation, coefficient of variation maps were generated assuming the same segmentation scheme (based on 0.2-mi segments) as that used for displaying average segment speeds. As shown in Chapter 7, this segmentation scheme enabled the detection of localized traffic effects when using a GPS-GIS technique for travel time data collection and data processing. From this perspective, coefficient of variation maps based on short segments (say 0.2-mi long or shorter) can only be produced when using a data collection technique like the one described in this dissertation. In practice, coefficient of variation maps can be produced at any scale as long as the speed and standard deviation

values used are consistent with that scale. This means that agencies which currently use a travel time data collection technique like AVI, which is normally based on long segments, should also be able to produce coefficient of variation maps (even on at almost real-time basis) at the scale they normally use. An interesting question, which was not addressed in this dissertation, would be to define the compatibility of coefficient of variation maps produced at different scales.

Future Work

This section examines some specific advantages and disadvantages of the GPS-GIS methodology and describes topics that warrant further research. The discussion focuses on computing platform issues, fixed segmentation as opposed to dynamic segmentation, computation of segment speeds, performance measures, database schema, and probe vehicle driving technique.

Computing platform

The procedures described in this dissertation were used to collect travel time data that the Baton Rouge, Shreveport, and New Orleans metropolitan areas needed to develop their congestion management systems. The GPS-GIS methodology was implemented in an Intergraph workstation running MGE because this was the platform that the Louisiana Department of Transportation and Development (DOTD) and the MPOs in the three metropolitan areas were using. Unfortunately, such a platform is quite expensive (around $15,000) which means that not many smaller agencies or groups within agencies would be able to afford it. This situation confines the applicability of the GPS-GIS methodology to large-scale travel time studies. However, many travel time studies like before-and-after studies and signal timing optimization studies are needed quite frequently by a large

number of organizations. As a result, the GPS-GIS methodology should be easily accessible. In recent years several relatively inexpensive GIS packages like TransCAD have emerged that cost less than $3,000 and can run on ordinary PCs. Therefore, it would be desirable to adapt the current GPS-GIS methodology to one of these cheaper packages so that district engineers and smaller MPOs would have the requisite tools for efficiently conducting the travel time studies they need.

Fixed Segmentation vs. Dynamic Segmentation

The GPS-GIS methodology was based on the assumption that fixed highway segments are used to represent the highway network. A comprehensive analysis was performed to evaluate the effect of using different segment lengths and it was observed that small segment lengths between 0.1 miles and 0.2 miles are generally required to detect localized traffic flow characteristics. However, traffic flow is essentially dynamic both in space and time. This means that depending on the circumstances, it may be more appropriate to use either shorter or longer segments than those defined by the hard segmentation process. This limitation can be overcome by the use of dynamic segmentation techniques. As a result, it would be desirable to modify the GPS-GIS methodology so that each GPS data point is assigned a milepost or cumulative linear distance tag along the route of interest before the GPS data are actually aggregated into highway segments (Figure 8-1).

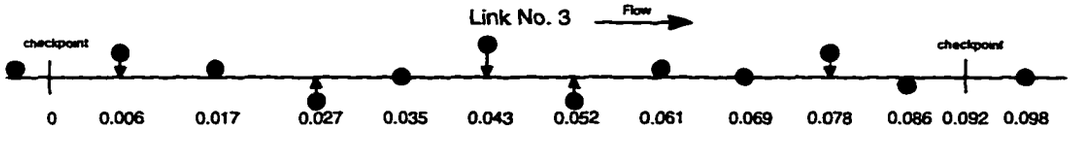

Figure 8-1: Linear referencing of GPS points

In Figure 8-1, checkpoints represent physical discontinuity points, and links are linear features connecting two adjacent checkpoints. For the sake of generality, a link may contain several segments. Similarly, several links can be joined together to form a corridor, which may be of use when the global traffic behavior of entire corridors is being analyzed.

Computation of Segment Speeds

This dissertation included a procedure to compute aggregated segment speeds based on individual GPS speeds and differences in time stamps between adjacent GPS points (equation (3-3)). However, as mentioned in Chapter 3, all segment speeds for the CMS study were computed using equation (3-4), i.e. ignoring the effect of variable GPS time intervals. Equation (3-4) produces good results most of the time because, in most cases, the variation of GPS speeds within a segment tends to be relatively small. However, in some cases, for instance when the probe vehicle approaches a signalized intersection, GPS speeds do vary greatly. For cases such as these, it may be advisable to use equation (3-2) instead of equation (3-4) to compute segment speeds. Current work involving extensions to the GPS-GIS methodology described here will use equation (3-2) directly. This will provide the capability to assess the actual effect of using equation (3-4) instead of the more accurate equation (3-2).

Performance Measures

This dissertation was based on the use of relatively short segments for the computation of segment speeds, standard deviations, and coefficients of variation. To show their spatial variability, color coded maps and tabular reports were produced using classification schemes that covered the entire range of observed values. However, no

attempt was made to compare these classification schemes with those reported in the literature, notably the Highway Capacity Manual [TRB, 1994]. In the case of average speeds, the main reason was that the classification schemes of the Highway Capacity Manual apply to long segments, say 2-5 mi, and the question arises as to whether classification schemes which are defined for a specific level of resolution can be exported freely to a different level of resolution. In the case of coefficients of variation, the literature is very scant in their use as a performance measure at any level of resolution. Therefore, it would be of interest to develop procedures to define thresholds that could be used to define comparable performance levels as a function of the level of resolution.

Database Schema

The database schema developed for this research provided a compact, simple model that provides the capability to manage highway segment travel time and speed data efficiently. However, there are components in the database schema that need to be modified to enhance the database performance. For example, the speed limit attribute (SPLIMIT) in table CORR_SEGMENTS (Table 5-1) is assumed to be fixed. In most cases, this assumption is valid. In practice, however, speed limits may change due to Legislative Bills, Chief Engineer's directives or temporary circumstances like a construction or rehabilitation work. Such changes could be accommodated by creating a separate segment speed limit table with explicit indications of dates, times, and circumstances under which the posted speed limit changes.

Time stamps (STARTTIME) in the travel time table (SEG_TRAVEL_TIME) (Table 5-1) are expressed in UTC time. The main reason for expressing time in the UTC scale was that time stamps in the original GPS data files were also expressed in UTC

scale. At the time when the database was being developed, it was thought that making all time stamps independent of seasonal variations (i.e. standard local time vs. daylight saving time) was a convenient feature. However, it also imposed a burden on the query preparation process. As shown in Appendix B, queries that involved the computation of average travel times or speeds by time period had to take into account when local time changed in October and April. A solution to this inconvenience would be to include an additional field defining time stamps in local time. This would make most regularly used queries much simpler. It would also allow traffic engineers to analyze the specific effects of time shifts in October and April because all travel time records would contain all the necessary information for the analysis.

Another area of database improvement would be the inclusion of data that affect the way travel time runs are made. Examples of this kind of data are weather conditions, driver name, vehicle mechanical conditions, GPS receiver characteristics, and incidents. In the CMS study, some of this log information was collected and stored in individual text files in a somewhat informal way. In the case of Baton Rouge, incident information was stored in a separate Access database. It would be desirable to modify the database schema so that this information becomes an integral part of the database.

Probe Vehicle Driving Technique

The methodology described in this dissertation assumed that travel time runs were made following the floating car technique. During the data collection process, an explicit and constant effort was made to instruct drivers to make sure that they passed as many cars as cars passed them. They were also instructed to drive in the middle lane whenever possible. Because of time constraints and because the objective was not to test the

floating car technique but to develop a workable methodology to collect travel time data, not much additional work was devoted to this issue. To test whether drivers actually follow the floating car technique would mean to have several probe vehicles in the same section of highway at the same time. Issues such as traffic interference, number of probe vehicles, and traffic conditions would need to be taken into consideration. This would make testing the floating car technique a self-contained study.

REFERENCES

Advanstar, 1996. "Receiver Survey." GPS World, 7(1), 32-51.

Benz, R.J., and Ogden, M.A., 1996. "Development and Benefits of Computer-Aided Travel Time Data Collection." Transportation Research Record 1551, TRB, National Research Council, Washington, DC, 1-7.

Box, P.C., and Oppenlander, J.C., 1976. "Manual of Traffic Engineering Studies." Institute of Transportation Engineers, 4th Edition, Washington DC.

Brewer, C.A., 1994. "Color Use Guidelines for Mapping and Visualization." Visualization in Modern Geography, MacEachren and Taylor (Eds), Oxford, New York, NY, 123-147.

Bullock, D., and Quiroga, C.A., 1996. "Development of a Congestion Management System Using GPS Technology - Volume I." Final Report, Louisiana Transportation Research Center, Baton Rouge, LA 132 p.

CAAA, 1990. Clean Air Act Amendment, US Code, Title 1, Section 103.

CUTR, 1996. "Demonstration of Video-Based Technology for Automation of Traffic Data Collection." Center for Urban Transportation Research, University of South Florida, Tampa, FL, 68 p.

David, H.A., 1981. "Order Statistics." 2nd Edition, John Wiley & Sons, New York, NY, 360 p.

DeVivo, P.J., 1997. "Evaluation of JHK and LSU GPS-Based Travel Time Systems." Internal Memo, Metropolitan Washington Council of Governments, Washington, DC, 8p.

Dowdy, S., and Wearden, S., 1985. "Statistics for Research." 2nd Edition, John Wiley & Sons, New York, NY, 629 p.

Duncan, A.J., 1986. "Quality Control and Industrial Statistics." Irwin, Homewood, IL, 5th Edition, 1123 p.

FHWA, 1995. "Our Nation's Highways - Selected Facts and Figures." Publication No. FHWA-PL-95-028, US Department of Transportation, Washington DC, 48 p.

FHWA, 1996. "Highway Statistics 1995." Publication No. FHWA-PL-96-017, US Department of Transportation, Washington DC, 325 p.

Gallagher, J., 1996. "Travel Time Data Collection Using GPS." National Traffic Data Acquisition Conference, Albuquerque, NM, May 6-9, 1, 147-161.

Gans, P., 1992. "Data Fitting in the Chemical Sciences." John Wiley & Sons, Chichester, England, 258 p.

Guo, P., and Poling, A.D., 1995. "Geographic Information Systems/Global Positioning Systems Design for Network Travel Time Study." Transportation Research Record 1497, TRB, National Research Council, Washington, DC, 135-139.

Hahn, G.J., and Meeker, W.Q., 1991. "Statistical Intervals. A Guide for Practitioners." John Wiley & Sons, New York, NY, 392 p.

Harding, J., Salwin, A., Shank, D., and Ghaman, R., 1996. "GPS Applications for Traffic Engineering Studies." Preprint 960214, Transportation Research Board, 75th Annual Meeting, Washington D.C., January 7-11.

HRB, 1950. "Highway Capacity Manual; Practical Applications of Research." National Research Council, Washington, DC, 147 p.

HRB, 1965. "Highway Capacity Manual." 2nd Edition, Special Report 87, National Research Council, Washington, DC, 397 p.

ISTEA, 1991. Intermodal Surface Transportation Efficiency Act US Code, Title 23, Chapter 3, Section 303.

JHK, 1996. "Performance Measures and Levels of Service in the Year 2000 Highway Capacity Manual." NCHRP Project 3-55(4), TRB, National Research Council, Washington, DC, 25 p.

Konvitz, J.W., 1995. "Improving the City Environment." The OECD Observer, 197, 17-22.

Laird, D., 1996. "Emerging Issues in the Use of GPS for Travel Time Data Collection." National Traffic Data Acquisition Conference, Albuquerque, NM, May 6-9, 1, 117-123.

Leick, A., 1995. "GPS Satellite Surveying." John Wiley & Sons, New York, NY, 560 p.

Liu, T.K., and Haines, M., 1996. "Travel Time Data Collection Field Tests - Lessons Learned." Report FHWA A-PL-96-010, US Department of Transportation, 116 p.

Lomax, T., et al., 1995. "Quantifying Congestion - Final Report." National Cooperative Highway Research Program, TRB, National Research Council, Washington, DC, 160 p.

Massey, F.J., 1951. "The Kolmogorov-Smirnov Test for Goodness of Fit." Journal of the American Statistical Association, 46(253), 68-78.

May, A.D., 1990. "Traffic Flow Fundamentals." Prentice-Hall, Englewood, NJ, 464 p.

Meeker, W.Q. and Escobar, L.A., 1997. "Statistical Methods for Reliability Data." To be published by John Wiley & Sons in 1998.

Messina, W.S., 1987. "Statistical Quality Control for Manufacturing Managers." John Wiley & Sons, New York, NY, 331 p.

Milton, J.S., and Arnold, J.C., 1990. "Introduction to Probability and Statistics: Principles and Applications for Engineering and the Computing Sciences." 2nd Edition, McGraw Hill, New York, NY, 700 p.

OECD, 1994. "Congestion Control and Demand Management." Road Transport Research Report, 139 p.

OSTP, 1996. "U.S. Global Positioning System Policy." Fact Sheet, Office of Science and Technology Policy, National Security Council, White House, Washington, DC., March 29.

Oppenlander, J.C., 1976. "Sample Size Determination for Travel Time and Delay Studies." Traffic Engineering, September, 25-28.

Ostle, B.. and Mensing, R.W., 1975. "Statistics in Research. Basic Concepts and Techniques for Research Workers." Third Edition, Iowa State University Press, 596 p.

Petro, C., 1996. "GPS Hits the Road: Pinpointing the Sources of Traffic Congestion." GPS World, 7(9), 42-52.

Quiroga, C.A., and Bullock, D., 1996. "Architecture of a Congestion Management System for Controlled-Access Facilities." Transportation Research Record 1551, TRB, National Research Council, Washington, DC, 105-113.

Quiroga, C.A., Bullock, D., and Schwehm, C, 1997. "Dissemination of Travel Time Information Using the World Wide Web". Preprint 970322, Transportation Research Board, 76th Annual Meeting, Washington DC, January 12-16.

Reilly, W.R., Gardner, C.C., and Kell, J.H., 1976. "A Technique for Measurement of Delay at Intersections. Volume I Technical Report." Report FHWA-RD-76-135, US Department of Transportation, 169 p.

Robertson, H.D., 1994. "Travel Time and Delay Studies". Manual of Transportation Engineering Studies, Robertson, H.D. (Ed), Institute of Transportation Engineers, Washington DC, 52-68.

Roden, D., 1996. "Travel Time Data Collection Using GPS Technologies." National Traffic Data Acquisition Conference, Albuquerque, NM, May 6-9, 163-182.

Sandlin, A., McDonald, K., and Donahue, A., 1995. "Selective Availability: To Be or Not to Be." GPS World, 6(9), 44-51.

Schrank, D.L., Turner, S.M., and Lomax, T.J., 1993. "Estimates of Urban Roadway Congestion - 1990." Report No. FHWA/TX-90/1131-5, US Department of Transportation, Texas Transportation Institute, 82 p.

Senna, L., 1994. "The Influence of Travel Time Variability on The Value of Time." Transportation, 21, 203-228.

Srinivasan, K.K., and Jovanis, P.P., 1996. "Determination of Number of Probe Vehicles Required for Reliable Travel Time Measurement in Urban Network." Transportation Research Record 1537, TRB, National Research Council, Washington, DC, 15-22.

Taylor, M.A.P., Young, W., and Bonsall, P.W., 1996. "Understanding Traffic Systems: Data, Analysis and Presentation." Avebury Technical, Aldershot, England, 443 p.

Tobler, W., 1987. "Measuring Spatial Resolution." International Workshop on Geographic Information Systems, Beijing, China, pp. 42-48.

TRB, 1985. "Highway Capacity Manual." 3rd Edition, Special Report 209, National Research Council, Washington, DC, 504 p.

TRB, 1994. "Highway Capacity Manual." 3rd Edition Update, Special Report 209, National Research Council, Washington, DC.

Trimble, 1993. "Placer GPS 400 Installation and Operator's Manual." Sunnyvale, CA.

Turner, S.M., 1996. "Advanced Techniques for Travel Time Data Collection." Transportation Research Record 1551, TRB, National Research Council, Washington, DC, 51-58.

Zito, R., D'Este, G., and Taylor, M.A.P., 1995. "Global Positioning Systems in the Time Domain: How Useful a Tool for Intelligent Vehicle-Highway Systems?" Transportation Research Part C, 3(4), 193-209.

Appendix A
ACCURACY OF TRAVEL TIME AND SPEED MEASUREMENTS USING GPS

This appendix provides supplementary information to illustrate why the speed of the probe vehicle is used to calculate travel time in equation (3-8).

Mathematical Formulation Using Time Interpolation

Assume a segment of length L. Assume that the time stamps associated with the segment entrance and exit points are determined using a linear time interpolation scheme. Figure A-1 shows two GPS points: one immediately before the end of a segment, and the other one immediately after the beginning of the following segment. The subscripts b and a indicate the before and after GPS points. The time stamp t_i represents the interpolated time associated with the beginning of a segment. The term ε represents GPS point spatial accuracy. The term ε_t represents the resulting accuracy associated with t_i.

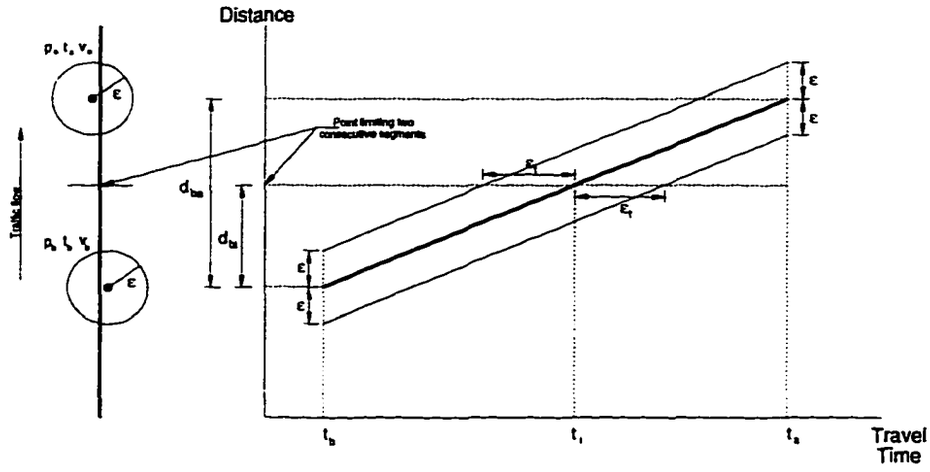

Figure A-1: GPS points before and after highway segment end points

Assuming a linear time interpolation scheme (or constant speed from b to a), t_i is given by

$$t_i = t_b + \frac{d_{bi}}{d_{ba}}(t_a - t_b) \tag{A-1}$$

The term ε_t is given by

$$\varepsilon_t = \frac{\varepsilon}{d_{ba}}(t_a - t_b) \tag{A-2}$$

For simplicity, assume that the time interval between any two consecutive GPS points is constant, say Δt. Calling v the assumed constant speed from b to a, equation (A-2) reduces to

$$\varepsilon_t = \frac{\varepsilon}{d_{ba}}\Delta t = \frac{\varepsilon}{v} \tag{A-3}$$

The average speed u associated with the segment of length L is

$$u = \frac{L}{t_{i+1} - t_i} \tag{A-4}$$

Because of ε_t, there are errors associated with u. Using error propagation theory [Gans, 1992], the standard deviation of u, σ_u, can be expressed as

$$\sigma_u = \sqrt{\left[\frac{\partial u}{\partial t_i}\right]^2 \sigma_{t_i}^2 + \left[\frac{\partial u}{\partial t_{i+1}}\right]^2 \sigma_{t_{i+1}}^2 + 2\frac{\partial u}{\partial t_i}\frac{\partial u}{\partial t_{i+1}} Cov(t_i, t_{i+1})} \tag{A-5}$$

where σ_{t_i} is the standard deviation associated with t_i, $\sigma_{t_{i+1}}$ is the standard deviation associated with t_{i+1}, and $Cov(t_i,t_{i+1})$ is the covariance between t_i and t_{i+1} defined as

$$Cov(t_i, t_{i+1}) = \rho\sigma_{t_i}\sigma_{t_{i+1}} \tag{A-6}$$

In equation (A-6), ρ is the correlation coefficient between t_i and t_{i+1}.

Assume, for simplicity, that σ_{t_i} and $\sigma_{t_{i+1}}$ are the same and equal to σ_t. Combining equations (A-4), (A-5), and (A-6) yields

$$\sigma_u = \sqrt{2\left[\frac{L}{(t_{i+1}-t_i)^2}\right]^2\sigma_t^2 - 2\rho\left[\frac{L}{(t_{i+1}-t_i)^2}\right]^2\sigma_t^2} = \frac{\sqrt{2}L\sigma_t}{(t_{i+1}-t_i)^2}\sqrt{1-\rho} \qquad \text{(A-7)}$$

Assume also that the relationship between σ_u and σ_t is the same as that between ε_u (accuracy associated with u) and ε_t. This means that

$$\varepsilon_u = \frac{\sqrt{2}L\varepsilon_t}{(t_{i+1}-t_i)^2}\sqrt{1-\rho} \qquad \text{(A-8)}$$

If t_i and t_{i+1} are perfectly correlated, $\rho = 1$, and $\varepsilon_u = 0$. If t_i and t_{i+1} are independent, $\rho = 0$. In this case,

$$\varepsilon_u = \frac{\sqrt{2}L\varepsilon_t}{(t_{i+1}-t_i)^2} \qquad \text{(A-9)}$$

Replacing L from equation (A-4) into equation (A-9) yields

$$\varepsilon_u = \frac{\sqrt{2}u\varepsilon_t}{t_{i+1}-t_i} \qquad \text{(A-10)}$$

Replacing ε_t from equation (A-3) into equation (A-10) and assuming that u is the same as v yields

$$\varepsilon_u = \frac{\sqrt{2}\varepsilon}{t_{i+1}-t_i} \qquad \text{(A-11)}$$

Equation (A-11) shows that the error associated with u is a function of the positional accuracy of individual GPS points and the segment travel time. Table A-1 shows a few sample values. Equation (A-11) provides an upper bound for ε_u. In practice,

ε_u values may be lower. This will happen if t_i and t_{i+1} are not truly independent variables, more specifically if the errors associated with individual values of t_i and t_{i+1} are both of the same sign and order of magnitude. Based on observations of data collected with the Trimble receiver, GPS position fixes appear to be affected by a shape smoothing algorithm that causes GPS point coordinates to follow smooth trajectories instead of erratic ones. The question is whether points which are 0.1 miles, 0.2 miles, or more apart are affected the same way by the smoothing algorithm, or whether the effect of this smoothing algorithm fades away after a few points in which case t_i and t_{i+1} could be considered to be independent for all practical purposes.

Table A-1: ε_u vs. $(t_{i+1}-t_i)$ (assuming $\varepsilon = 5$ m)

$t_{i+1}-t_i$ (sec)	ε_u (mph)
1	15.82
2	7.91
5	3.16
10	1.58
20	0.79
30	0.53
60	0.26
120	0.13
240	0.07
480	0.03
960	0.02

Mathematical Formulation Using GPS Speeds

For a segment of length L, the average speed u can be expressed using equation (3-2). For completeness, this equation is repeated here:

$$u = \frac{d}{t_d} = \frac{1}{t_d}\left\{ v_0\left(\frac{t_1 - t_0}{2}\right) + \left[\sum_{k=1}^{p-1} v_k\left(\frac{t_{k+1} - t_{k-1}}{2}\right)\right] + v_p\left(\frac{t_p - t_{p-1}}{2}\right)\right\} \qquad \text{(A-12)}$$

Assuming that the time interval between consecutive GPS points is constant (Δt) yields

$$u = \frac{\Delta t}{t_d}\left[\frac{v_0}{2} + \left(\sum_{k=1}^{p-1} v_k\right) + \frac{v_p}{2}\right] = \frac{1}{p}\left[\frac{v_0}{2} + \left(\sum_{k=1}^{p-1} v_k\right) + \frac{v_p}{2}\right] \tag{A-13}$$

Following a procedure similar to that of equation (A-5) yields

$$\sigma_u = \sqrt{\frac{1}{4p^2}\sigma_0^2 + \sum_{k=1}^{p-1}\frac{1}{p^2}\sigma_k^2 + \frac{1}{4p^2}\sigma_p^2 + \frac{1}{4p^4}\sigma_0\sigma_1 Cov(v_0, v_1) + \ldots} \tag{A-14}$$

GPS speed measurements are almost instantaneous and are made independently of position fixes. Therefore, it is reasonable to assume that individual GPS speeds are independent from each other. As a result, the covariance terms vanish and equation (A-14) reduces to

$$\sigma_u = \sqrt{\frac{1}{4p^2} + \frac{p-1}{p^2} + \frac{1}{4p^2}}\sigma_v = \frac{\sqrt{p-0.5}}{p}\sigma_v \tag{A-15}$$

where σ_v is the standard deviation associated with a typical GPS speed measurement. As before, assume that the relationship between σ_u and σ_v is the same as that between ε_u and ε_v (accuracy associated with individual measurements of speed). In the case of the Trimble GPS Placer 400, which was the receiver used for this research, ε_v was 0.1 mph (1 sigma) [Trimble, 1993]. Finally,

$$\varepsilon_u = \frac{\sqrt{p-0.5}}{p}\varepsilon_v \tag{A-16}$$

Equation (A-16) shows that the error associated with u is a function of the accuracy of individual measurements of speed and the number of GPS points associated with a segment (and also of the segment travel time if Δt is equal to 1 second). Table A-2 shows a few sample values, assuming $\varepsilon_v = 0.1$ mph.

A comparison between the values of Table A-1 and those of Table A-2 clearly indicates that the error associated with u is much larger when a time interpolation scheme is followed to computed segment speeds than when GPS speeds are used to compute segment speeds. Notice that the differences are particularly noticeable for small travel times, say smaller than 10 seconds. For travel times larger than 10 seconds, the differences between the two approaches decrease rapidly, but do not disappear.

Table A-2: ε_u as a function of p and ε_v (assuming $\varepsilon_v = 0.1$ mph)

p	ε_u
1	0.071
2	0.061
5	0.042
10	0.031
20	0.022
30	0.018
60	0.013
120	0.009
240	0.006
480	0.005
960	0.003

Appendix B
DATABASE QUERIES

This appendix provides supplementary information that demonstrates how the data model described in Chapter 5 can be used. The following queries are described here:

- Selection of records associated with a specific segment
- Computation of minimum, average, and maximum speed per date range and per time period
- Computation of median speed per date range and per time period
- Determination of free flow speeds
- Computation of segment travel time delay
- Computation of speed and travel time at the corridor level

Selection of Records Associated with Specific Segments

Suppose that all records associated with segment 12444 (Figure 3-3) from September 1995 to May 1996 during the AM peak (7:00-8:00 am) are needed. The corresponding query would be:

```
SELECT    SEGCODE, GPSDATE, STARTTIME, GPSSPEED
FROM      SEG_TRAVEL_TIME
WHERE     (SEGCODE = 12444
          AND GPSDATE > '01-SEP-95' AND GPSDATE <= '28-OCT-95'
          AND STARTTIME > 43200 AND STARTTIME <= 46800)
OR        (SEGCODE = 12444
          AND GPSDATE > '28-OCT-95' AND GPSDATE <= '7-APR-96'
          AND STARTTIME > 46800 AND STARTTIME <= 50400)
OR        (SEGCODE = 12444
          AND GPSDATE > '7-APR-96' AND GPSDATE <= '3-MAY-96'
          AND STARTTIME > 43200 AND STARTTIME <= 46800);
```

Figure 5-2 shows some of the resulting records. Notice that the WHERE condition includes three date ranges to account for the change from daylight saving time to standard

time and then back to daylight saving time. For completeness, Table B-1 shows the equivalence between UTC time, standard time, and daylight saving time, with an indication of the AM peak and PM peak time periods in Baton Rouge, Louisiana.

Table B-1: Equivalence between UTC time, standard time, and daylight saving time for Baton Rouge, Louisiana

UTC Time		Standard Time		Daylight Saving Time	
(seconds)	(hh:mm)	(hh:mm)	Peak	(hh:mm)	Peak
39,600	11:00	5:00 am		6:00	
41,400	11:30	5:30		6:30	
43,200	12:00	6:00		7:00	X
45,000	12:30	6:30		7:30	X
46,800	13:00	7:00	X	8:00	
48,600	13:30	7:30	X	8:30	
50,400	14:00	8:00		9:00	
52,200	14:30	8:30		9:30	
54,000	15:00	9:00		10:00	
55,800	15:30	9:30		10:30	
57,600	16:00	10:00		11:00	
59,400	16:30	10:30		11:30	
61,200	17:00	11:00		12:00 pm	
63,000	17:30	11:30		12:30	
64,800	18:00	12:00 pm		1:00	
66,600	18:30	12:30		1:30	
68,400	19:00	1:00		2:00	
70,200	19:30	1:30		2:30	
72,000	20:00	2:00		3:00	
73,800	20:30	2:30		3:30	
75,600	21:00	3:00		4:00	
77,400	21:30	3:30		4:30	X
79,200	22:00	4:00		5:00	X
81,000	22:30	4:30	X	5:30	
82,800	23:00	5:00	X	6:00	
84,600	23:30	5:30		6:30	
86,400	24:00	6:00		7:00	

Suppose now that the total number of weekday records per segment for the same date range and time periods is needed. The corresponding query would be:

```
SELECT    SEGCODE, COUNT (*)
FROM      SEG_TRAVEL_TIME, WEEK_DAYS
WHERE     (SEG_TRAVEL_TIME.GPSDATE > '01-SEP-95'
          AND SEG_TRAVEL_TIME.GPSDATE <= '28-OCT-95'
          AND STARTTIME > 43200 AND STARTTIME <= 46800
          AND SEG_TRAVEL_TIME.GPSDATE = WEEK_DAYS.GPSDATE
          AND DAYWEEK <> 'SA'
          AND DAYWEEK <> 'SU')
OR        (SEG_TRAVEL_TIME.GPSDATE > '28-OCT-95'
          AND SEG_TRAVEL_TIME.GPSDATE <= '7-APR-96'
          AND STARTTIME > 46800 AND STARTTIME <= 50400
```

```
                AND SEG_TRAVEL_TIME.GPSDATE = WEEK_DAYS.GPSDATE
                AND DAYWEEK <> 'SA'
                AND DAYWEEK <> 'SU')
OR              (SEG_TRAVEL_TIME.GPSDATE > '7-APR-96'
                AND SEG_TRAVEL_TIME.GPSDATE <= '3-MAY-96'
                AND STARTTIME > 43200 AND STARTTIME <= 46800
                AND SEG_TRAVEL_TIME.GPSDATE = WEEK_DAYS.GPSDATE
                AND DAYWEEK <> 'SA'
                AND DAYWEEK <> 'SU')
GROUP BY        SEGCODE;
```

Table B-2 shows some of the results from this query.

Table B-2: Sample of results from query to determine number of weekday records

SEGCODE	COUNT
12444	32
12445	11
12446	11
12447	11
12448	11
12449	12
12450	12
12451	12
12453	20
12454	20
12455	21
12456	22
12457	16
12458	15
12462	11
12463	12
12464	12

Computation of Minimum, Average, and Maximum Speed

Suppose that color coded maps containing minimum, average, and maximum speeds for the PM peak period (4:30-5:30 pm) from September 1995 to May 1996 are needed. To do this, it would be necessary to execute queries to retrieve minimum, average, and maximum speeds by segment, and then use GIS query tools to join the resulting segment speed data to their location on the design map. This process is summarized in Figure B-1. For simplicity, only the process to generate average speed color coded maps is shown. The processes to generate minimum speed and maximum speed color coded maps are similar. A description of each step is provided below.

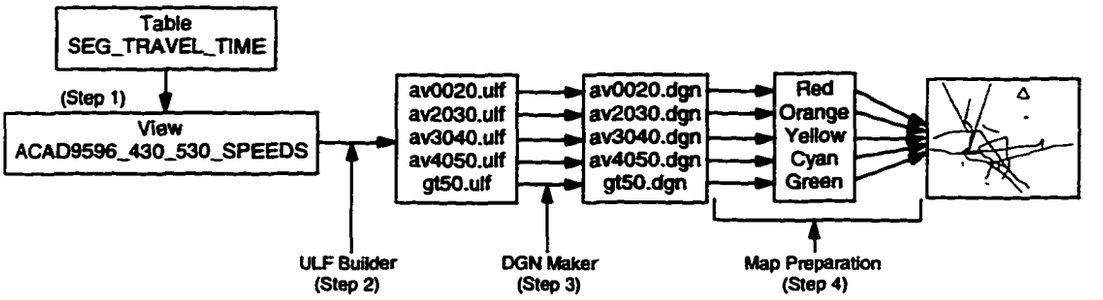

Figure B-1: Description of process to produce segment speed color coded maps

1. A query is executed to retrieve average speeds per segment. Because results from this query are needed as input to the rest of the process, a name is assigned to it. In database packages such as Oracle (the underlying database package used in this research), query naming is usually handled by the use of virtual tables called views. The corresponding query would be:

```
CREATE VIEW     ACAD9596_430_530_SPEEDS (SEGCODE, RCOUNT, MINSPEED,
                AVSPEED, MAXSPEED)
AS      SELECT  SEGCODE, COUNT (*), MIN(GPSSPEED), 1/AVG(1/GPSSPEED),
                MAX(GPSSPEED)
        FROM    SEG_TRAVEL_TIME, WEEK_DAYS
        WHERE   (SEG_TRAVEL_TIME.GPSDATE > '01-SEP-95'
                AND SEG_TRAVEL_TIME.GPSDATE <= '28-OCT-95'
                AND STARTTIME > 77400 AND STARTTIME <= 81000
                AND SEG_TRAVEL_TIME.GPSDATE = WEEK_DAYS.GPSDATE
                AND DAYWEEK <> 'SA'
                AND DAYWEEK <> 'SU')
        OR      (SEG_TRAVEL_TIME.GPSDATE > '28-OCT-95'
                AND SEG_TRAVEL_TIME.GPSDATE <= '7-APR-96'
                AND STARTTIME > 81000 AND STARTTIME <= 84600
                AND SEG_TRAVEL_TIME.GPSDATE = WEEK_DAYS.GPSDATE
                AND DAYWEEK <> 'SA'
                AND DAYWEEK <> 'SU')
        OR      (SEG_TRAVEL_TIME.GPSDATE > '7-APR-96'
                AND SEG_TRAVEL_TIME.GPSDATE <= '3-MAY-96'
                AND STARTTIME > 77400 AND STARTTIME <= 81000
                AND SEG_TRAVEL_TIME.GPSDATE = WEEK_DAYS.GPSDATE
                AND DAYWEEK <> 'SA'
                AND DAYWEEK <> 'SU')
        GROUP BY SEGCODE;
```

Table B-3 shows some of the results from this query.

Table B-3: Sample of results from query to determine minimum, average, and maximum speeds by segment (View ACAD9596_430_530_SPEEDS)

SEGCODE	COUNT	MINSPEED (mph)	AVSPEED (mph)	MAXSPEED (mph)
12444	30	24.02	40.76	55.35
12445	9	52.03	55.01	62.20
12446	9	52.47	55.82	63.03
12447	9	52.61	56.46	64.47
12448	9	53.66	57.07	64.15
12449	12	9.02	15.79	54.72
12450	12	6.69	17.03	54.52
12451	12	11.90	30.57	54.53
12453	18	31.79	47.64	57.80
12454	18	35.57	51.75	61.84
12455	18	36.36	54.75	64.93
12456	19	39.06	55.53	63.68
12457	10	50.42	56.85	64.70
12458	11	50.32	55.49	63.93
12462	9	52.79	56.64	63.92
12463	12	10.88	20.00	54.39
12464	12	12.79	20.53	53.75

2. A set of speed ranges is defined, for example, 0-20 mph, 20-30 mph, 30-40 mph, 40-50 mph, and >50 mph. The MGE universal list file (ULF) Builder tool is then used to locate which segments fall within each speed range considered, and then stores this information in a set of ULFs. For example, for the 0-20 mph range, the ULF Builder would run the following query:

```
SELECT   MSLINK
FROM     CORR_SEGMENTS, ACAD9596_430_530_SPEEDS
WHERE    CORR_SEGMENTS.SEGCODE = ACAD9596_430_530_SPEEDS.SEGCODE
AND      AVSPEED <= 20;
```

and would store the corresponding results in a file called, say, av0020.ulf. Similarly, for the 20-30 mph range, the ULF Builder would run the following query:

```
SELECT   MSLINK
FROM     CORR_SEGMENTS, ACAD9596_430_530_SPEEDS
WHERE    CORR_SEGMENTS.SEGCODE = ACAD9596_430_530_SPEEDS.SEGCODE
AND      AVSPEED > 20 AND AVSPEED <= 30;
```

and would store the corresponding results in a file called, say, av2030.ulf. The procedure for generating the remaining ULFs (av3040.ulf, av4050.ulf, and gt50.ulf) is similar.

3. The MGE DGN Maker tool is used to generate a design file for each ULF. For example, av0020.dgn would be the design file resulting from av0020.ulf; av2030.dgn would be the design file resulting from av2030.ulf; and so on.
4. All design files are merged and assigned a unique color code by speed range. For example, red would represent average speeds in the 0-20 mph range; green would represent average speeds > 50 mph; and so on. Examples of color coded maps are included in Chapter 6.

Computation of Median Speeds

Database packages such as Oracle and Microsoft Access lack functions to compute common statistics such as median values. As a result, it becomes necessary either to create a utility outside these packages or to use a tool like Excel to replace the missing function. The external utility reads data from a generic database table that contains only segment and speed data. This generic table can be the result of a query that produces all GPS speed values for specific date ranges and time periods.

Suppose that median speeds for the PM peak period (4:30-5:30 pm) from September 1995 to May 1996 are needed. The query to generate the input Oracle table would be:

```
CREATE TABLE    ACAD9596_430_530 (SEGCODE, SPEED)
AS      SELECT  SEGCODE, GPSSPEED
        FROM    SEG_TRAVEL_TIME, WEEK_DAYS
        WHERE   (SEG_TRAVEL_TIME.GPSDATE > '01-SEP-95'
                AND SEG_TRAVEL_TIME.GPSDATE <= '28-OCT-95'
                AND STARTTIME > 77400 AND STARTTIME <= 81000
                AND SEG_TRAVEL_TIME.GPSDATE = WEEK_DAYS.GPSDATE
                AND DAYWEEK <> 'SA'
                AND DAYWEEK <> 'SU')
        OR      (SEG_TRAVEL_TIME.GPSDATE > '28-OCT-95'
                AND SEG_TRAVEL_TIME.GPSDATE <= '7-APR-96'
                AND STARTTIME > 81000 AND STARTTIME <= 84600
                AND SEG_TRAVEL_TIME.GPSDATE = WEEK_DAYS.GPSDATE
                AND DAYWEEK <> 'SA'
                AND DAYWEEK <> 'SU')
```

```
OR      (SEG_TRAVEL_TIME.GPSDATE > '7-APR-96'
        AND SEG_TRAVEL_TIME.GPSDATE <= '3-MAY-96'
        AND STARTTIME > 77400 AND STARTTIME <= 81000
        AND SEG_TRAVEL_TIME.GPSDATE = WEEK_DAYS.GPSDATE
        AND DAYWEEK <> 'SA'
        AND DAYWEEK <> 'SU');
```

Table B-4a shows some of the results from this query. With these results, the external utility computes median speeds (Table B-4b).

Table B-4: Sample of results from query to compute median speeds by segment

a) Table ACAD9596_430_530[1]

SEGCODE	SPEED (mph)
12444	41.51
12444	38.31
12444	45.22
12445	55.15
12445	60.04
12445	60.39
12446	55.38
12446	47.51
12446	51.43

b) Median speeds[2]

SEGCODE	SPEED (mph)
12444	42.54
12445	53.91
12446	55.02

[1] Only 3 records per segment are shown here

[2] The median values shown here are based on all database records (30 for segment 12444; 9 for segment 12445; and 9 for segment 12446, as shown in Table B-3)

Determination of Free Flow Speeds

There are three options for estimating free flow speeds: (1) based on posted speed limits; (2) based on runs conducted specifically for this purpose; or (3) based on maximum observed speeds. Assume that posted speed limits are chosen to represent free flow speeds. The corresponding query would be:

```
CREATE VIEW     FREE_FLOW_SPEEDS (SEGCODE, FFSPEED)
AS      SELECT  SEGCODE, SPLIMIT
        FROM    CORR_SEGMENTS;
```

A view is created because free flow speed data will be used to compute travel time delays. Alternatively, assume that Sunday morning runs are conducted specifically to obtain free flow speeds. The corresponding query would be:

```
CREATE VIEW     FREE_FLOW_SPEEDS (SEGCODE, FFSPEED)
AS      SELECT  SEGCODE, 1/AVG(1/GPSSPEED)
        FROM    SEG_TRAVEL_TIME, WEEK_DAYS
        WHERE   SEG_TRAVEL_TIME.GPSDATE = WEEK_DAYS.GPSDATE
        AND     DAYWEEK = 'SU';
        GROUP BY SEGCODE;
```

when using average Sunday morning speeds, or

```
CREATE VIEW     FREE_FLOW_SPEEDS (SEGCODE, FFSPEED)
AS      SELECT  SEGCODE, MAX(GPSSPEED)
        FROM    SEG_TRAVEL_TIME, WEEK_DAYS
        WHERE   SEG_TRAVEL_TIME.GPSDATE = WEEK_DAYS.GPSDATE
        AND     DAYWEEK = 'SU';
        GROUP BY SEGCODE;
```

when using maximum Sunday morning speeds. Assume now that maximum observed speeds, regardless of day of week, are chosen to represent free flow speeds. The corresponding query would be:

```
CREATE VIEW     FREE_FLOW_SPEEDS (SEGCODE, FFSPEED)
AS      SELECT  SEGCODE, MAX(GPSSPEED)
        FROM    SEG_TRAVEL_TIME
        GROUP BY SEGCODE;
```

Table B-5 shows some of the results from these queries. Notice the differences between the four values of speed, particularly those between posted speed limits and maximum observed speeds. One problem with using posted speed limits is that motorists routinely drive faster than the posted speed limit if traffic conditions permit it. In the case of Baton Rouge, a set of runs were made on selected Sunday mornings with the hope that more realistic free flow conditions or nearly free flow conditions would be measured. However, it was observed that some speeds during Sunday morning runs were actually smaller than some weekday speeds. One possible explanation for this phenomenon is that drivers tend to be less aggressive on Sunday mornings and are therefore more willing to drive at speeds closer to the posted speed limits. For simplicity, in this dissertation it is assumed that maximum observed speeds, regardless of day of week, represent free flow speeds. However, it is clear, as reported in the literature [JHK, 1996], that further

research is needed to clarify the issue so that appropriate free flow speed values are used as a reference to compute free flow travel times and travel time delays.

Table B-5: Sample of results from query to retrieve free flow speeds by segment in Baton Rouge

SEGCODE	Free Flow Speed FFSPEED (mph)			
	Speed Limit	Sunday Morning Runs		Max. Speeds
		Avg. Speeds	Max. Speeds	
12444	55	57.54	61.27	63.14
12445	55	54.53	57.07	68.14
12446	55	55.16	57.90	67.88
12447	55	55.28	58.00	67.79
12448	55	56.05	58.18	67.81
12449	55	56.42	62.06	67.14
12450	55	55.86	59.08	62.05
12451	55	55.63	58.52	61.34
12453	55	56.09	59.94	64.72
12454	55	55.73	58.38	63.75
12455	55	56.03	61.98	65.07
12456	55	58.09	62.60	67.70
12457	55	59.93	63.59	66.34
12458	55	59.31	60.08	65.92
12459	55	58.28	58.28	58.76
12460	55	54.70	54.70	56.66
12461	55	56.03	56.03	58.26
12462	55	54.79	56.85	70.32
12463	55	56.48	60.64	62.69
12464	55	56.64	62.21	66.09

Computation of Segment Travel Time Delay

Segment travel time delay can be computed using table CORR_SEGMENTS, view FREE_FLOW_SPEEDS, and one of the views containing representative segment speed values such as ACAD9596_430_530_SPEEDS. The basic relationships among tables and views needed to compute delay are shown in Figure B-2. First, free flow and representative travel times are computed. Then, free flow times are subtracted from representative travel times to compute delays.

The query to compute free flow travel times would be:

```
CREATE VIEW     FREE_FLOW_TIMES (SEGCODE, FFTIME)
AS      SELECT  FREE_FLOW_SPEEDS.SEGCODE, 3600*SEGLENGTH/FFPEED
```

```
FROM      FREE_FLOW_SPEEDS, CORR_SEGMENTS
WHERE     FREE_FLOW_SPEEEDS.SEGCODE=CORR_SEGMENTS.SEGCODE;
```

with FFTIME given in seconds. The query to compute summary travel times would be:

```
CREATE VIEW     ACAD9596_430_530_TRAV_TIMES (SEGCODE, MINTIME, AVTIME,
                MAXTIME)
AS      SELECT  ACAD9596_430_530_SPEEDS.SEGCODE,
                3600*SEGLENGTH/MAXSPEED, 3600*SEGLENGTH/AVSPEED,
                3600*SEGLENGTH/MINSPEED
        FROM    ACAD9596_430_530_SPEEDS, CORR_SEGMENTS
        WHERE   ACAD9596_430_530_SPEEDS.SEGCODE = CORR_SEGMENTS.SEGCODE;
```

The query to compute travel time delays would be:

```
CREATE VIEW     ACAD9596_430_530_DELAYS (SEGCODE, MINDELAY, AVDELAY,
                MAXDELAY)
AS      SELECT  FREE_FLOW_TIMES.SEGCODE, MINTIME - FFTIME, AVTIME - FFTIME,
                MAXTIME - FFTIME
        FROM    FREE_FLOW_TIMES, ACAD9596_430_530_TRAV_TIMES
        WHERE   ACAD9596_430_530_TRAV_TIMES.SEGCODE =
                FREE_FLOW_TIMES.SEGCODE;
```

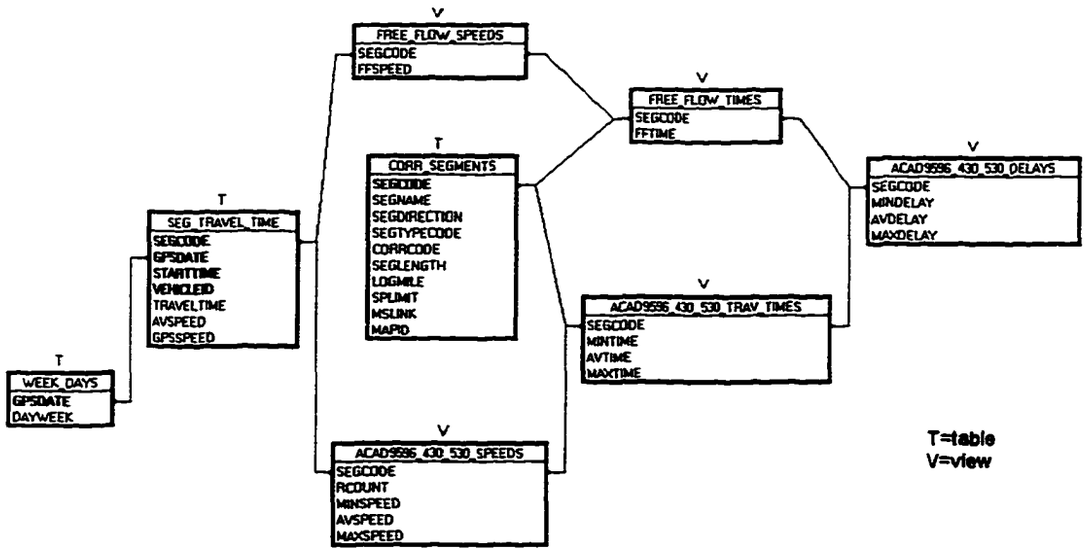

Figure B-2: Travel delay query schema

Table B-6 shows a sample of results from the application of these queries. Free flow time (FFTIME) values were obtained from the maximum observed speeds shown in Table B-5. Minimum, average, and maximum travel time (MINTIME, AVTIME, and

MAXTIME) values were obtained from maximum, average, and minimum speed (MAXSPEED, AVSPEED, and MINSPEED) values shown in Table B-3.

Table B-6: Sample of results from queries to determine travel time delay by segment

SEGCODE	LENGTH (mi)	FFTIME (sec)	MINTIME (sec)	AVTIME (sec)	MAXTIME (sec)	MINDELAY (sec)	AVDELAY (sec)	MAXDELAY (sec)
12444	0.200	11.4	13.0	17.7	30.0	1.6	6.3	18.6
12445	0.176	9.3	10.2	11.5	12.2	0.9	2.2	2.9
12446	0.200	10.6	11.4	12.9	13.7	0.8	2.3	3.1
12447	0.200	10.6	11.2	12.8	13.7	0.5	2.1	3.1
12448	0.200	10.6	11.2	12.6	13.4	0.6	2.0	2.8
12449	0.200	10.7	13.2	45.6	79.8	2.4	34.9	69.1
12450	0.104	6.0	6.9	21.9	55.9	0.8	15.9	49.8
12451	0.104	6.1	6.8	12.2	31.4	0.8	6.1	25.3
12453	0.106	5.9	6.6	8.0	12.0	0.7	2.1	6.1
12454	0.106	6.0	6.2	7.4	10.7	0.2	1.4	4.7
12455	0.200	11.1	11.1	13.2	19.8	0.0	2.1	8.7
12456	0.200	10.6	11.3	13.0	18.4	0.7	2.3	7.8
12457	0.200	10.9	11.1	12.7	14.3	0.3	1.8	3.4
12458	0.200	10.9	11.3	13.0	14.3	0.3	2.1	3.4
12462	0.200	10.2	11.3	12.7	13.6	1.0	2.5	3.4
12463	0.200	11.5	13.2	36.0	66.2	1.8	24.5	54.7
12464	0.200	10.9	13.4	35.1	56.3	2.5	24.2	45.4

Computation of Speed and Travel Time at the Corridor Level

Occasionally it may be of interest to compute speeds and travel time for an entire corridor. Because segments follow directional centerlines, queries must take direction into account. Suppose that average speed and total travel time for the PM peak period (4:30-5:30 pm) from September 1995 to May 1996 is needed. Only segments located on the main routes are considered. These segments are characterized by having SEGTYPECODE = 1 (Figure 5-2). The corresponding query would be

```
SELECT     CORRCODE, SEGDIRECTION, COUNT(*) "NRECORDS",
           SUM(SEGLENGTH) "LENGTH", SUM(AVTIME)/60 "TRTIME",
           SUM(SEGLENGTH)*3600/SUM(AVTIME) "SPEED"
FROM       CORR_SEGMENTS, ACAD9596_430_530_TRAV_TIMES
WHERE      ACAD9596_430_530_TRAV_TIMES.SEGCODE =
           CORR_SEGMENTS.SEGCODE
AND        SEGTYPECODE = 1
GROUP BY   CORRCODE, SEGDIRECTION;
```

Length is given in miles; travel time is given in minutes; and speed is given in mph. Table B-7 shows the results from this query.

Table B-7: Total travel time and average speed for highway corridors in Baton Rouge (September 1995 - May 1996, 4:30-5:30 pm data)

CORRCODE	SEGDIRECTION	NRECORDS	LENGTH (mi)	TRTIME (mm:ss)	SPEED (mph)
I-10	EB	95	16.53	31:12	31.78
	WB	96	16.57	18:13	54.56
I-110	NB	58	8.84	09:34	55.42
	SB	57	8.58	10:03	51.28
I-12	EB	97	17.56	21:08	49.84
	WB	96	17.62	18:16	57.87
LA 19	NB	34	5.62	11:33	29.20
	SB	34	5.61	10:08	33.22
Plank Rd	NB	90	14.63	32:35	26.95
	SB	88	14.49	30:34	28.45
Airline Hwy	SB	137	22.85	41:29	33.05
	NB	136	22.84	39:23	34.81
Florida Blvd	EB	91	14.66	34:56	25.17
	WB	91	14.66	33:50	26.00
Mickens Rd	EB	17	3.01	04:47	37.74
	WB	17	3.01	04:50	37.33
Sherwood For.	NB	41	6.74	22:00	18.38
	SB	41	6.72	20:23	19.79
Siegen Lane	NB	16	2.47	12:12	12.12
	SB	16	2.47	06:06	24.30
N Foster Dr	NB	5	0.77	01:33	29.63
	SB	5	0.78	07:04	6.59
Government	EB	25	3.43	10:47	19.06
	WB	25	3.44	09:49	21.04
Jefferson Hwy	EB	33	5.40	13:28	24.05
	WB	33	5.41	11:00	29.49
Staring Lane	NB	10	1.99	04:34	26.15
	SB	10	1.99	05:02	23.70
Essen Lane	NB	14	1.86	09:42	11.48
	SB	14	1.85	09:05	12.23
Bluebonnet Rd	NB	9	1.31	05:49	13.53
	SB	9	1.31	03:30	22.48
Burbank Dr	EB	5	0.92	01:52	29.49
	WB	5	0.92	02:06	26.40
Nicholson Dr	NB	6	1.08	02:14	28.97
	SB	8	1.25	02:30	30.03
LA 1	NB	2	0.27	00:20	49.68
	SB	3	0.45	00:30	52.89
Greenwell Sp.	EB	35	5.23	13:16	23.67
	WB	35	5.24	11:03	28.46
Scenic Hwy	NB	57	9.76	12:30	46.86
	SB	62	10.65	14:24	44.40
Range Ave	NB	15	2.29	07:21	18.65
	SB	15	2.29	05:43	23.99

VITA

Cesar Augusto Quiroga was born in Bogota, Colombia, on August 26, 1961. His education includes an undergraduate degree (1982) in Civil Engineering from Escuela Colombiana de Ingenieria (Colombian School of Engineering) in Bogota, and a Master's degree (1986) in Civil Engineering from Louisiana State University in Baton Rouge. Currently, he is a Research Associate in the Remote Sensing and Image Processing Laboratory at Louisiana State University in Baton Rouge.

His professional and research activities have covered a broad spectrum of topics ranging from applications of remote sensing and GIS to transportation engineering, to the analysis and design of drainage, flood control, and erosion control projects. His work has been published in several peer-reviewed technical journals, conference proceedings, and book chapters. His most recent project, which gave origin to this dissertation, involved the development and application of a methodology based on GPS and GIS for collecting travel time data needed for the Baton Rouge, Shreveport, and New Orleans Congestion Management Systems. This project has now been extended to apply the methodology to a wider variety of travel time studies.

He is a member of the American Society of Civil Engineers, the Institute of Transportation Engineers, the Transportation Research Board, and the Society of Hispanic Professional Engineers.

He is fluent in Spanish and English.

DOCTORAL EXAMINATION AND DISSERTATION REPORT

Candidate: Cesar A. Quiroga

Major Field: Civil Engineering

Title of Dissertation: An Integrated GPS-GIS Methodology for Performing Travel Time Studies

Approved:

Major Professor and Chairman

Dean of the Graduate School

EXAMINING COMMITTEE:

Chester G. Wilmot

Date of Examination:

June 17, 1997